SYSTEMS BIOLOGY OF PRO- AND ANTI-INFLAMMATORY INTRA- AND INTER-KINGDOM SIGNALING IN MAMMALIAN CELLS

A Dissertation

by

SHREYA MAITI

Submitted to the Office of Graduate and Professional Studies of
Texas A&M University
in partial fulfillment of the requirements for the degree of

DOCTOR OF PHILOSOPHY

Chair of Committee,	Arul Jayaraman
Committee Members,	Robert C. Alaniz
	Zhilei Chen
	Katy Kao
Head of Department,	M. Nazmul Karim

May 2015

Major Subject: Chemical Engineering

ABSTRACT

Inflammation is a beneficial self-defense mechanism that is usually triggered by injury or infection and is designed to return the body to homeostasis. However, uncontrolled inflammation can be deleterious and has been shown to be involved in the etiology of several diseases, such as inflammatory bowel disorder, rheumatoid arthritis and asthma. Inflammation is counter-balanced by host-derived anti-inflammatory immune responses of the body thereby maintaining immune homeostasis. Millions of bacteria categorized under commensal (non-pathogenic), probiotic (mutualistic) and pathogenic (disease causing) species that inhabit gastro-intestinal (GI) tract of mammalian host have been reported to influence host immune homeostasis. Host immune response is tolerant towards beneficial bacteria and provide them with shelter and food, in turn these bacteria help the host by digesting carbohydrates and proteins and preventing colonization of GI tract by invading pathogens and potentially harmful indigenous bacteria. Intestinal microbiota-derived indole has been shown to exhibit anti-inflammatory properties by down regulating inflammatory markers. A shift in indigenous bacterial population (dysbiosis) has been recently found to initiate and perpetuate chronic inflammation resulting in the etiology of inflammatory bowel diseases (comprising ulcerative colitis and Crohn's disease). However, the inter-play between pro- and anti-inflammatory signaling as well as molecular mechanism involved in host-microbiota interactions are not fully understood.

In this dissertation, we developed a mathematical model to describe integrated pro- and anti-inflammatory signaling in macrophages. The model incorporates the feedback

effects of *de novo* synthesized pro-inflammatory (tumor necrosis factor α; TNF-α) and anti-inflammatory (interleukin-10; IL-10) cytokines on the activation of the transcription factor named nuclear factor -κ B (NF-κB) under continuous lipopolysaccharide (LPS) stimulation (mimicking bacterial infection). In the model, IL-10 upregulates its own production (positive feedback) and also downregulates TNF-α production through NF-κB (negative feedback). In addition, TNF-α upregulates its own production through NF-κB (positive feedback). We validated the mathematical model predictions by measuring phosphorylated NF-κB, *de novo* synthesized TNF-α and IL-10 in murine RAW 264.7 macrophages when exposed to LPS. This integrated model was used to incorporate bacteria-derived indole signaling through a potential aryl hydrocarbon receptor (AHR) activated signal transduction pathway in human intestinal epithelial HCT-8 cells. The work described in this dissertation is a step towards modeling integrated pro- and anti-inflammatory immune responses in host (intra-kingdom signaling) and their cross-talk with intestinal microbiota-derived metabolite (inter-kingdom signaling) to maintain homeostasis in the body.

DEDICATION

To my parents for their unconditional love…

The best and the most beautiful things in the world
cannot be seen or even touched,
they must be felt with the heart….
-Helen Keller

ACKNOWLEDGMENTS

I thank all my committee members, Dr. Jayaraman, Dr. Hahn, Dr. Alaniz, Dr. Chen and Dr. Kao for their invaluable guidance. My advisor, Dr. Arul Jayaraman has been immensely supportive and encouraging throughout my Ph.D. Brainstorming ideas and hypotheses with him were both a pleasure and a learning experience. His guidance in analyzing data and scientific writing has been very helpful. Moreover, flexibility in thinking and accepting new ideas is something I learnt from him which has and always will be helpful.

I would also like to thank Dr. Juergen Hahn for guiding me through the modeling part of the work and instilling a keen eye for precision. A special thanks to Dr. Robert Alaniz for helping me get familiar with flow cytometry and analyzing FACS data. He has always been there to answer my queries and discuss experimental designs. Ms. Jane Miller ran my first samples on the flow cytometer and has always helped me with troubleshooting while running samples to obtain data for my experiments.

My friends and colleagues in Dr. Jayaraman, Dr. Alaniz and Dr. Hahn's lab have been of great help and a support system for me. I have enjoyed doing research thoroughly in such a friendly environment. I have had a great time with all my friends here at College Station/Bryan during the course of my graduate school.

My teacher from elementary, middle and high schools have played an integral part in my upbringing. I would like to thoroughly acknowledge their contributions in shaping my analytical abilities and a quest for knowledge.

My father (Biswanath) has been an inspiration to me and motivated me to pursue a doctoral degree. He is my friend, philosopher and guide who has answers to all my questions. My mother (Anupa) has laid the foundation for who I am today. I dedicate all my little achievements to her. My parents are and always will be a big part of my existence. My brother (Shoumik) inspires me to keep learning something new every day. A special thanks to all my grandparents, aunts, uncles, cousins and my little nephews for their love and memorable times spent together.

NOMENCLATURE

TNF-α	Tumor Necrosis Factor- alpha
IL-8	Interleukin 8
IL-10	Interleukin 10
NF-κB	Nuclear Factor- kappa B
AHR	Aryl Hydrocarbon Receptor
STAT3	Signal Transducer and Activator of Transcription 3

TABLE OF CONTENTS

Page

Page

LIST OF FIGURES

Page

Page

LIST OF TABLES

Page

CHAPTER I

INTRODUCTION

1.1 BACKGROUND

The human immune system is a highly complex network of organs, cells and biochemical mediators that work in conjunction with each other to prevent entry of foreign particles, spread of infection and is primarily designed to return the body to homeostasis. Acute inflammation (visibly perceived as tissue swelling and localized redness in case of external injuries or internal cytotoxicity leading to cell apoptosis in case of exposure to environmental pollutants such as dioxin) is the first wave of immune response post injury in multicellular eukaryotic organisms. It can be defined as a self-defense mechanism of the body, targeted towards protecting broken epithelial layer (at the site of injury) from microbial invasion and also spread of infection from food and airborne pathogens. Circulating blood comprises immune cells such as macrophages, dendritic cells, neutrophils, T lymphocytes and B lymphocytes that pick up cues of pathogenic invasion and eradicate invading pathogens, protect injured tissue from further insult and prevent spread of infection to other parts of the body. Inflammation is a double-edged sword. As indispensable as acute inflammation is, chronic inflammation can result in the body attacking its own cells even in absence of pathogens, which leads to autoimmune and inflammatory disorders such as rheumatoid arthritis (inflammation of small diarthrodial joints) [1], asthma (inflammation of respiratory tract) [2], psoriasis (inflammation of skin) [3], multiple sclerosis (inflammation of myelin sheath of nerve cells) [4] and inflammatory

bowel disorder (IBD) classified as ulcerative colitis (distal gastro-intestinal inflammation) and Crohn's disease (pan gastro-intestinal inflammation) [5]. Under healthy conditions, pro-inflammatory responses are counter-balanced by anti-inflammatory responses to maintain homeostasis (equilibrium) in the body. However under disease conditions, the fine balance between pro- and anti-inflammatory responses is disturbed (or lost) and the resulting uncontrolled inflammation leads to pathogenesis of autoimmune and auto-inflammatory disorders [6].

Pro-inflammatory responses of immune and epithelial cells are marked by extracellular secretion of pro-inflammatory cytokines such as tumor necrosis factor alpha (TNF-α) and interleukin 8 (IL-8) on recognition of inflammatory cues like lipopolysaccharide (LPS) of bacterial cells through specialized cell surface receptor called toll-like receptor 4 (TLR4) [7]. The *de novo* synthesis of these cytokines is regulated by the transcription factor nuclear factor kappa B (NF-κB) which is sequestered as an inactive complex in the absence of inflammatory signals. Pro-inflammatory responses on the other hand are regulated and mitigated by anti-inflammatory cytokines such as interleukin 10 (IL-10) which inhibit *de novo* synthesis of TNF-α and IL-8 through NF-κB down regulation [8].

For a long time the sole function of sophisticated immune responses was thought to be eradication of invading microbes however, recently a whole new facet of the mammalian immune response, i.e., tolerance towards indigenous microflora has been unraveled. Bacteria, bacteriophages, viruses and fungi inhabit different parts of the mammalian body such as oral cavity, ear, skin, urogenital tract and most prominently the

gastro-intestinal (GI) tract (especially the large intestine) [9]. In humans, microbial cell population exceeds the number of host cells by a factor of ten [10], thereby constituting 90% of the cumulative genes of the host-microbiota system. The human GI tract houses approximately 10^{14} bacterial cells belonging to approximately 1000 different species of commensal (non-pathogenic), probiotic (mutualistic) and pathogenic (disease causing) bacteria in close proximity to host cells [11].

The continuous exchange of signals between endogenous microbial community and host cells make the GI tract a classic example of intra- and inter-kingdom signaling ecosystem. The host immune response is extremely tolerant towards the non-pathogenic bacteria as opposed to the pathogenic ones. The specific host immune tolerance towards non-pathogenic species indicates a co-operative relationship between host and its beneficial microbiota (comprising commensal and probiotic bacteria) [12]. A primary function of the beneficial microbiota is preventing colonization of the GI tract by exogenous pathogenic bacteria or even potentially harmful indigenous microorganisms by directly competing with them for limited nutrients as well as by modulating host immune response [13] (Figure 1). Dysbiosis (alteration in microbiota population triggered by genetic pre-disposition or environmental factors), has been reported to be associated with the etiology of auto-inflammatory disorders such as inflammatory bowel disease (IBD) [14,15] (Figure 1). The intestinal microbiota's involvement in digestion and metabolism of carbohydrates, synthesis of vitamins and recently discovered contribution in host immunity have made researchers term it as a novel organ in mammals [16].

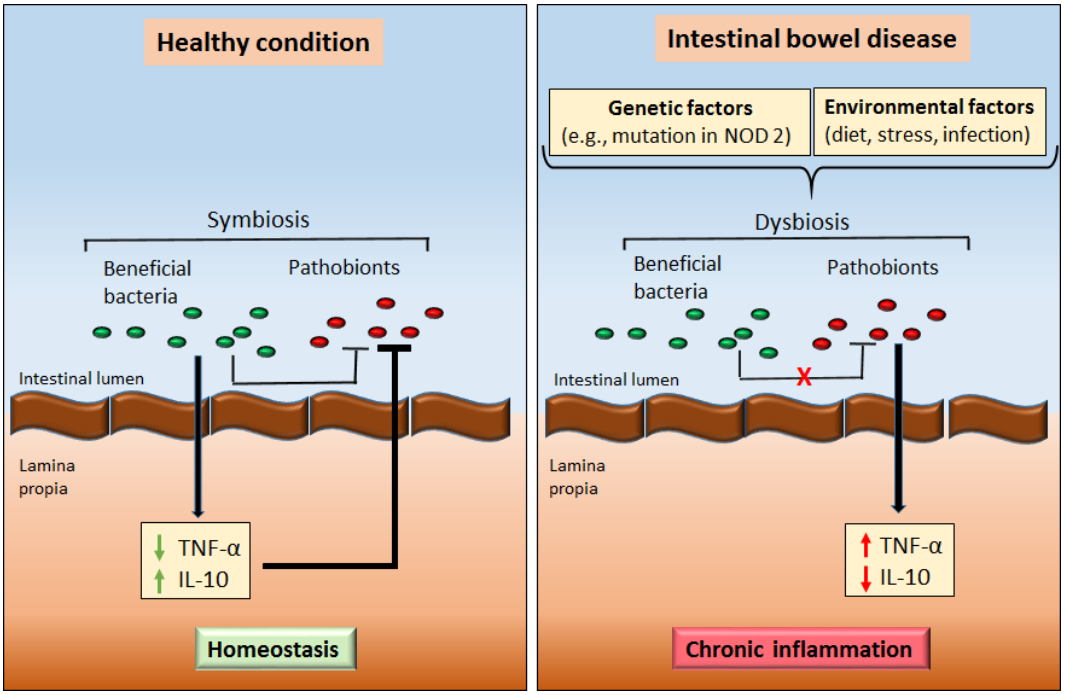

Figure 1. Immunoregulation by intestinal microbiota.

Although intestinal microbiota has been reported to have beneficial effects on the host, molecular mechanisms involved in signal transduction pathways activated by bacteria-derived molecules in host cells and the subsequent cross-talk between host-derived pro- and anti-inflammatory signaling are not well understood. The main focus of this work is investigating pro- and anti-inflammatory responses in host immune cells, specifically macrophages, under chronic inflammatory signal exposure and bacterial metabolite indole-induced signaling in host intestinal epithelial cells in the context of host GI homeostasis. The dissertation is divided into two sections; first, development of a mathematical model describing pro- and anti-inflammatory immune signaling in

macrophages under chronic inflammatory signal exposure (in the context of overall immune homeostasis) and second, extending this model to studying the effects of host-microbiota interactions for inflammatory signaling in intestinal epithelial cells in the context of GI immune homeostasis under the conditions of chronic inflammation (mimicking IBD).

1.2 MOTIVATION

Patients suffering from chronic inflammatory disease like IBD have diarrhea, rectal bleeding, abdominal pain, fatigue, and weight loss problems on a regular basis. All of these restrict the quality of life to a severe extent, trigger emotional stress and pose financial burden. It is a life-long ailment that currently has several treatments but no cure for absolute remission. According to Crohn's and Colitis Foundation of America (CCFA) funded by Centers for Disease Control and Prevention (CDC), 70,000 new cases of IBD are diagnosed every year in the United States of America, among which 38,000 are cases of ulcerative colitis (UC) and 33,000 of Crohn's disease (CD) with a median age for diagnosis of UC and CD being 34.9 and 29.5 years respectively. In USA, approximately 1.6 million people are currently affected by IBD and 5% are less than 20 years in age. IBD diagnosed in children is more severe than that diagnosed in adults [17] and often causes delayed puberty and growth failure [18]. CCFA reports that in 2010 187,000 patients were hospitalized for CD and 107,000 for UC. The root cause for the incidence of such disorders is not completely known, however, besides genetic pre-disposition, environmental factors

such as lifestyle, diet, and gut microbiota are found to play an important role in the etiology of IBD [19].

The medications currently available for treatment of IBD cause non-specific suppression of immune response, e.g., corticosteroids that inhibit ability of the body to initiate and sustain inflammatory responses [20]. Corticosteroids are prescribed to patients only for short-term control of flare-ups and not recommended for long-term use because of their strong side effects associated with bone loss, weight gain, cataracts, sleep disturbance and mood swings. On the other hand immunomodulators such as 6-mercaptopurine, azathioprine and methotrexate are prescribed to patients in remission who have only responded to steroids [21]. Amino salicylates (introduced orally or rectally) help reduce inflammation of the intestinal wall, however, is effective in ulcerative colitis only and not in the case of Crohn's disease [22,23]. The latest development in the treatment for IBD is the use of targeted inhibitors such as infliximab (approved by FDA for treatment of CD in 1998 as intravenous infusion) [24], golimumab (approved by FDA for treatment of UC in 2013 as subcutaneous injection) [25] which are monoclonal antibodies against tumor necrosis factor alpha (TNF-α), a major pro-inflammatory cytokine (description in section 2.3.2.1). Vedolizumab (approved by FDA for treatment of UC and CD in 2014) is a monoclonal antibody against lymphocytes, preventing them from entering inflamed tissues [26]. In cases of severe UC and CD, intravenous infusions are prescribed every 4-6 weeks along with regular intake of immunomodulators like 6-mercaptopurine. IBD patients resort to surgical methods when no medication seem to relieve their discomfort. By means of surgery the affected regions of GI tract (usually large intestine) are amputated

or in severe cases large intestine is completely removed and the ileum (distal end of small intestine) is brought out onto the surface of the abdominal skin creating an opening for the passage of intestinal waste to be collected in a pouch outside the body [27,28]. All these procedures force the patient to adopt a drastic lifestyle change.

Most of the current IBD treatments focus at immunosuppression either for short-term remission of flare-ups or for keeping symptoms under control. For complete non-invasive cure of IBD, we still need to understand the root cause behind the etiology of the disease and design therapy that keeps pro-inflammatory responses in check but does not suppress them completely. Clinically IBD is identified as ulcerations at the small or large bowel mucosa [19]. Although genetic pre-disposition influences prevalence of the disease, recent research has established that environmental factors are essential for the pathogenesis and growing incidence of IBD all over the world [19]. Diet, prolonged use of antibiotics and microbial exposure during childhood and adulthood have been reported to be in direct relation with incidence of IBD [19]. Moreover, all these factors modify intestinal microbiota to a great extent, thereby indicating that a shift in normal microbiota population can play a critical role in the pathogenesis and perpetuation of IBD [19]. Bansal *et al*. reported that bacterial metabolite, for example, indole (released by endogenous bacteria upon tryptophan metabolism) has the potential to down regulate pro-inflammatory signals, such as NF-κB (transcription factor) and IL-8 (chemokine) and induce anti-inflammatory signals such as IL-10 (cytokine) [29] in human intestinal epithelial cells.

Knowledge of the co-operative relationship between host and intestinal microbiota [12,15,16] and the possibility that the microbiota can exert anti-inflammatory effects on the host [29,30] laid the foundation for this work. This dissertation aims at understanding the host-microbiota interactions in the context of immune regulation in the GI tract using a systems biology approach. We developed experimentally validated mathematical models to study intra-host pro- and anti-inflammatory immune responses induced by bacterial LPS in macrophages and bacteria-derived metabolite indole signaling through a potential signal transduction pathway that influences immune responses of human intestinal epithelial cells.

1.3 RESEARCH OBJECTIVES, IMPORTANCE AND NOVELTY

Biochemical interactions among different components of a biological signaling network is highly complex and difficult to comprehend solely through experimental studies. Mathematical modeling of such biological networks expands the opportunity to infer experimental data and understand network interactions in a much broader context. The deterministic computational models developed in the current work in conjunction with experimental data are composed of important biochemical reactions (represented in the form of ordinary differential equations using MATLAB) of signal transduction pathways corresponding to LPS and TNF-α stimulation, involving transcription factor activation and subsequent cytokine synthesis that can help elucidate molecular mechanisms associated with regulating immune homeostasis in host. Host-microbiota interactions have been reported to have profound effect on host homeostasis and thus

investigating mechanistic dynamics of these interactions computationally and experimentally can shed some light on the pathogenesis of several inflammatory diseases. Microbiota-derived indole has been reported to regulate inflammation in host, however, the molecular mechanism involved in indole signaling is not clearly understood. This dissertation focuses at investigating a possible molecular mechanism of indole-induced signal transduction that influences pro- and anti-inflammatory immune responses of the host. We developed experimentally validated computational models that can predict host responses in the context of immune homeostasis for conditions that are not experimentally achievable due to lack of suitable techniques or resources. We selected essential biochemical reactions involved in the signal transduction pathway that are experimentally verifiable to reduce uncertainty in the values of reaction parameters. The biochemical network of host immune responses and host-microbiota interactions as mentioned in sections 1.1 and 1.2 comprise several feed-forward and feed-back regulatory loops that influence the overall outcome of the biological reactions. We incorporated known regulatory feed-back loops in our deterministic models, something which has not been done before. Most of the deterministic computational models that have been developed so far in the context of inflammation have either considered synthesis of only one pro-inflammatory cytokine [31,32] or represented stimulatory effects of multiple extracellular cytokines [33]. In this work we studied cross-talk between *de-novo* synthesized pro-inflammatory cytokine and anti-inflammatory cytokines in murine macrophages under continuous LPS stimulation and the effect of indole on immune responses of human intestinal epithelial cells under continuous TNF-α stimulation. The models developed here

are a step towards assimilating our knowledge on host-derived pro- and anti- inflammatory immune responses as well as intra- and inter-kingdom signaling as studied in mammalian gastro-intestinal tract. The experimental data obtained and mathematical models developed in this work provide a quantitative and dynamic profile of the cytokines and transcription factors involved in the signal transduction pathways studied.

The specific objectives of this work are:

- Development of a computational module representing pro-inflammatory immune response in macrophages induced by lipopolysaccharide (LPS) resulting in activation of NF-*κ*B signal transduction pathway and *de novo* synthesis of TNF-α positive feedback effect of TNF-α on NF-κB activation.
- Development of an anti-inflammatory module representing LPS-induced *de novo* synthesis of anti-inflammatory cytokine (IL-10) through NF-κB and STAT3 activation and positive feedback effect of IL-10 on STAT3 activation and negative feedback effect on NF-κB.
- Assimilation of pro- and anti-inflammatory modules as described above into an integrated immune response model where TNF-α synthesis is inhibited by IL-10 through down regulation of NF-κB activation.
- Extension of the above integrated model to incorporate indigenous bacterial metabolite indole and predict its effect on NF-κB activation and *de novo* IL-8 synthesis in human intestinal epithelial cells.
- Investigation of a possible signal transduction pathway to mediate indole-induced immune responses in host.

CHAPTER II

LITERATURE REVIEW

2.1 MAMMALIAN IMMUNE RESPONSE

Mammalian immune response is mediated through an intricate network of lymphoid organs (thymus, bone marrow, spleen, lymph nodes and tonsils), different cell types (dendritic cells, macrophages, neutrophils, T-cells, B-cells and more), messenger molecules (cytokines) and humoral factors (antibodies, complement proteins and antimicrobial peptides) that protect the body from foreign entities such as bacteria, viruses, and fungi that might invade through broken skin at the site of injury or airborne and foodborne pathogens. The response of the immune system can be broadly classified into two categories on the basis of speed and specificity of action, namely innate and adaptive immune response. Disruption in innate immune responses can lead to auto-inflammatory diseases such as IBD [34], whereas, hyperactive adaptive immune responses result in autoimmune diseases, allergy and allograft rejection [35].

2.1.1 Innate immune response in mammalian host

Innate immune responses are initiated immediately after injury and are primarily mediated through dendritic cells, macrophages, neutrophils, eosinophils, leukocytes, mast cells, monocytes and natural killer cells. These cells circulate in blood and are localized in specific niches of different organs such as liver [36], spleen (which stores half the body's monocytes that differentiate into dendritic cells and macrophages upon tissue

injury) [37] and Peyer's patches (specialized lymphoid nodules adjacent to epithelial cell layer in ileum) [38]. Innate immune response is a defense mechanism that has been conserved through evolution in plants and animals (invertebrates and vertebrates) [35] which indicates its presence even before the split of the two kingdoms.

Communication between different cell types of innate immune system is accomplished through biochemical messenger molecules called cytokines like tumor necrosis-factor alpha (TNF-α), interferon gamma (IFN-γ) and interleukin 8 (IL-8). Though the innate immune response is immediate post injury and an indispensable part of the immune system, it damages some of the host cells due to its lacks of specificity. However, innate immune cells like dendritic cells, macrophages and neutrophils can differentiate between self and non-self entities on the basis of specialized structures present on microbial cells called pathogen-associated-membrane-proteins (PAMPs), for example, flagellin of bacterial flagella [39], lipopolysaccharides (LPS) of gram negative bacteria and peptidoglycan of gram positive bacteria [35] that can trigger an immune response.

Resting macrophages are activated by both bacterial as well as host-derived inflammatory signals such as LPS and pro-inflammatory cytokines like TNF-α respectively. Macrophages respond by releasing more pro-inflammatory cytokines and phagocytizing pathogens [40]. The central feature of innate immune response is the activation and recruitment of specialized neutrophils to the site of injury to phagocytose pathogens [41]. Phagocytizing neutrophils and macrophages extend their cytoplasmic membranes to form pseudopodia which in turn form phagosomes (membrane bound

vesicles) around the targeted particles which in turn fuse with lysosomes and to form phagolysosome that can lyse the microbe, as shown in Figure 2.

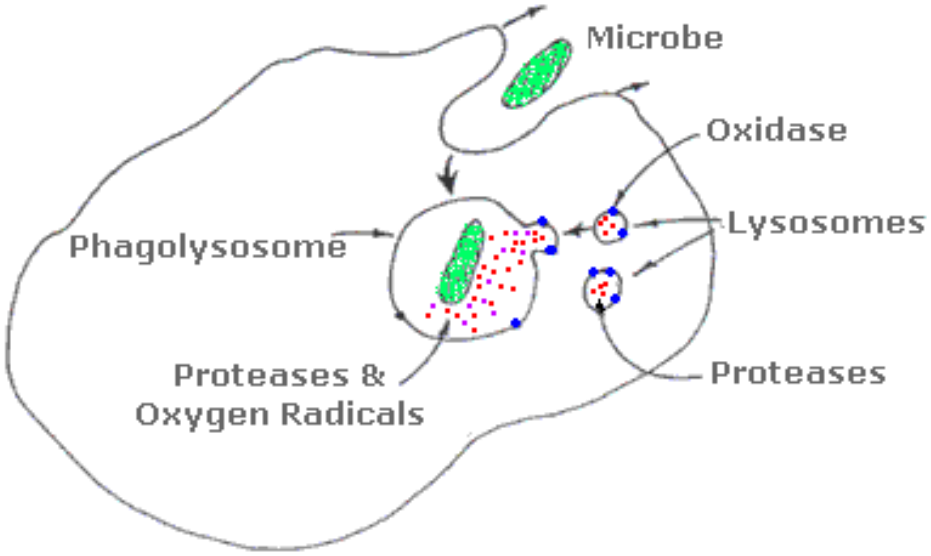

Figure 2. Phagocytosis of microbes by macrophages and neutrophils: an integral part of innate immune response [42].

Dendritic cells are found in circulation as well as in tissues that have contact with external environment such as skin, outer lining of nose, lungs and gastro-intestinal tract [43]. Due to their specific location close to the external environment they are usually the first ones to sample the surrounding with their extendable dendrite-like structures that can protrude through intracellular spaces of the epithelial lining. Dendritic cells are antigen-presenting cells that process antigen material upon sampling the environment and present them to B and T lymphocytes in lymph nodes. Immature dendritic cells circulating in blood upon activation migrate to lymph nodes and interact with T and B lymphocytes to induce adaptive immune response [43]. Dendritic cells thus link the innate and adaptive immune responses.

2.1.2 Adaptive immune response in mammalian host

Invertebrates and simpler animals defend themselves from pathogens by virtue of their protective barriers, phagocytic cells and secretion of toxic molecules, much similar to the innate immune system of vertebrates. However, adaptive immune system is a characteristic feature of vertebrates [35]. It is called upon when innate immune responses are not sufficient to eradicate pathogenic invasion [35]. It is mediated by two types of lymphocytes, namely, B and T cells, and unlike innate immune responses, adaptive responses are highly specific to the type of pathogen invading the body (can differentiate proteins on the basis of single amino acid or distinguish between optical isomers of the same molecule). Adaptive immune responses can be regarded as the second wave of

protective immune response, called upon by the innate immune system and is effective only if the body has been exposed to the pathogens *a priori* [43].

The adaptive immune response can be further classified under two categories, antibody mediated responses (regulated by B lymphocytes) and cell mediated responses (regulated by T lymphocytes). B cells are activated by innate immune cells to secrete antibodies called immunoglobulins targeted to bind specific pathogens (antigens) and render them inactive. Antibody bound inactive pathogens are marked for phagocytic elimination by innate immune cells. On the other hand, T-cells can detect pathogens inside the host and either kill the infected cells themselves or secrete signaling molecules to activate phagocytizing cells like macrophages to eliminate the pathogen.

2.1.3 Pro-inflammatory immune response

Visibly, inflammation is swelling and redness around injured tissues due to increased blood flow to the site of injury. Secretion of pro-inflammatory cytokines by host cells such as TNF-α, IFN-γ, interleukin 1-beta (IL-1β) and chemokine IL-8 under bacterial stimulation are indicators of pro-inflammatory responses. A broad range of cell types such as macrophages, T lymphocytes, B lymphocytes, mast cells, endothelial cells and fibroblasts release such cytokines. Cytokines are extremely potent signaling molecules and vary in size between 8 and 30 kDa. The *de novo* synthesis of cytokines in immune cells upon pro-inflammatory signal activation is regulated by transcription factors. Nuclear factor kappa B (NF-κB; described in section 2.3.3.1) is one of the most abundant transcription factors that mediate pro-inflammatory responses and induce synthesis of

TNF-α, IL-8, and IL-1β [44]. The major sources of pro-inflammatory cytokines are Th-1 type cells that secrete high levels of IL-1, TNF-α and IFN-γ that in turn activate macrophages and induce innate immune responses against invading pathogens [45]. Other transcription factors that are involved in pro-inflammatory responses are signal transducer and activator of transcription (STAT3), activator protein 1 (AP-1) and nuclear factor of activated T cells (NFAT) [46]. Acute pro-inflammatory responses of the innate immune system play an integral role in self-defense, however uncontrolled inflammatory responses can lead to the etiology of auto-inflammatory disorders like intestinal bowel disease (IBD). In healthy conditions, pro-inflammatory responses are counter balanced by anti-inflammatory responses to maintain homeostasis in the body.

2.1.4 Anti-inflammatory immune response

The prominent anti-inflammatory cytokines that play integral role in maintaining homeostasis in the body are interleukin 10 (IL-10) and tumor growth factor beta (TGF-β). IL-4, IL-13, and IL-1 receptor antagonist (IL-1ra) are other well-known anti-inflammatory cytokines that are mostly secreted by Th-2 type cells [45]. Regulatory T cells (Treg cells) formerly known as suppressor T cells are a subpopulation of T cells that modulate pro-inflammatory responses of the immune system and maintain tolerance towards self-antigens. Treg cells are a source of IL-10 and TGF-β [47]. Macrophages, an integral part of the innate immune response exhibit dual phenotype classified as M1 and M2 [48]. M1 is the pro-inflammatory phenotype that is activated by inflammatory signals and secrete pro-inflammatory cytokines such as TNF-α, IL-1β and IFN-γ. On the other hand, the M2

phenotype exhibits anti-inflammatory responses marked by *de novo* synthesis and secretion of IL-10, IL-4 and IL-13 [49] as shown in Figure 3. IL-10 and TGFβ secreted by intestinal epithelial cells and resident macrophages play an important role in maintaining homeostasis in the host gastro-intestinal (GI) tract which is inhabited by ~10^{14} bacterial cells.

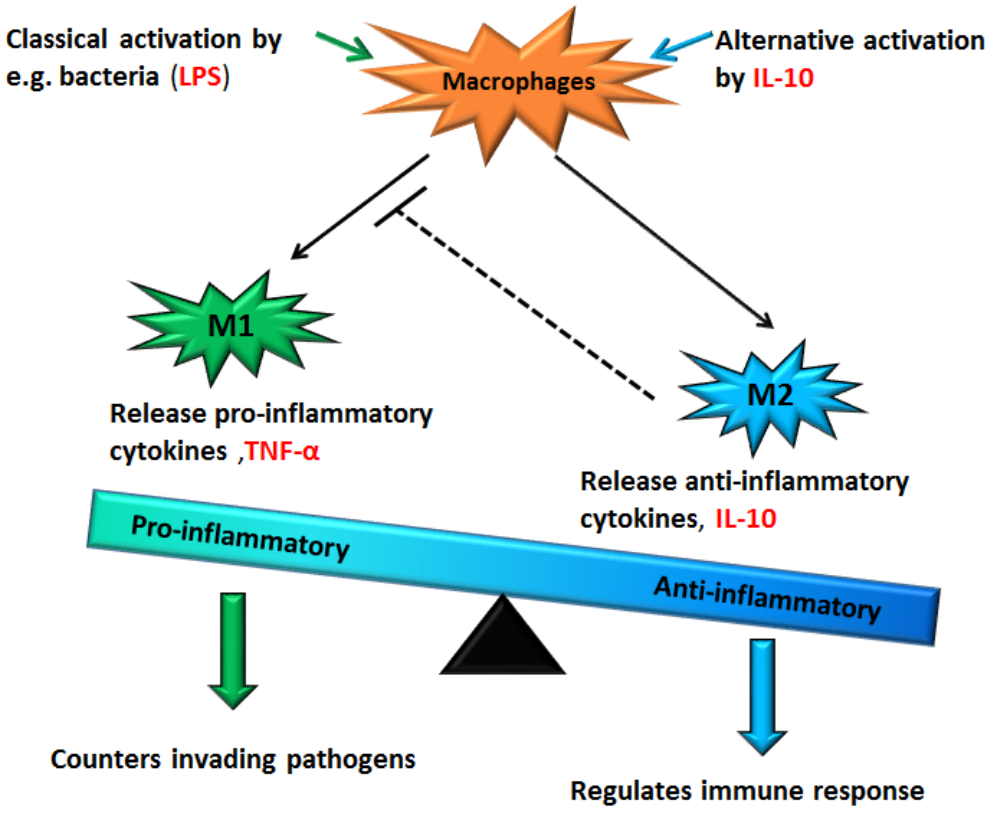

Figure 3. M1 (pro-) and M2 (anti-inflammatory) macrophage activation and responses.

2.2 HOST-MICROBIOTA INTERACTIONS IN GASTRO-INTESTINAL TRACT

A dynamic interaction exists between host immune cells and the microorganisms that colonize the gastro-intestinal (GI) tract. The intestinal microbiota is embedded in the mucous layer adjacent to the intestinal epithelial lining as shown in Figure 4. Colonization of GI tract by microbiota is initiated by maternally acquired bacteria during birth followed by large number of microflora that are acquired from the environment [15]. The microbiota composition varies between individuals; however, the two major bacterial phylotypes are *Firmicutes* ssp. and *Bacteroidetes* spp. [50], and are mostly gram negative anaerobes [51].

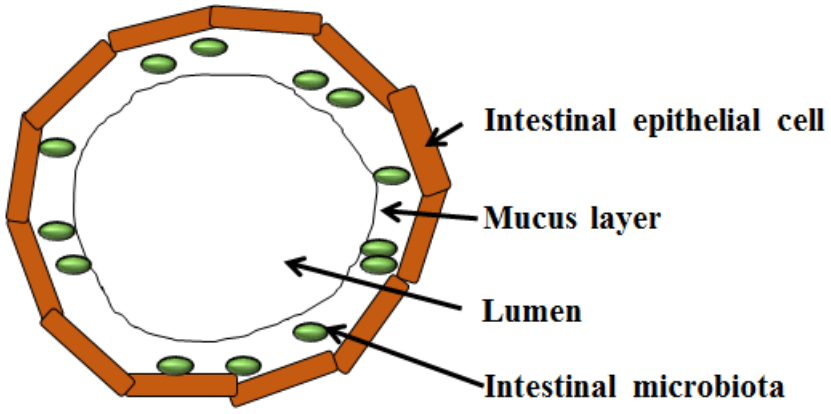

Figure 4. Cross-sectional view of mammalian gastro-intestinal tract.

Not much is known about the composition and functions of the intestinal microbiota, as almost 80% of the microbiota cannot be cultivated *in vitro* in the laboratory [51]. The indigenous microbiota anaerobically converts undigested carbohydrates and proteins in the large intestine to short chain fatty acids such as acetate, propionate, butyrate [52] that have been reported to induce T cell differentiation into T_{reg} cells and promote secretion of the anti-inflammatory cytokine IL-10 [53]. Host-microbiota mutualistic relationship is represented in the fermentation of undigested dietary components by the microbiota to produce energy from carbohydrates and proteins that might have been discarded by host, which in turn promotes growth and sustenance of microbiota. The intestinal microbiota is referred to as a virtual organ by some authors due to its multifaceted metabolic and immunomodulatory functions [54]. Its activity depends largely on substrate availability and its retention time before being discharged out of the body with intestinal waste [52]. Other than metabolic functions, intestinal microbiota has been found to modulate mucosal immune response and colonization by invading endogenous pathogens and potential harmful indigenous bacteria [13].

Immune cells in the GI tract are located in specialized lymphoid tissues such as GALT (gut associated lymphoid tissue), ILT (intestinal lymphoid tissue) and Peyer's patches (usually in ileum of small intestine as shown in Figure 5**)**.

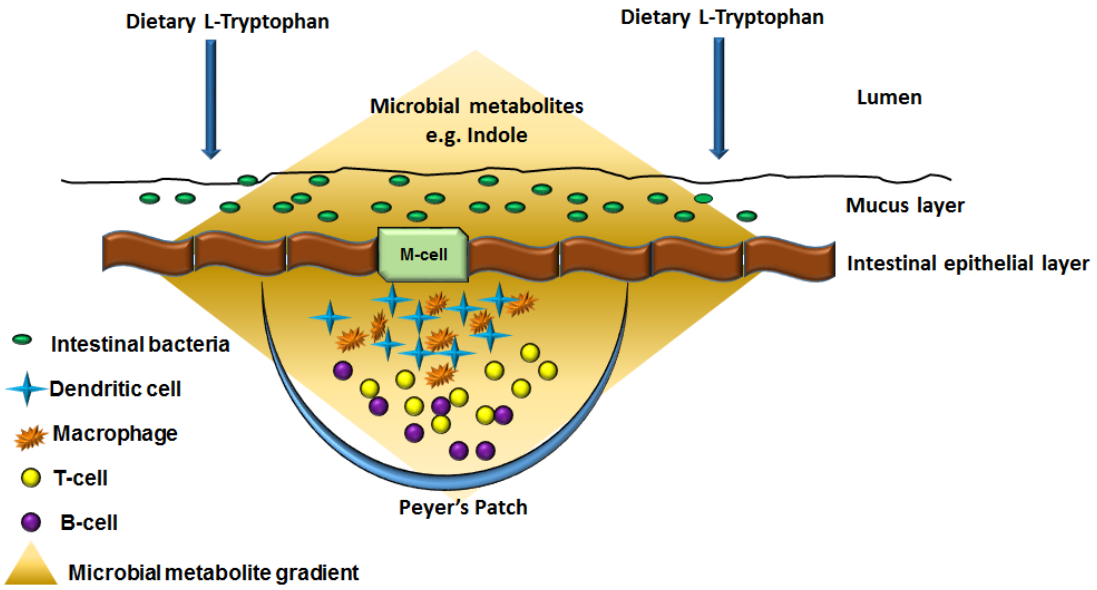

Figure 5. Small intestine organization.

The intestinal epithelial lining forms a boundary between host cells and bacterial colonies and are interspaced with specialized M-cells that allow passage of selective molecules between host and the bacterial compartments [55]. The close proximity of different cell types and molecules made by them, as well as exchange of molecules between host and microbiota [56] facilitates intra- and inter-kingdom signaling. Previous studies have shown that both the microbiota and intestinal epithelial cell responses are altered by molecules produced by the other cell type. For example, previous work from our laboratory showed that norepinephrine (hormone) released by host cells affects bacterial colonization and virulence [57]; similarly, indole produced by the microbiota modulates indicators of inflammation in intestinal epithelial cells [29].

2.2.1 Microbiota-derived indole as an inter-kingdom signaling molecule

Escherichia coli, one of the bacteria found in mammalian GI tract produces ~600µM indole in suspension culture [58] and it has also been detected in feces at comparable concentrations [59,60]. *E. coli*, possesses *tnaA* and *tnaB* genes which encode for enzyme tryptophanase A (TnaA) and transporter protein TnaB. TnaB helps in internalizing dietary tryptophan (amino acid) which then gets hydrolyzed by TnaA to produce indole, pyruvate and ammonia [61,62] as shown below:

$$L - Tryptophan + water \leftrightarrow Indole + Pyruvate + Ammonia$$

Unlike tryptophan, it is not clearly known if indole readily diffuses through the cell membrane or if it requires a transport complex to facilitate its uptake and secretion [62]. Indole had been identified as a bacterial metabolite as early as in the 19th century and was regularly used as a test for distinguishing cholera spirilla from other spirilla [63]. However, only recently has indole been recognized as an intercellular signaling molecule that regulates diverse physiological processes in bacteria such as motility [57], biofilm formation [57], antibiotic resistance (by inducing xenobiotic exporter genes) [64] and virulence [65] as well as increases intestinal epithelial tight junction resistance and attenuates pro-inflammatory responses in host by downregulating NF-κB under continuous TNF-α stimulation *in vitro* [29]. This makes indole an important intercellular signaling molecule that influences both bacterial as well as host responses, thereby shaping host-microbiota crosstalk. Almost 85 species of gram positive and gram negative bacteria are known to produce indole including certain pathogenic bacteria such as *Bacillus alvei*, *Vibrio cholera*, several *Shigella* strains, *Enterococcus faecalis* and

pathogenic *E. coli* [62]. However, it is not known if indole concentrations vary between healthy and diseased individuals.

Several non-indole producing bacteria and host cells in the GI tract and liver possess genes that can convert indole to produce several derivatives such as indole-3-propionic acid (identified as a powerful anti-oxidant), indoxyl sulphate [66] and 5-hydroxyindole [67]. These derivatives have also been identified by our laboratory in luminal contents [68] indicating its potential contribution in systemic immune response. The anti-inflammatory properties of indole (as an inhibitor of NF-κB and down regulator of IL-8) as reported by previous work from our laboratory [29] makes it a potential therapeutic candidate for inflammatory bowel disease. However, the molecular mechanisms underlying the reported effect of indole are not known. In order to study the effect of indole in modulating chronic inflammation in host and its potential contribution as a therapeutic molecule, it is necessary to identify and characterize the signal transduction pathways involved and its interaction with other pro- and anti-inflammatory signaling pathways in host cells.

2.3 SIGNAL TRANSDUCTION

Signal transduction refers to the biological process of conveying an extracellular signal from the cell membrane to the intracellular nucleus to activate target genes by stimulating or inhibiting cytosolic proteins in a specific order. Immune responses are examples of signal transduction where an extracellular stimulus such as bacterial membrane component LPS triggers pro-inflammatory responses by activating

transcription factor (such as NF-κB) that leads to transcription and *de novo* synthesis of TNF-α.

Cytokines (TNF-α, IL-8, IL-10 and more), hormones (estrogen, melatonin and more) and neurotransmitters (serotonin, acetylcholine and more) are usually the extracellular signals that initiate communication between different cell types in an organism. MEDLINE (Medical Literature Analysis and Retrieval System Online, or MEDLARS Online), a medical bibliographic database reported the first entry of the term "signal transduction" in 1972. Some early articles used "signal transmission" and "sensory transduction" to explain present day signal transduction phenomena [69,70]. Signal transduction pathways started getting attention from researchers post late 1980s following advancement in experimental techniques to test complex biochemical interactions. The first step in signal transduction pathway is the recognition of extracellular signaling molecule (ligand) by its corresponding receptor on the surface of a cell. Ligand-receptor binding leads to conformational change of receptor that triggers cascade of subsequent intracellular biochemical reactions. The essential components of a signal transduction pathway are the ligands, the cell surface receptors, intracellular proteins that affect the functioning of the cell, target genes and proteins.

2.3.1 Cell surface receptors

Usually cell surface receptors are transmembrane proteins with extracellular, transmembrane and intracellular domains. An extracellular ligand binds to the extracellular domain of the receptor, changing the conformation of the transmembrane domain which in turn relays the effect to signaling proteins associated with the intracellular domain, without the need of internalizing the ligand. Cell surface receptors can be categorized into three classes based on their mode of relaying extracellular signal to the internal proteins of a cell, namely, ion-channel-linked receptor, G-protein-linked receptor and enzyme-linked receptor. These are expressed in very low numbers varying between a few hundred and few thousand per cell [71].

2.3.1.1 Ion-channel-linked receptors

These receptors are usually associated with neuronal signaling in excitable cells such as neurons, muscle cells and touch receptor cells where chemical signal (e.g., acetylcholine) or mechanical signal (e.g., touch) is converted to electrical signal. Ion-channel linked receptors are multimeric transmembrane proteins that undergo conformational change when a ligand binds to them such that an opening is created through the cell membrane to allow passage of ions such as sodium (Na^+) and potassium (K^+) as shown in Figure 6 (A). Flow of ions through the channel in the receptor alters the charge across the cell membrane thereby creating an electrical signal. These receptors are specific with regard to the type of ion that flows through their opening. The ions channels are open only for few milliseconds, past which the ligands dissociate from the receptor

and the ion channels enter a resting stage, unresponsive to signals for a short period of time.

2.3.1.2 G-protein-linked receptors

These receptors are also called seven transmembrane domain receptors (7TM receptors) as they traverse the cell membrane seven times, as shown in Figure 6 (B). The commonly known ligands for this receptor are hormones, neurotransmitters and pheromones. Most of the chemokine receptors, for example, receptor for IL-8 (CXCR1) is of this type [72]. The receptor is associated with 3 G proteins, α, β and γ that are physically connected in a preformed complex. In an unstimulated state, the receptor and G proteins are inactive. Extracellular ligand binding induces conformational change of the receptor which in turn alters conformation of α subunit that allows it to exchange its guanosine-diphosphate (GDP) for guanosine-triphosphate (GTP). Activated α subunit separates from βγ complex, both of which can then activate target proteins in the plasma membrane. After α subunit activates its target proteins, it inactivates itself by hydrolyzing its bound GTP to GDP. Inactive α subunit then re-associates with βγ to form an inactive G protein.

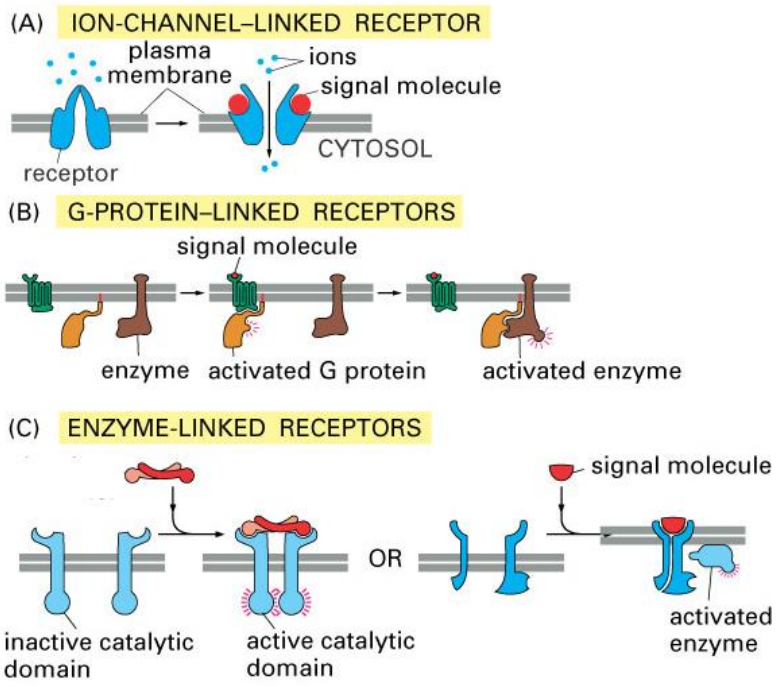

Figure 6. Different cell surface receptors found in mammals. (A) Ion-channel-linked receptor, (B) G- coupled receptor, (C) Enzyme-linked receptor [73].

2.3.1.3 Enzyme-linked receptors

Enzyme-linked receptors are composed of single or multiple polypeptide domains that span the cell membrane once as shown in Figure 6 (C). The characteristic feature of these receptors are the association of their cytosolic domain with intracellular enzymes that either phosphorylate (kinase enzyme) or de-phosphorylate (phosphatase enzyme) proteins that are involved in the specific signal transduction pathway activated by the corresponding ligand. Most of the cytokine receptors that influence immune regulation are usually of the enzyme-linked type. Toll-like receptors (TLR) and TGFβ receptors are

examples of enzyme-linked receptors. Since the late 1980s, studies pertaining to cytokine receptors have significantly increased, owing to the successful large-scale bioprocessing and synthesis of recombinant cytokines [71]. In recent years, cytokine receptors have gathered considerable attention from investigators as their deficit in cells has been directly co-related to several immunodeficiency disorders due to alteration in signal transduction.

2.3.2 Cytokines as extracellular messenger molecules

Cytokines are important extracellular messenger molecules that constitute an integral part of immune response in vertebrates. Some of the cytokines that have been studied in this research work are TNF-α, IL-8 and IL-10.

2.3.2.1 Tumor necrosis factor alpha (TNF-α)

TNF-α is one of the most prominent pro-inflammatory cytokines that influences innate and adaptive immune responses. It belongs to the TNF superfamily of proteins that is composed of 19 members and 29 corresponding receptors which are characterized by cysteine rich residues in the extracellular domain [74]. It is known to be synthesized by macrophages, T lymphocytes, B lymphocytes, smooth muscle cells, endothelial cells, epithelial cells, adipocytes as well as fibroblasts [75]. In 1893, Coley *et al.* reported tumor necrotic activities of a biological factor in cancer patients who were exposed to several bacterial infections [76]. In 1975, Carswell *et al*. [77] reported that the tumor necrotic factor was TNF, currently known as TNF-α, a glycoprotein that is released into the blood in response to endotoxin (lipopolysaccharide from *Escherichia coli*) treatment of mice

already primed with *mycobacterium bovis* strain Bacillus Calmette-Guérin (BCG) inoculation. Carswell *et al*. conjectured that TNF-α might be secreted by activated macrophages upon bacterial infection [77]. Later in 1985, Beutler *et al*. showed that TNF-α synthesis could be i by endotoxin alone in absence of pathogen priming [78] and is secreted at detectable levels two hours post endotoxin stimulation. Lot of research has since been done on TNF-α and is currently considered a canonical pro-inflammatory signal that is associated with the pathogenesis of inflammatory bowel diseases [79,80].

TNF-α has a molecular weight of 17 kDa [81] and is usually found as a trimer in solution and when bound to its receptor [82]. TNF-α trimers are at least 8-fold more active and have higher receptor binding affinity than their monomeric counterparts. TNF-α has two kinds of receptors, TNFR1 (55kDa) and TNFR2 (75kDa) which trigger different pathways when activated by ligand binding [83]. Few decades back TNF-α was considered as one of the candidates for cancer therapy due to its cytocidal effects on tumors [84]. However, clinical trials could not be completed owing to its systemic toxicity at effective concentrations [85]. Recently it has been reported to play a significant role in etiology of type II diabetes, cancer, auto-inflammatory and autoimmune disorders [74]. TNF-α is a classical pro-inflammatory cytokine and prototypical activator of transcription factor NF-κB, *de novo* synthesis of itself being induced by NF-κB, thereby indicating a positive feed-back effect on its own production. TNF-α production has been shown to be inhibited by anti-inflammatory IL-10 [86].

2.3.2.2 Interleukin 8 (IL-8)

Cytokines that induce migration or "chemotaxis" of cells are called chemokines. Interleukin-8 (IL-8) is a chemokine that is secreted by macrophages, epithelial cells, endothelial cells and smooth muscle cells in response to an inflammatory signal. IL-8 is among the first chemokines identified and is also known as *neutrophil chemotactic factor* due to its function as an inducer of neutrophil, basophil and T lymphocyte migration towards the site of infection [87] . In addition, IL-8 also induces migrated cells to phagocytize invading pathogens. The characteristic feature of most chemokines is the presence of four cysteine residues and on the basis of the motif displayed by first two cysteine residues, they are categorized into four classes, namely, CXC (alpha), CC (beta), C (gamma) and CX3C (delta) [88]. IL-8 belongs to the CXC chemokine family comprising four members [87]. Chemokine receptors are usually of the G-protein coupled type, of which CXCR1 and CXCR2 bind IL-8 [88]. The synthesis of IL-8 is primarily regulated by transcription factor NF-κB [87]. However, response element pertaining to nuclear factor-interleukin 6 (NF-IL-6) has been characterized in the promoter region of IL-8 gene [89]. IL-8 is synthesized as a 99 amino acid peptide and is proteolysed to form several isoforms among which peptides comprising 72 (in immune cells) and 77 (in non-immune cells) amino acids are most biologically relevant [87]. IL-8 has a molecular weight of 8 kDa and readily forms homodimer and even oligomers at higher concentrations in solution [90]. However, IL-8 monomer is the active form of the chemokine and is recognized by the receptor in the monomeric form [90,91]. Inflammatory signals such as TNF-α, IL-1, IL-6, lipopolysaccharide, reactive oxygen species and other cellular stresses can induce

synthesis and secretion of IL-8 whereas, IL-4 and IL-10 can inhibit IL-8 synthesis [87]. IL-8 has been reported to be involved in the pathogenesis of cancer autoimmune, inflammatory and infectious diseases [87,92].

2.3.2.3 Interleukin 10 (IL-10)

IL-10 belongs to the IL-10 family of cytokines (consisting of nine members, e.g., IL-19, IL-20, IL-22, IL-24), members of which are closely related to interferon (IFN) family of cytokines [93]. IL-10 is a prominent anti-inflammatory cytokine that can repress pro-inflammatory responses by inhibiting synthesis of pro-inflammatory cytokines such as TNF-α and IL-8 [86,87]. IL-10 is mainly secreted by dendritic cells, macrophages, natural killer cells, mast cells, neutrophils, eosinophils, T lymphocytes (notably T_{reg} cells) and B lymphocytes and targets primarily leukocytes [93]. IL-10 was first identified in 1989 and reported by Fiorentino *et al*. as a "cytokine synthesis inhibitory factor (CSIF)", based on its ability to inhibit synthesis of pro-inflammatory cytokines such as IL-2, IL-3, TNF-α, IFN-γ and granulocyte-macrophage colony stimulating factor (GM-CSF) [94]. Mature human and mouse IL-10 comprises 160 amino acids and binds to a chain of two receptors, IL-10R1 and IL-10R2 [93]. The association of IL-10 with IBD was first established in 1993 by Kühn *et al*. [95] where IL-10-deficient mice ($Il10^{-/-}$) showed normal immune response during development but spontaneously developed colitis, marked by abnormal mucosal architecture and infiltration of leukocytes. This showed that bowel inflammation is a manifestation of uncontrolled immune response triggered by enteric antigens and IL-10 is an essential immunomodulator, especially for the gastro-intestinal

tract. Unlike other members of the IL-10 family of cytokines, IL-10 itself is prominent mainly during the recovery phase of inflammation and repairs cellular damage caused due to inflammation [93]. IL-10 activates transcription factor signal transducer and activator of transcription 3 (STAT3) and activated STAT3 itself triggers IL-10 transcription indicating a possible positive feed-back effect on IL-10 synthesis.

2.3.3 Transcription factors in mammalian signal transduction

According to the human genome sequencing data published in 2004, there are approximately 24,000 genes that encode proteins [96]. Gene expression is tightly controlled at multiple levels, and transcription factors are one such regulatory mechanism. Transcription factors are regulatory proteins that induce transcription of specific genes when activated by corresponding signals. They can regulate genes involved in immune response, growth, proliferation and other physiological functions of the body. Monitoring activation of transcription factors by corresponding stimuli gives a measure of the dynamics of the signal transduction pathway.

2.3.3.1 Nuclear factor-kappa B (NF-κB)

Nuclear factor-kappa B (NF-κB) is a transcription factor that is found in almost all cell types and is known to mediate pro-inflammatory responses. It promotes anti-apoptotic functions, thereby maintaining tumors. In 1986, Sen *et al*. [97] discovered NF-κB in B-cell tumors as a factor that bound to κ light chain enhancer with a sequence of GGGACTTTCC. In a follow-up study, Sen *et al*. [98] reported that lipopolysaccharide (LPS) or phorbol ester could induce activation of NF-κB in absence of protein synthesis, indicating NF-κB to be present in an inactive form prior to LPS stimulation. In 1988, Baeuerle *et al*. [99] described an inhibitory protein (IκB) that binds to cytoplasmic NF-κB and sequesters its activity. Baeuerle *et al*. also reported that phorbol ester treatment of lymphoblastoids could induce dissociation of inactive NFκB-IκB complex, thereby releasing NF-κB that can translocate into the nucleus to activate target genes as shown in Figure 7. NF-κB is a pivotal transcription factor and has been reported to be involved in in the pathogenesis of chronic inflammatory diseases [100]. NF-κB works in concert with other transcription factors to mediate immune responses in host cells.

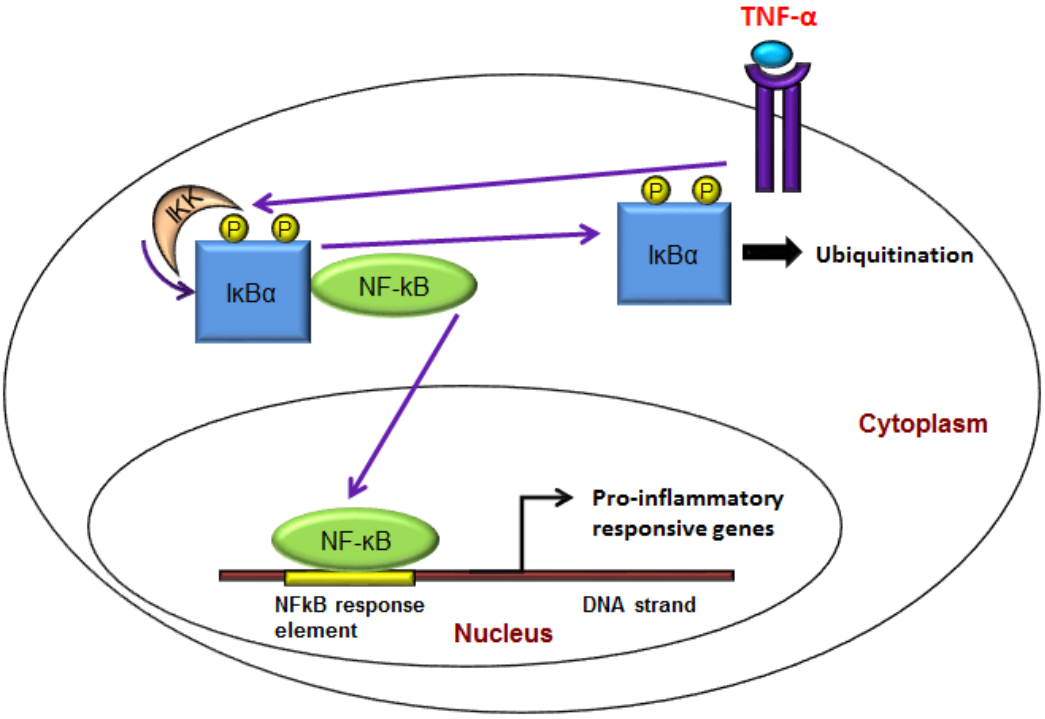

Figure 7. Schematic representation of signal transduction pathway mediated by nuclear factor kappa B (NF-κB).

2.3.3.2 Aryl hydrocarbon receptor (AHR)

Aryl hydrocarbon receptor is a cytosolic ligand activated transcription factor that is known to bind to a large number of exogenous aromatic hydrocarbons such as dioxins, polyclyclic aromatic hydrocarbons (PAH), plant flavonoids and polyphenolics. The prototypic ligand for AHR is 2,3,7,8-tetracholorodibenzo-p-dioxin (TCDD, a by-product of industrial synthesis of herbicide) [101] and is known to regulate xenobiotic degrading enzymes such as cytochrome P450. AHR has been reported to be involved in regulatory T cell (T_{reg}) differentiation and down regulation of pro-inflammatory responses and use of

natural AHR ligands (for example, plant flavonoids) have been reported as potential therapeutics for inflammatory disorder [102]. Microbiota-derived indole is an aromatic hydrocarbon and due to its structural similarity with AHR ligand TCDD as shown in Figure 8 it is hypothesized that indole could be a potential ligand for AHR and mediate immunoregulation of host through AHR activation.

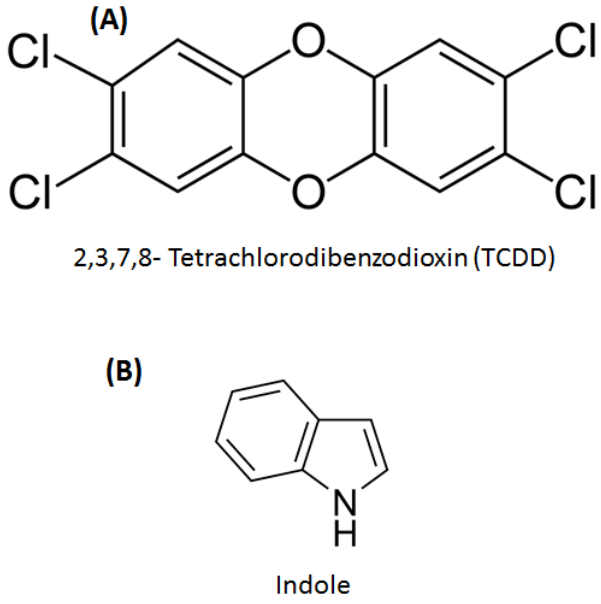

Figure 8. Aromatic ligands for aryl hydrocarbon receptor (AHR)
(A) 2,3,7,8-tetrachlorodibenzodioxin (TCDD) – canonical AHR ligand; (B) indole – potential AHR ligand.

AHR belongs to PAS (Per-ARNT-Sim) domain of the family of basic-helix-loop-helix (bHLH) transcription factors [103]. AHR is sequestered in the cytoplasm as an inactive complex with a 90kDa heat shock protein (HSP90), XAP2 and p23 in absence of a ligand [101]. The prototypic ligand for AHR is 2,3,7,8-tetracholorodibenzo-p-dioxin (a by-product of industrial synthesis of herbicide) [101]. AHR signaling is tightly controlled by the chaperon proteins (HSP90, XAP2 and p23) and AHR nuclear translocator (ARNT). HSP90 helps mask the constitutive DNA binding affinity of AHR and maintains the receptor in a conformation that promotes high ligand binding affinity. XAP2 prevents ubiquitination of AHR prior to ligand binding and p23 prevents nuclear translocation of AHR complex and non-specific binding to ARNT in absence of bound ligand. Ligand binding causes conformational change in AHR complex (comprising AHR, three chaperon proteins and a ligand) that facilitates binding of importin β to the corresponding nuclear localization signal (NLS) which in turn promotes nuclear translocation of the complex. In the nucleus, ARNT binding to AHR complex induces dissociation of chaperon proteins and AHR-ARNT complex then binds to the corresponding DNA response elements in the promoter regions of their responsive genes that encode xenobiotic metabolizing enzymes such as CYP1A1 [101] (Figure 9).

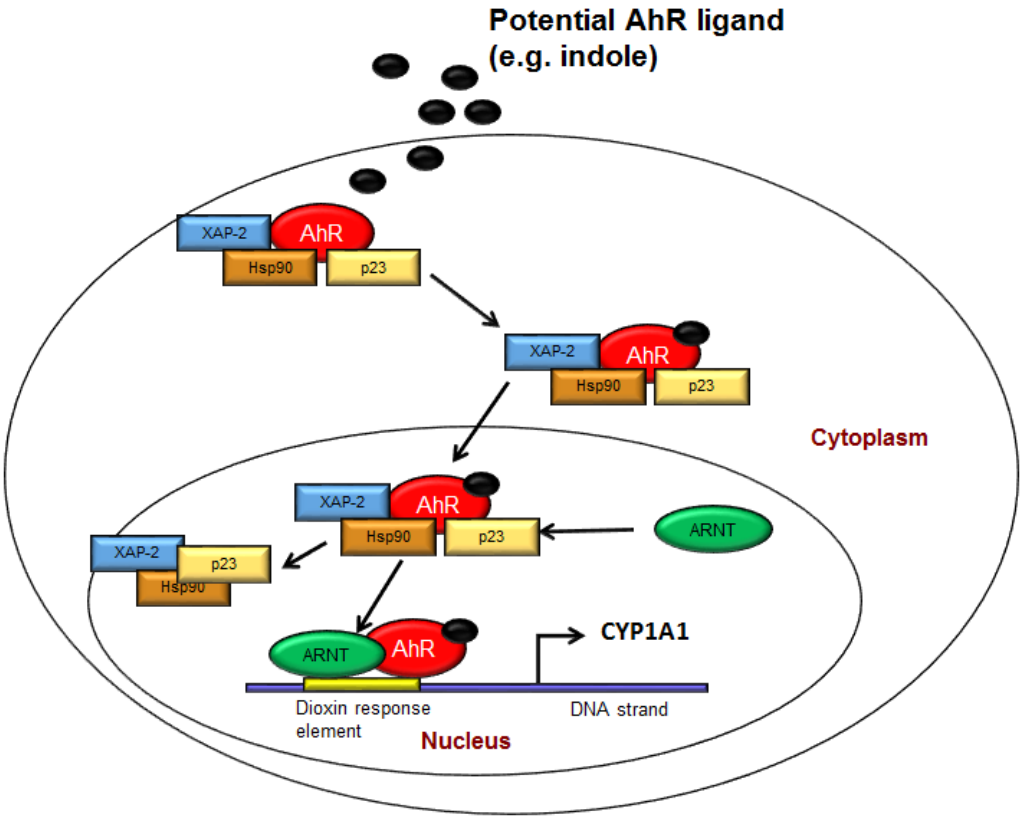

Figure 9. Schematic representation of signal transduction pathway mediated by aryl hydro carbon receptor (AHR).

The main focus of this dissertation is to develop quantitative models that can predict dynamics of transcription factors and cytokines involved in signal transduction pathways triggered by bacterial components lipopolysaccharide (gram negative bacteria) and indole (derived from indigenous bacteria upon tryptophan metabolism and representing microbiota metabolism). The next chapter gives an overview of systems biology approach towards studying mammalian immune response and host-microbiota interactions by integrating experimental and mathematical techniques.

CHAPTER III

SYSTEMS BIOLOGY APPROACH TOWARDS STUDYING MAMMALIAN IMMUNE RESPONSE

3.1 MATHEMATICAL MODELING OF SIGNAL TRANSDUCTION PATHWAYS

Systems biology is the quantitative study of biological interactions through integration of mathematical modeling and experimental measurements with the goal of being able to predict biological responses and outcomes. Model predictions and experimental measurements follow a cyclical loop where each is refined by the other (Figure 10). Model predictions can be used to design experiments whereas experimental data can validate and estimate model parameters

Systems biology is a holistic study of biological systems as opposed to the reductionist approach and hence aims at studying a network of both extra- and intracellular interactions. Systems biology has evolved from the integration of complex biological interactions with simultaneous developments in high throughput technologies for data acquisition (e.g., genome sequencing, as shown in top line of Figure 11) and the identification of intricate networks in single and multi-cellular organisms (as shown in the bottom line of Figure 11).

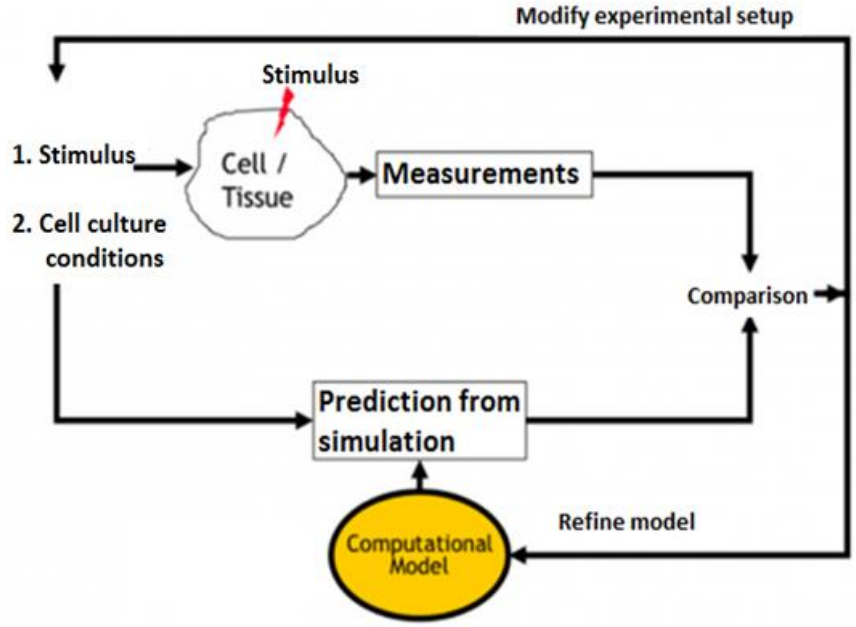

Figure 10. Systems biology: integration of computational model predictions and experimental measurements.

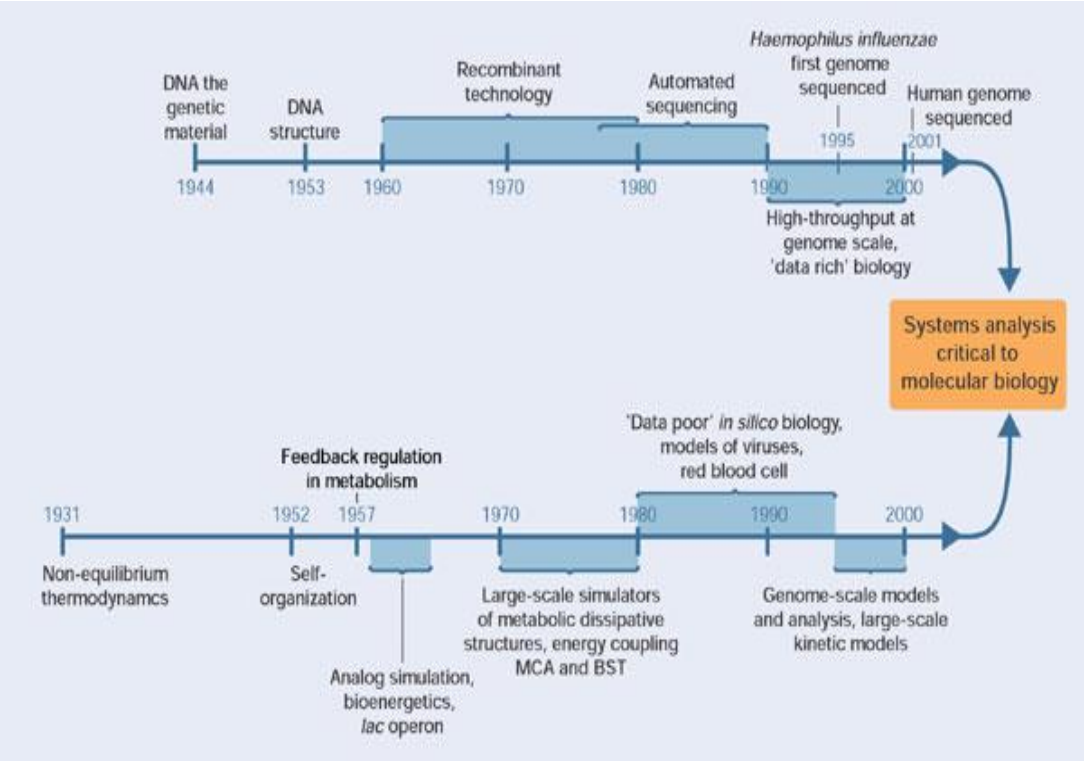

Figure 11. History of systems biology [104].

Cellular networks in biological systems can be broadly classified into three categories, namely, signal transduction pathways, metabolic networks and gene regulatory networks [105-107]. Signal transduction pathway refers to the steps involved in extra cellular stimulus initiating intracellular cascade of biochemical reactions (activation/deactivation of transcription factors) and altering cellular functions (through gene expression). Metabolic networks involve conversion of small biomolecules (that serve as carbon and nitrogen sources) to produce energy and intermediate products that are critical for cell survival and growth. Gene regulatory networks on the other hand deal with interaction of proteins (such as transcription factors) with DNA to induce gene expression. All three constitute integral parts of an organism and are highly interconnected to facilitate proper functioning of a cell. For example, energy derived from metabolic networks is essential to carry out signal transduction which in turn influences gene regulatory networks depending on the extracellular stimulus.

Signal transduction is instantaneous and downstream effects are observed rapidly. For example cytoplasmic NF-κB gets activated within five minutes of extracellular stimulation [108]. Hence information about transient dynamics of activated proteins in signal transduction pathway is important to understand how the signaling pathway contributes to cellular responses. Elucidating signal transduction pathways involved in immune responses is non-trivial due to the sheer complexity and highly evolved interconnectivity between biomolecules. One extracellular stimulus can activate multiple signaling pathways; conversely, several extracellular molecules can activate the same signaling pathway as well. This complexity makes it extremely difficult to establish cause-

and-effect relationships. Hence integration of mathematical modeling and experimental validation is needed to bridge the gap between what is already known and what needs to be known about signal transduction in highly complex organisms such as mammals.

Several aspects of single signal transduction pathways have been fully understood till now because of the unavailability of experimental data or techniques to experimentally investigate certain biochemical reactions. However, computational models serve as a promising substitute for unexplored areas of experimental biology. Certain biochemical reactions in signal transduction pathways are so rapid that they are difficult to be monitored experimentally. However, computational models that can predict the nature of the reaction would be a good complement to experimental studies. Computational models are currently used in pharmaceutical industries to predict the feasibility of specific drugs or help select the right candidates for clinical trials, which eliminates the need for expensive experimental data.

Though pro-inflammatory immune responses have been studied using computational models [31,107-109], no significant work has been done with respect to integrating pro- and anti-inflammatory responses which underlies homeostasis in our body. Mathematical modeling has attracted attention from systems biology researchers not only to help design experiments but also to predict their outcomes. Some of the common computational approaches to study biological systems are ordinary differential equations, Bayesian networks, Boolean networks and fuzzy logic [110]. Bayesian and Boolean networks are usually used to represent and predict steady state data for metabolic and gene regulatory networks [111]. However, ordinary differential equations are used in transiently

dynamic signal transduction models [31,112]. A good understanding of signal transduction pathways and quantitative predictions from model simulations can help study the feasibility of certain therapeutic molecules. This dissertation focuses at studying dynamic pro- and anti-inflammatory responses and how it might be regulated by host-microbiota interactions using ordinary differential equation models.

3.1.1 Ordinary differential equations (ODE) for component balance

Dynamic profiles of components in a signal transduction pathway can be quantitatively predicted using non-linear ordinary differential equation (ODE) models. ODEs in such cases represent concentration balance for different components involved in the particular signaling pathway. The ODEs are usually of the form:

$$\frac{dx}{dt} = f(x, u, p) \tag{3.1}$$

where *x* is a vector of states (concentrations of biological components), *u* is a vector of inputs (stimulus) and *p* is a vector of parameters (reaction rate constants).

The cell is considered a single batch reactor where biochemical reactions take place. Equation 3.1 represents the rate of change of the concentration of component 'x' at the rate 'p' under the effect of stimuli 'u'. Component balance in signal transduction pathways are represented in two forms:

- **Mass action kinetics** where the rate of change of a component depends on the rate of production and rate of consumption, as shown in equation (3.2)

$$\frac{dx_i}{dt} = \sum \nu_{i_{produced}} - \sum \nu_{i_{consumed}} \tag{3.2}$$

Where, $\nu_{i_{produced}}$ and $\nu_{i_{consumed}}$ are the rates of component x_i production and consumption respectively, following chemical kinetics of reactions it is involved with. Most of the biochemical reactions, for example, activation of transcription factor NF-κB under pro-inflammatory stimulus (as described in Chapter II) are represented in mass action kinetics form.

- **Michaelis-Menten kinetics** is used to represent the process of gene expression (transcription) induced by transcription factor binding to the promoter region of the target gene. The enzyme kinetics of invertase as described in [113] is the basis for ODE models comprising mass action kinetics and Michaelis-Menten kinetics.

3.2 REVIEW OF SOME SIGNAL TRANSDUCTION AND HOST-MICROBIOTA INTERACTOME MODELS

A large number of databases are readily available online to refer to the different biochemical reactions taking place in physiological processes. Some popular databases are BioCarta (http://www.biocarta.com), BioCyc (www.biocyc.org), and KEGG (http://www.genome.jp/kegg/pathway.html). Mathematical models written in Systems Biology Makeup Language (SBML) are also available online for reference purposes (http://www.ebi.ac.uk/biomodels-main/). Among the pro-inflammatory transcription factors, TNF-α-induced activation of NF-κB is most widely studied and computationally modeled [31,32,108,112]. Lipniacki *et al*. [31], and Rangamani *et al*. [112], developed deterministic models comprising the cascade of intra-cellular biochemical reactions that are initiated by pro-inflammatory TNF-α signal. Moya *et al*. [114] developed a mathematical model that describes signal transduction pathways initiated by extracellular IL-6 (pro-inflammatory) and IL-10 (anti-inflammatory) signals, both targeted towards activation of transcription factor STAT3 in human hepatic cells. This was the first model that integrated pro- and anti-inflammatory responses in mammalian cells.

With the growing knowledge of intricate relationship shared by mammals and their intestinal microbiota, several experimental studies have been directed towards investigating complex host-microbiota interactions. Alteration in the intestinal microbiota population has been linked to the pathogenesis of intestinal bowel disease, obesity, and allergic reactions (as discussed in Chapter II). Several genome-scale metabolic models (GSMM) using big data sets have integrated knowledge of genes, reactions and metabolic

pathways in human intestinal microbiota and information about host and microbial metabolism and signaling to investigate metabolic pathways involved in digestion of polysaccharides and proteins in the gastro-intestinal tract by microbiota and in turn generation of small chain fatty acids such as acetate, propionate and butyrate [115,116].

Marino *et al*. [117] developed a mathematical model to study inter-population interactions among murine microbiota. Their model is based on co-relation analysis of data obtained from laboratory colonization of germ-free mice with cecal contents of a mature mouse. The model simulations predict a lack of mutualistic interactions with in a community of bacteria with significant parasitic interactions observed among the members of Bacteroidetes and competition among Firmicutes. Thus computational models based on metagenomics can elucidate interspecies interactions of intestinal microbiota that might have a potential contribution to host metabolism and transition from health to disease.

Most of the computational models of studying host-microbiota interactions focus on metabolic pathways because of the availability of huge sets of metagenomic data and genome-scale metabolic models for some bacteria [118]. Research focused on studying the effect of intestinal microbiota on host immune responses (as discussed in Chapter II). Several host-pathogen computational models have been developed to study molecular mechanisms involved in the interactions between host and pathogenic micro-organisms while transitioning from health to disease in cases of HIV [119], malaria [120], tuberculosis [121] and influenza [122]. However, to our knowledge, no mathematical models have yet been developed to investigate the complex host-microbiota interactions that are essential in maintaining mucosal homeostasis (in the gastro-intestinal tract) and

alteration of which can lead to pathogenesis of inflammatory diseases. This is because the signal transduction pathways activated by bacterial metabolites in hosts are poorly understood.

This dissertation focuses at investigating a possible molecular mechanism involved in host-microbiota interactions through indole-induced signaling and its effect on host immune responses and homeostasis. Immune homeostasis in host is essentially regulated by maintaining a balance between pro- and anti-inflammatory responses and their positive/negative feed-back regulatory loops. Chapter IV describes a mathematical model that is developed to study pro- and anti-inflammatory immune responses and feed-back effects of host macrophages to maintain homeostasis under a continuous inflammatory signal from gram negative bacteria-derived lipopolysaccharide (LPS). Chapter V expands this by including for the first time signaling effects mediated by a bacterial metabolite indole.

CHAPTER IV

MATHEMATICAL MODELING OF PRO- AND ANTI-INFLAMMATORY IMMUNE RESPONSES IN MACROPHAGES*

4.1 OVERVIEW

Inflammation is a beneficial mechanism that is usually triggered by injury or infection and is designed to return the body to homeostasis. However, uncontrolled or sustained inflammation can be deleterious and has been shown to be involved in the etiology of several diseases, including inflammatory bowel disorder and asthma. Therefore, effective anti-inflammatory signaling is important in the maintenance of homeostasis in the body. However, the inter-play between pro- and anti-inflammatory signaling is not fully understood. In the present study, we develop a mathematical model to describe integrated pro- and anti-inflammatory signaling in macrophages. The model incorporates the feedback effects of *de novo* synthesized pro-inflammatory (tumor necrosis factor α; TNF-α) and anti-inflammatory (interleukin-10; IL-10) cytokines on the activation of the transcription factor nuclear factor -κ B (NF-κB) under continuous lipopolysaccharide (LPS) stimulation (mimicking bacterial infection). In the model, IL-10 upregulates its own production (positive feedback) and also downregulates TNF-α production through NF-κB (negative feedback). In addition, TNF-α upregulates its own

*Reprinted with permission from "Mathematical modeling of pro- and anti-inflammatory signaling in macrophages" by Maiti, S.; Dai, W.; Alaniz, R.; Hahn, J.; Jayaraman, A., 2014. *Processes*, 3, 1-18, Copyright 2014 by MDPI.

production through NF-κB (positive feedback). Eight model parameters are selected for estimation involving sensitivity analysis and clustering techniques.

We validate the mathematical model predictions by measuring phosphorylated NF-κB, *de novo* synthesized TNF-α and IL-10 in RAW 264.7 macrophages exposed to LPS. This integrated model represents a first step towards modeling the interactions between pro- and anti-inflammatory signaling.

4.2 INTRODUCTION

Inflammation is a beneficial self-defense mechanism that is initiated by the body to eliminate pathogens and prevent the spread of infection [123]. The inflammatory responses to pathogens and other inflammatory stimuli are mediated by innate (dendritic cells and macrophages) and adaptive immune cells (T-cells and B-cells) [124]. Immune cells have transmembrane receptors called Toll-like receptors (TLR) that recognize foreign molecules based on pathogen-associated molecular patterns (PAMPs), such as flagellin of bacterial flagella [39], lipopolysaccharide (LPS) of Gram-negative bacteria and peptidoglycan of Gram-positive bacteria [35]. Recognition of PAMPs by immune cells (such as macrophages) triggers the *de novo* synthesis and secretion of pro-inflammatory cytokines, which leads to the recruitment of phagocytic cells, such as neutrophils [125], for eliminating pathogens. While inflammation is a beneficial body response, unabated (chronic) inflammation is deleterious, as it can result in immune cells attacking other host cells. Chronic inflammation has been shown to be involved in the etiology of several diseases, including inflammatory bowel disease (IBD) [126] and

asthma [127]. Chronic inflammation can also arise in the absence of pathogen infection. Since the mucosal immune cells in the gastro-intestinal (GI) tract are in close proximity with intestinal microbiota [128], any alteration in the intestinal microbial community (*i.e.*, dysbiosis) can also lead to uncontrolled pro-inflammatory responses. This sustained inflammation in the absence of any infection has been shown to result in ulcerative colitis or Crohn's disease [126].

Nuclear factor –κ B (NF-κB) is an important transcription factor that plays a pivotal role in mediating inflammatory responses in immune cells, such as macrophages [129]. NF-κB is made up of two subunits, p50 and p65 [130], and is sequestered as an inactive complex in the cytosol by an inhibitor protein, IκBα [129]. When macrophages detect the presence of bacteria (by recognizing LPS) through their cell surface receptor, TLR4, an LPS-TLR4 complex is formed that triggers the activation of IκBα kinase (IKK), resulting in phosphorylation of IκBα-NFκB and subsequent ubiquitination and degradation of IκBα [129]. NF-κB, which is catalytically released from the inactive IκBα-NFκB complex, translocates into the nucleus and binds to response elements in the promoter region of its target genes to activate their transcription [129]. Several target genes with functions in inflammation and immune regulation have been identified for NF-κB [131], of which TNF-α and IL-10 are the most prominent pro- and anti-inflammatory cytokines, respectively [132-134]. In addition to TNF-α and IL-10, other NF-κB responsive genes that have significant NF-κB regulatory functions are IκBα (sequesters free NF-κB) [135] and A20 (inactivates IKK) [136]. However, NF-κB is not the only transcription factor that regulates IL-10 and TNF-α signaling and often acts in concert

with other transcription factors. For example, signal transducer and activator of transcription 3 (STAT3) is a well-studied transcription factor involved in IL-10 signaling [137,138]. STAT3 not only regulates transcription of IL-10, but is itself activated by IL-10 [139] and LPS [140] in a feedback manner. The effects of pro-inflammatory cytokines, such as TNF-α and IL-1β, are countered by signaling initiated by anti-inflammatory cytokines. IL-10 is a potent anti-inflammatory cytokine and suppresses the production of pro-inflammatory cytokines, like TNF-α [141], by downregulating NF-κB through inhibition of IKK activation and suppression of free phosphorylated NF-κB translocation from cytosol to nucleus [142,143].

Several computational models of inflammatory signaling have been previously developed. These include a model for the IL-6 signal transduction pathway by Singh *et al.* [144], the TNF-α signaling pathway by Huang *et al.* [32], Lipniacki *et al.* [31], Rangamani *et al.* [112] and Hoffmann *et al.* [108]. A characteristic feature of these models is that they describe the dynamics of signaling initiated by a single pro-inflammatory cytokine. Moya *et al.* [114] developed a mathematical model to represent interactions between IL-6 (pro-inflammatory) and IL-10 (anti-inflammatory) in hepatocytes when both of these cytokines were used as stimuli to the cells. The current work describes an interplay between *de novo* synthesized pro-inflammatory (TNF-α) and anti-inflammatory (IL-10) cytokines in macrophages exposed to LPS (Figure 12). Since the inter-play between the pro- and anti-inflammatory signaling in macrophages is poorly understood, our integrated model represents a first step towards modeling the interaction between pro- and anti-

inflammatory signaling mediators that is important in inflammation and maintaining homeostasis.

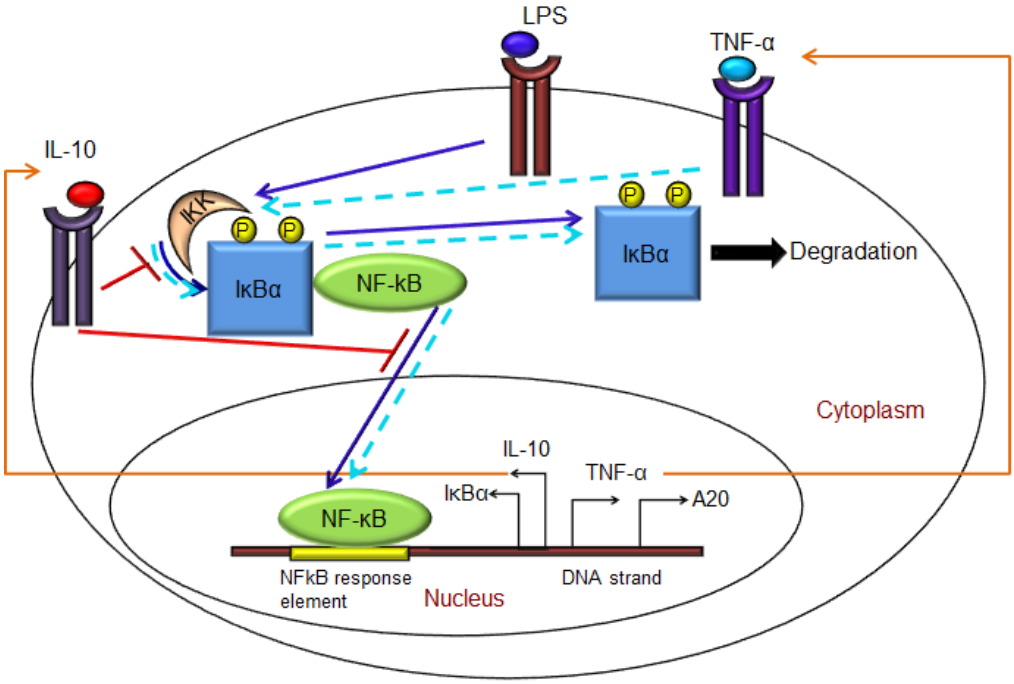

Figure 12. Schematic representation of LPS-induced signal transduction resulting in NF-κB activation and *de novo* synthesis of TNF-α and IL-10 in macrophages. LPS-induced NF-κB activation is indicated in solid blue arrows. TNF-α-induced positive feedback regulation of NF-κB is indicated in dashed cyan arrows, and IL-10-induced negative feedback regulation of NF-κB is indicated in solid red lines.

4.3 MATERIAL AND METHODS

4.3.1 Model formulation

The mathematical model presented in this paper is an integration of an inflammatory module and an anti-inflammatory module. The model is developed by representing biochemical reactions involved in the signal transduction pathway as a set of non-linear ordinary differential equations (ODEs) of the form:

$$\frac{dx}{dt} = f(x, u, p) \tag{4.1}$$

where x is a vector of states, u is a vector of inputs and p is a vector of parameters in equation 4.1. The model comprises 29 differential equations and 37 parameters. Each differential equation represents the rate of change of the concentration of a particular protein involved in the pathway.

The inflammatory (TNF-α) module is adapted from Huang *et al.* [32] and Lipniacki *et al.* [31]. While these models use TNF-α as the input, our model describes LPS (input)-induced signaling through TLR4 (LPS receptor), which leads to TNF-α production. Besides adding TLR4 to the model, the TNF-α receptor description is retained to represent the positive feedback of *de novo* synthesized TNF-α on NF-κB regulation. We have included a kinetic term for TNF-α mRNA transcription initiated by nuclear NF-κB and component balances for TNF-α in the cytoplasm and the supernatant. In addition, Lipniacki *et al.*, included TRADD, TRAF2, RIP-1, FADD, caspase-3 and caspase-8 proteins, which are left out of the model presented here, as we focus mainly on some of the key biochemical reactions involved in LPS-induced NF-κB activation, its effect on the

production of TNF-α and IL-10 and in turn, the role of these cytokines on the feedback regulation of NF-κB. The similarities between the model described in Lipniacki *et al.* [31], and our current ODE model lie in the formulation of the biochemical reactions involved in IKK activation, IκBα-NFκB phosphorylation, dissociation and nuclear transport of NF-κB, nuclear NF-κB-induced I*κ*Bα, A20 mRNA transcription, free NF-*κ*B sequestration by *de novo* synthesized I*κ*Bα and IKK inactivation by A20. We added a balance for phosphorylated IκBα, as it is known to degrade after dissociation from the IκBα-NFκB complex.

The anti-inflammatory (IL-10) module is adapted from the IL-6 and IL-10 model by Moya *et al.* [114]. Only the ODEs involved in IL-10 signaling through the IL-10 receptor (as mentioned in Moya *et al.* [114]) are included in the anti-inflammatory module of our current model to formulate the feedback effects of IL-10 on its own production (through positive feedback regulation of STAT3) and TNF-α production (through negative feedback regulation of NF-κB). Biochemical reactions, as described in Moya *et al.*, for STAT3 phosphorylation, dimerization and nuclear translocation to initiate transcription are retained in our current model. Transcription and translation of SOCS3 due to STAT3 and downstream biochemical reactions associated with SOCS3 are not included in the model presented here. A Michaelis–Menten-type kinetics for IL-10 transcription, initiated by the transcription factors, NF-κB and STAT3, and component balances for IL-10 in the cytoplasm and supernatant, have been included here.

Some values of the parameters and initial concentrations of proteins are adapted from the TNF-α signaling models by Huang *et al.* [32], Lipniacki *et al.* [31], Rangamani *et al.* [112], Hoffmann *et al.* [108] and the IL-6 and IL-10 model by Moya *et al.* [114]. The previously developed models consisted of 37 differential equations and 60 parameters for the TNF-α model by Huang *et al.* and 68 differential equations and 118 parameters for the IL-6 and IL-10 model by Moya *et al.* [114] Among the proteins included in these models, very few are quantifiable by experimental methods, making parameter estimation difficult. In our current integrated model, we have reduced the number of differential equations to 29 and the number of parameters to 37 by only focusing on the key proteins of the pathway. Using a smaller model increased parameter identifiability and simplified parameter estimation.

The ODE model is structurally divided into pro-inflammatory (TNF-α) and anti-inflammatory (IL-10) modules that are both initiated by LPS stimulation and NF-*κ*B activation.

Pro-Inflammatory Module:

1. Exogenous LPS binds to the cell surface receptor (TLR4).
2. LPS-TLR4 complex initiates activation of $IKK_{neutral}$ to IKK_{active}.
3. IKK_{active} phosphorylates I*κ*Bα-NFκB and initiates dissociation of the inactive IκBα-NFκB complex into phosphorylated IκBα and NF-κB species.
4. Free phosphorylated IκBα undergoes ubiquitination and degradation, whereas free cytoplasmic NF-κB translocates into nucleus.

5. Nuclear NF-κB binds to response elements in the promoter regions of TNF-α, IκBα and A20 genes and leads to transcription and translation of the corresponding proteins and subsequent secretion of TNF-α into the supernatant. *de novo* intracellular IκBα sequesters both free cytoplasmic and nuclear NF-κB by binding to them, and A20 catalyzes the change of IKK_{active} to the $IKK_{inactive}$ form.
6. Secreted TNF-α in the cell culture supernatant binds to its cell surface receptor to form a complex that initiates similar pathways as LPS, resulting in the production of more TNF-α through a positive feedback regulation on NF-κB.

Anti-Inflammatory Module:

1. Nuclear NF-κB binds to the IL-10 gene promoter and initiates transcription of IL-10 mRNA and subsequent translation into IL-10 protein in the cytoplasm, which gets secreted into the supernatant.
2. IL-10 secreted into the supernatant binds to its cell surface receptor, forming a ligand-receptor complex that inhibits activation of $IKK_{neutral}$ to IKK_{active} and translocation of activated free cytoplasmic NF-κB into the nucleus as well.
3. The IL-10 + receptor complex activates a second transcription factor, presumably STAT3, which, in turn, regulates transcription of the IL-10 gene in a feed-forward manner.

Below is the schematic representation of the implemented reaction network (Figure 13).

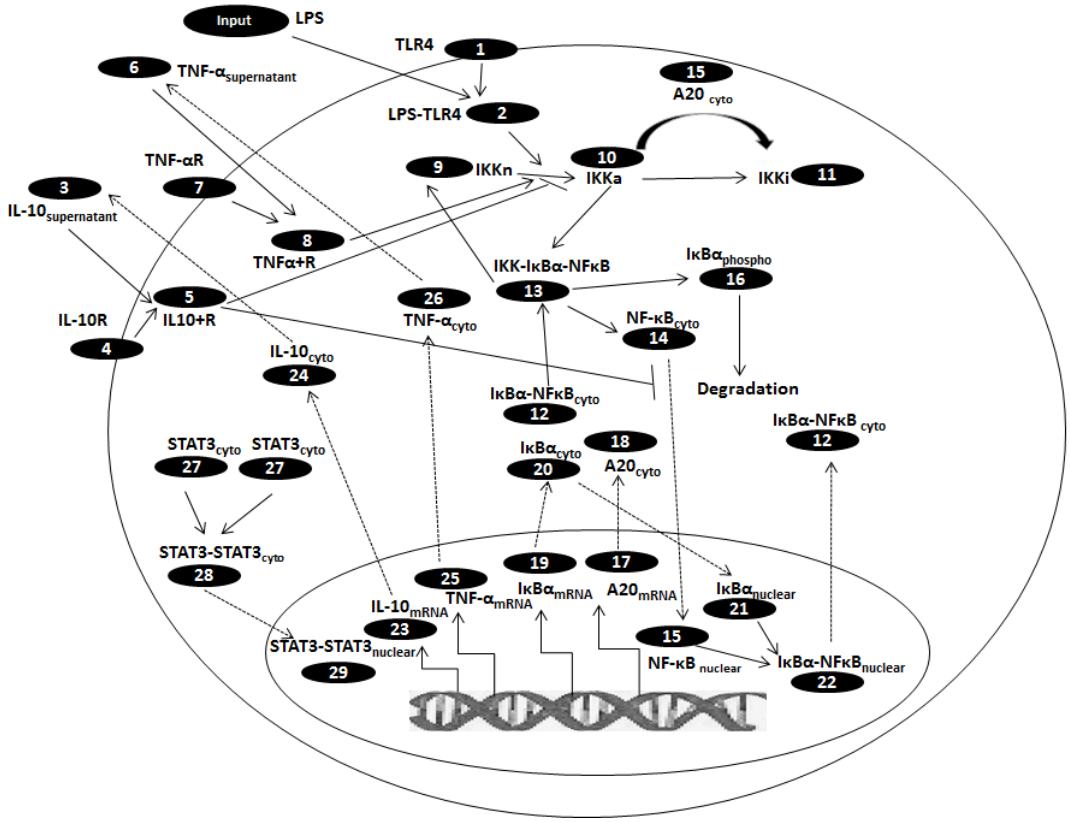

Figure 13. Implemented reaction network for LPS-induced NF-*κ*B signal transduction pathway with TNF-α (positive) and IL-10 (negative) feedback regulations.

Different LPS concentrations (0, 0.1, 1, 10 μg/mL) are used to stimulate the model. The IKK complex and NF-κB dimer (p50–p65) are considered as single proteins in the model. The signal transduction model comprises feedback regulatory loops involving TNF-α and IL-10. The positive feedback of TNF-α on its own production is represented by *de novo* TNF-α binding to its cell surface receptor, activating $IKK_{neutral}$ to IKK_{active}, leading to phosphorylation and dissociation of the IκBα-NFκB complex to release NF-κB,

which translocates to the nucleus to initiate transcription of TNF-α. IL-10 has a negative feedback effect on TNF-α production by inhibiting NF-κB activation (phosphorylation and dissociation), and the extent of this inhibition is calculated on the basis of the ligand bound IL-10 receptor complex (IL10-IL10R) concentration, which is represented as k_{in} as shown in equation 4.2.

$$k_{in} = \max\left[\left(1 - \frac{[\mathrm{IL10{-}IL10R}]}{[\mathrm{IL10{-}IL10R_{max}}]}\right), 0\right] \tag{4.2}$$

The maximum attainable concentration of IL10-IL10R is denoted by IL10-$IL10R_{max}$ with an assumed value of 2.56×10^{-6}. k_{in} is multiplied to factors that are inhibited by IL-10, such as IKK activation and nuclear translocation of free cytoplasmic NF-κB [142,143]. The higher the concentration of the IL10-IL10R complex, the lower will be the value of k_{in} and, hence, the lower will be the contribution of the terms mentioned above to the total outcome of NF-κB signaling, resulting in suppression of TNF-α production by IL-10. Positive feedback of IL-10 on its own production is represented by a set of differential equations that describe the IL-10 bound receptor complex phosphorylating transcription factor STAT3, which then dimerizes and translocates into the nucleus, binds to the promoter region of the IL-10 gene and initiates transcription of IL-10 mRNA and subsequent translation and secretion of IL-10 protein. The differential equations used in formulating the current model and the initial concentrations of the state variables (different components of the model) are shown in Table 1 and Table 2.

Table 1. Differential equations representing biochemical reactions involved in LPS-induced NF-κB signal transduction pathway, as used in the pro- and anti-inflammatory ODE model.

1.	$\frac{\mathrm{d[TLR4]}}{\mathrm{dt}} = -kf_1 \times [\mathrm{LPS}][\mathrm{TLR4}] + kr_1 \times [\mathrm{LPS-TLR4}]$
2.	$\frac{\mathrm{d[LPS-TLR4]}}{\mathrm{dt}} = kf_1 \times [\mathrm{LPS}][\mathrm{TLR4}] - kr_1 \times [\mathrm{LPS-TLR4}]$
3.	$\frac{\mathrm{d[IL-10_{sup}]}}{\mathrm{dt}} = -kf_2 \times [\mathrm{IL-10_{sup}}][\mathrm{IL-10R}] + kr_2 \times [\mathrm{IL10-IL10R}] + ksec_{IL10} \times [\mathrm{IL-10_{cyto}}] \times \frac{0.36}{200} - kdeg_{IL-10sup} \times [\mathrm{IL-10_{sup}}]$
4.	$\frac{\mathrm{d[IL-10R]}}{\mathrm{dt}} = -kf_2 \times [\mathrm{IL-10}][\mathrm{IL-10R}] + kr_2 \times [\mathrm{IL10-IL10R}]$
5.	$\frac{\mathrm{d[IL10-IL10R]}}{\mathrm{dt}} = kf_2 \times [\mathrm{IL-10_{sup}}][\mathrm{IL-10R}] - kr_2 \times [\mathrm{IL10-IL10R}]$
6.	$\frac{\mathrm{d[TNF-\alpha_{sup}]}}{\mathrm{dt}} = -kf_3 \times [\mathrm{TNF-\alpha_{sup}}][\mathrm{TNF-\alpha R}] + kr_3 \times [\mathrm{TNF\alpha\ -TNF\alpha R}] + ksec_{TNF\alpha} \times [\mathrm{TNF-\alpha_{cyto}}] \times \frac{0.36}{200} - kdeg_{TNF\alpha sup} \times [\mathrm{TNF-\alpha_{sup}}]$
7.	$\frac{\mathrm{d[TNF-\alpha R]}}{\mathrm{dt}} = -kf_3 \times [\mathrm{TNF-\alpha_{sup}}][\mathrm{TNF-\alpha R}] + kr_3 \times [\mathrm{TNF\alpha\ -TNF\alpha R}]$
8.	$\frac{\mathrm{d[TNF\alpha-TNF\alpha R]}}{\mathrm{dt}} = kf_3 \times [\mathrm{TNF-\alpha_{sup}}][\mathrm{TNF-\alpha R}] - kr_3 \times [\mathrm{TNF\alpha\ -TNF\alpha R}]$
9.	$\frac{\mathrm{d[IKK_n]}}{\mathrm{dt}} = -kfi \times k_{in} \times ([\mathrm{LPS-TLR4}] + [\mathrm{TNF\alpha\ -TNF\alpha R}]) \times [\mathrm{IKK_n}] + ti_3 \times [\mathrm{IKK_a} - \mathrm{I\kappa B\alpha NF\kappa B_{cyto}}]$ where, $k_{in} = \max[(1 - \frac{[\mathrm{IL10-IL10R}]}{[\mathrm{IL10-IL10R_{max}}]}), 0]$
10.	$\frac{\mathrm{d[IKK_a]}}{\mathrm{dt}} = kfi \times k_{in} \times ([\mathrm{LPS-TLR4}] + [\mathrm{TNF\alpha-TNF\alpha R}]) \times [\mathrm{IKK_n}] - kk_3 \times k_{in} \times [\mathrm{IKK_a}] \times [\mathrm{I\kappa B\alpha - NF\kappa B_{cyto}}] - kk_1 \times [\mathrm{IKK_a}] \times [\mathrm{A20_{cyto}}]$
11.	$\frac{\mathrm{d[IKK_i]}}{\mathrm{dt}} = kk_1 \times [\mathrm{IKK_a}] \times [\mathrm{A20_{cyto}}]$
12.	$\frac{\mathrm{d[I\kappa B\alpha-NF\kappa B_{cyto}]}}{\mathrm{dt}} = kf_4 \times [\mathrm{NF\kappa B_{cyto}}][\mathrm{I\kappa B\alpha_{cyto}}] + eni \times [\mathrm{I\kappa B\alpha - NF\kappa B_{nuclear}}] \times kv - kk_3 \times k_{in} \times [\mathrm{IKK_a}] \times [\mathrm{I\kappa B\alpha - NF\kappa B_{cyto}}]$
13.	$\frac{\mathrm{d[IKK_a-I\kappa B\alpha NF\kappa B_{cyto}]}}{\mathrm{dt}} = kk_3 \times k_{in} \times [\mathrm{IKK_a}] \times [\mathrm{I\kappa B\alpha - NF\kappa B_{cyto}}] - ti_3 \times [\mathrm{IKK_a - I\kappa B\alpha NF\kappa B_{cyto}}]$
14.	$\frac{\mathrm{d[NF\kappa B_{cyto}]}}{\mathrm{dt}} = -kf_4 \times [\mathrm{NF\kappa B_{cyto}}][\mathrm{I\kappa B\alpha_{cyto}}] + ti_3 \times [\mathrm{IKK_a - I\kappa B\alpha NF\kappa B_{cyto}}] - iln \times k_{in} \times [\mathrm{NF\kappa B_{cyto}}]$
15.	$\frac{\mathrm{d[NF\kappa B_{nuclear}]}}{\mathrm{dt}} = iln \times k_{in} \times \frac{[\mathrm{NF\kappa B_{cyto}}]}{\mathrm{kv}} - kf_4 \times [\mathrm{NF\kappa B_{nuclear}}][\mathrm{I\kappa B\alpha_{nuclear}}]$
16.	$\frac{\mathrm{d[I\kappa B\alpha_{phopsho}]}}{\mathrm{dt}} = ti_3 \times [\mathrm{IKK_a - I\kappa B\alpha NF\kappa B_{cyto}}] - kdeg_{I\kappa B\alpha} \times [\mathrm{I\kappa B\alpha_{cyto}}]$
17.	$\frac{\mathrm{d[A20_{mRNA}]}}{\mathrm{dt}} = Sm \times p \times \frac{[\mathrm{NF\kappa B_{nuclear}}]}{\mathrm{C}+[\mathrm{NF\kappa B_{nuclear}}]} - Dm \times [\mathrm{A20_{mRNA}}]$
18.	$\frac{\mathrm{d[A20_{cyto}]}}{\mathrm{dt}} = a20_{trans} \times [\mathrm{A20_{mRNA}}] - kdeg_{A20} \times [\mathrm{A20_{cyto}}]$
19.	$\frac{\mathrm{d[I\kappa B\alpha_{mRNA}]}}{\mathrm{dt}} = Sm \times p \times \frac{[\mathrm{NF\kappa B_{nuclear}}]}{\mathrm{C}+[\mathrm{NF\kappa B_{nuclear}}]} - Dm \times [\mathrm{I\kappa B\alpha_{mRNA}}]$
20.	$\frac{\mathrm{d[I\kappa B\alpha_{cyto}]}}{\mathrm{dt}} = -kf_4 \times [\mathrm{NF\kappa B_{cyto}}][\mathrm{I\kappa B\alpha_{cyto}}] + i\kappa b\alpha_{trans} \times [\mathrm{I\kappa B\alpha_{mRNA}}] - iki \times [\mathrm{I\kappa B\alpha_{cyto}}] + eki \times [\mathrm{I\kappa B\alpha_{nuclear}}] \times kv$

Table 1. Continued.

21. $\frac{\mathrm{d[I\kappa B\alpha_{nuclear}]}}{\mathrm{dt}} = -kf_4 \times [\mathrm{NF\kappa B_{nuclear}}][\mathrm{I\kappa B\alpha_{nuclear}}] + iki \times \frac{[\mathrm{I\kappa B\alpha_{cyto}}]}{\mathrm{kv}} - eki \times [\mathrm{IkB\alpha_{nuclear}}]$
22. $\frac{\mathrm{d[I\kappa B\alpha - NF\kappa B_{nuclear}]}}{\mathrm{dt}} = kf_4 \times [\mathrm{NF\kappa B_{nuclear}}][\mathrm{I\kappa B\alpha_{nuclear}}] - eni \times [\mathrm{I\kappa B\alpha - NF\kappa B_{nuclear}}]$
23. $\frac{\mathrm{d[IL-10_{mRNA}]}}{\mathrm{dt}} = 0.4 \times Sm \times p \times \frac{[\mathrm{NF\kappa B_{nuclear}}]}{\mathrm{C}+[\mathrm{NF\kappa B_{nuclear}}]} + 0.6 \times Sm\_il10 \times p \times \frac{[\mathrm{STAT3_{nuclear}}]}{\mathrm{C\_STAT3}+[\mathrm{STAT3_{nuclear}}]} - Dm \times [\mathrm{IL-10_{mRNA}}]$
24. $\frac{\mathrm{d[IL-10_{cyto}]}}{\mathrm{dt}} = il10_{trans} \times [\mathrm{IL-10_{mRNA}}] - ksec_{IL10} \times [\mathrm{IL-10_{cyto}}] - Dn \times [\mathrm{IL-10_{cyto}}]$
25. $\frac{\mathrm{d[TNF-\alpha_{mRNA}]}}{\mathrm{dt}} = Sm \times p \times \frac{[\mathrm{NF\kappa B_{nuclear}}]}{\mathrm{C}+[\mathrm{NF\kappa B_{nuclear}}]} - Dm \times [\mathrm{TNF-\alpha_{mRNA}}]$
26. $\frac{\mathrm{d[TNF-\alpha_{cyto}]}}{\mathrm{dt}} = tnf\alpha_{trans} \times [\mathrm{TNF-\alpha_{mRNA}}] - ksec_{TNF\alpha} \times [\mathrm{TNF-\alpha_{cyto}}] - Dn \times [\mathrm{TNF-\alpha_{cyto}}]$
27. $\frac{\mathrm{d[STAT3_{cyto}]}}{\mathrm{dt}} = -2 \times k_1 \times [\mathrm{IL10-IL10R}][\mathrm{STAT3_{cyto}}]^2 + 2 \times k_2 \times [\mathrm{STAT3-STAT3_{cyto}}]$
28. $\frac{\mathrm{d[STAT3-STAT3_{cyto}]}}{\mathrm{dt}} = k_1 \times [\mathrm{IL10-IL10R}][\mathrm{STAT3_{cyto}}]^2 - k_2 \times [\mathrm{STAT3-STAT3_{cyto}}] - i_{stat3} \times [\mathrm{STAT3-STAT3_{cyto}}] + eni \times [\mathrm{STAT3-STAT3_{nuclear}}] \times kv$
29. $\frac{\mathrm{d[STAT3-STAT3_{nuclear}]}}{\mathrm{dt}} = i_{stat3} \times \frac{[\mathrm{STAT3-STAT3_{cyto}}]}{\mathrm{kv}} - eni \times [\mathrm{STAT3-STAT3_{nuclear}}]$

Table 2. State variables and their initial values as used in the pro- and anti-inflammatory ODE model.

Sr. No.	State variables	Initial values, μM
1.	TLR4	1.0×10^{-1}
2.	LPS-TLR4	0
3.	IL-$10_{supernatant}$	4.6×10^{-6}
4.	IL-10R	1.0×10^{-1}
5.	IL10-IL10R	0
6.	TNF-$\alpha_{supernatant}$	0
7.	TNF-αR	1.0×10^{-1}
8.	TNFα-TNFαR	0
9.	$IKK_{neutral}$	2.0×10^{-1}
10.	IKK_{active}	0
11.	$IKK_{inactive}$	0
12.	IκBα-NFκB_{cyto}	2.5×10^{-1}
13.	IKK- IκBαNFκB	0
14.	NFκB_{cyto}	3.0×10^{-3}

Table 2. Continued.

Sr. No.	State variables	Initial values, μM
15.	$NF\kappa B_{nuclear}$	0
16.	$I\kappa B\alpha_{phopsho}$	0
17.	$A20_{mRNA}$	0
18.	$A20_{cyto}$	4.8×10^{-3}
19.	$I\kappa B\alpha_{mRNA}$	0
20.	$I\kappa B\alpha_{cyto}$	2.5×10^{-3}
21.	$I\kappa B\alpha_{nuclear}$	0
22.	$I\kappa B\alpha$-$NF\kappa B_{nuclear}$	0
23.	$IL\text{-}10_{mRNA}$	0
24.	$IL\text{-}10_{cyto}$	0
25.	$TNF\text{-}\alpha_{mRNA}$	0
26.	$TNF\text{-}\alpha_{cyto}$	0
27.	$STAT3_{cyto}$	5.92×10^{-1}
28.	$STAT3\text{-}STAT3_{cyto}$	0
29.	$STAT3\text{-}STAT3_{nuclear}$	0

4.3.2 Parameter selection and estimation

The parameter estimation problem for a dynamic system described by ordinary differential equations (ODEs) can be mathematically formulated as follows:

$$\min_{p} \sum_{i} \sum_{k} w_{ik}(y_{ik} - \hat{y}_{ik})^2 \tag{4.3}$$

Subject to,

$$\dot{x}(t) = f(x, u, p), x(0) = x_0 \tag{4.4}$$

$$y = g(x) \tag{4.5}$$

$$x^{lb} \leq x \leq x^{ub} \tag{4.6}$$

$$p^{lb} \leq p \leq p^{ub} \tag{4.7}$$

where y_{ik} and $\hat{y}_{ik}$ are the simulated and measured output data of the *i*-th component at sampling time t_k, respectively, as shown in equation (4.3); p are the parameters to be estimated, which are selected by local sensitivity analysis; x are the state variables of the dynamic system with initial values x_0; and u are the inputs to the system in equation (4.4). The output y is a function of x, as shown in equation (4.5). In addition, the state variables x and parameters p are restricted within certain ranges, as shown in equations (4.6) and (4.7), determined by the underlying biology and prior knowledge based on mathematical models developed by Lipniacki *et al.* [31], Huang *et al.* [32] and Rangamani *et al.* [112].

In this study, the simulated output vector y in equation (4.5), which is validated by experimental data, includes the intracellular ratio of phosphorylated NF-κB to total NF-κB (relative to the control) and the concentration of the cytokines, TNF-α and IL-10, in

the cell culture supernatant. Since the experiments are conducted with four different levels of the input u (*i.e.*, different concentrations of LPS, 0, 0.1, 1 and 10 µg/mL), four sets of measured outputs $\hat{y}_{ik}$ are obtained. Three sets of data obtained for 0, 0.1 and 1 µg/mL LPS stimulations are used for parameter estimation, and the fourth dataset for 10 µg/mL LPS stimulation is used for model validation.

First, the set of parameters that are to be estimated are selected by local sensitivity analysis and hierarchical clustering. Following this, the trust-region optimization technique is used to estimate the selected parameters. This technique is used in this work, as it is able to handle singular Hessian matrices, significant uncertainty in the parameters of the models and noisy data. In this technique, an optimization algorithm is applied in an outer loop, while the evaluation of the objective function and its gradients are performed by numerical integration of the ODEs in the inner loop [145,146] (shown in Figure 14). The trust-region method is guaranteed to converge to local optima with much weaker assumptions than line search methods. In this work, *fmincon* (MATLAB function) is used as the NLP (non-linear programming) solver and *ode15s* (MATLAB function) is used as the ODE integrator. It is worth noting that *ode15s* is specifically designed for stiff systems, such as the model discussed here, where both fast and slow dynamics exist, e.g., in our system, phosphorylation of NF-κB is a much faster process than *de novo* synthesis of TNF-α and IL-10. Values of the parameters used in the model and initial concentrations of proteins are shown in Table 3.

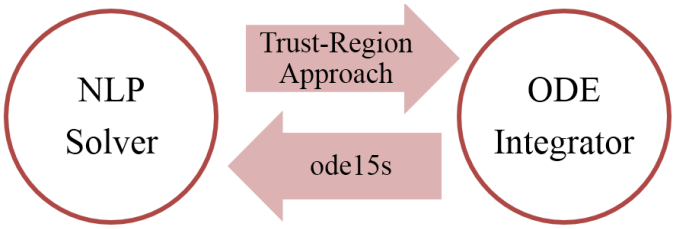

Figure 14. Algorithm for parameter estimation used to optimize pro- and anti-inflammatory ODE model parameters.

Table 3. List of parameters used in the pro- and anti-inflammatory ODE model. Estimated parameters are indicated in boldface.

Sr. No.	Parameter	Description	Value	Units	Comment
1.	***kv***	**Nuclear: Cytoplasmic (Volume)**	**1.17**	**NA**	**Estimated**
2.	$\boldsymbol{kf_1}$	**LPS binding to receptor**	$\mathbf{2.64 \times 10^{-1}}$	$\mathbf{(\mu M^{-s})^{-1}}$	**Estimated**
3.	kr_1	Dissociation of LPS + receptor complex	1.25×10^{-3}	$(\mu M^{-s})^{-1}$	Huang *et al.* (2008) [32]
4.	kf_2	IL-10 binding to receptor	2.50×10^{-4}	$(\mu M^{-s})^{-1}$	Assumed
5.	kr_2	Dissociation of IL-10 + receptor complex	6.11×10^{-4}	$(\mu M^{-s})^{-1}$	Assumed
6.	kf_3	TNF-α binding to receptor	2.50×10^{-3}	$(\mu M^{-s})^{-1}$	Gray *et al.* [147]
7.	kr_3	Dissociation of TNF-α + receptor complex	1.25×10^{-3}	$(\mu M^{-s})^{-1}$	Rangamani *et al.* (2007) [112]
8.	kf_4	Iκ*B*a and NF-κ*B* association	2.5×10^{-3}	$(\mu M^{-s})^{-1}$	Assumed
9.	***kfi***	**IKK activation**	$\mathbf{1.62 \times 10^{-3}}$	$\mathbf{s^{-1}}$	**Estimated**

Table 3. Continued.

Sr. No.	Parameter	Description	Value	Units	Comment
10.	kk_1	Inactivation of IKK by A20	2.5×10^{-4}	$(\mu M^{-s})^{-1}$	Assumed
11.	kk_3	Association of IKK with IκBα-NFκB	1.0	$(\mu M^{-s})^{-1}$	Lipniacki *et al.* (2004) [31]
12.	$\boldsymbol{ti_3}$	**Catalytic breakdown of IKK-IκBα-NFκB**	$\mathbf{1.72 \times 10^{-4}}$	$\mathbf{s^{-1}}$	**Estimated**
13.	***iln***	**NF-κB nuclear import**	$\mathbf{1.52 \times 10^{-3}}$	$\mathbf{s^{-1}}$	**Estimated**
14.	$a20_{trans}$	A20 translation	5.00×10^{-1}	s^{-1}	Lipniacki *et al.* (2004) [31]
15.	$kdeg_{A20}$	Degradation of A20 protein	3.00×10^{-4}	s^{-1}	Lipniacki *et al.* (2004) [31]
16.	$ikb\alpha_{trans}$	IκBα translation	5.00×10^{-1}	s^{-1}	Lipniacki *et al.* (2004) [31]
17.	$kdeg_{IκBα}$	Degradation of phosphorylated IκBα	1.28×10^{-4}	s^{-1}	Assumed half-life of 90 min
18.	$il10_{trans}$	IL-10 translation	5.00×10^{-1}	s^{-1}	Lipniacki *et al.* (2004) [31]
19.	$ksec_{IL10}$	Secretion of IL-10 from cytoplasm to supernatant	2.03×10^{-5}	s^{-1}	Assumed
20.	$kdeg_{IL10sup}$	Degradation of IL-10 in supernatant	7.40×10^{-5}	s^{-1}	Half-life of 2.6 h in supernatant. Fedorak *et al.* [148]
21.	$tnf\alpha_{trans}$	TNF-α translation	5.00×10^{-1}	s^{-1}	Lipniacki *et al.* (2004) [31]
22.	$\boldsymbol{ksec_{TNFα}}$	**Secretion of TNF-α from cytoplasm to supernatant**	$\mathbf{5.16 \times 10^{-5}}$	$\mathbf{s^{-1}}$	**Estimated**
23.	$\boldsymbol{kdeg_{TNFαsup}}$	**Degradation of TNF-α in supernatant**	$\mathbf{7.46 \times 10^{-5}}$	$\mathbf{s^{-1}}$	**Estimated**
24.	*Dn*	Degradation of intracellular cytokine	1.04×10^{-2}	s^{-1}	Huang *et al.* (2008) [32]
25.	*iki*	IκBα nuclear import	1.00×10^{-3}	s^{-1}	Lipniacki *et al.* (2004) [31]
26.	*eki*	IκBα nuclear export	5.00×10^{-4}	s^{-1}	Lipniacki *et al.* (2004) [31]

Table 3. Continued.

Sr. No.	Parameter	Description	Value	Units	Comment
27.	*eni*	IκBα -NFκB nuclear export	1.00×10^{-2}	s^{-1}	Lipniacki *et al.* (2004) [31]
28.	k_1	STAT3 activation and dimerization	1.54×10^{-2}	$(\mu M^{-s})^{-1}$	Assumed
29.	k_2	Dissociation of STAT3 dimer	3.3×10^{-5}	s^{-1}	Assumed
30.	$\boldsymbol{i_{stat3}}$	**STAT3 dimer nuclear import**	$\mathbf{3.56 \times 10^{-5}}$	$\mathbf{s^{-1}}$	**Estimated**
31.	*Sm*	Transcription due to NF-κB	1.00×10^{-1}	s^{-1}	Huang *et al.* (2008) [32]
32.	*Sm_il10*	IL-10 Translation due to STAT3	1.5	s^{-1}	Assumed
33.	*p*	Transcription parameter	5.00×10^{-3}	μM	Huang *et al.* (2008) [32]
34.	*Dm*	Degradation of mRNA	1.04×10^{-2}	s^{-1}	Huang *et al.* (2008) [32]
35.	*C*	Maximum NF-κB concentration in nucleus	1.08×10^{-1}	μM	Huang *et al.* (2008) [32]
36.	C_{STAT3}	Maximum STAT3 concentration in nucleus	5.00×10^{-2}	μM	Assumed
37.	$IL10\text{-}IL10R_{max}$	IL10-IL10R maximum concentration	2.56×10^{-6}	μM	Assumed

4.3.3 Cell culture and experimental set-up

The murine macrophage cell line RAW264.7 which is derived from ascites (American Type Culture Collection, Manassas, VA) was routinely cultured in Dulbecco's Modified Eagle Medium (DMEM) with 10% FBS (heat inactivated at 56℃ for 30 minutes), 100 U/ml penicillin and 100 µg/ml streptomycin. LPS (heat-killed *Salmonella enterica*) was purchased from Sigma Aldrich (St. Louis, MO, USA).

4.3.3.1. LPS stimulation of macrophages

RAW264.7 cells were seeded at a density of ~2.0 × 105 cells/well in a 96-well tissue culture plate and allowed to attach overnight. Cells were stimulated with different concentrations (0, 0.1, 1and 10 µg/mL) of LPS diluted in growth medium. Whole cells were used to measure total and phosphorylated NF-κB after 5, 15, 30, 45, 60, 120 and 240 minutes post-LPS stimulation. Culture supernatants were collected after 2, 4, 8, 12, 16, 20 and 24 hours post-LPS stimulation to measure secreted TNF-α and IL-10 concentrations.

4.3.3.2. Transcription factor NF-κB quantification by ELISA

The relative concentrations of total and phosphorylated NF-κB in LPS-stimulated RAW264.7 macrophage cells were determined using a commercially-available enzyme-linked-immunosorbent assay (ELISA) kit (R&D Systems, Minneapolis, MN, USA) according to the manufacturer's suggested protocol.

4.3.3.3 Cytokines TNF-α and IL-10 quantification by ELISA

The concentrations of *de novo* synthesized TNF-α and IL-10 in LPS-stimulated RAW264.7 macrophage culture supernatant were determined by commercially available enzyme-linked immunosorbent assay (ELISA) kits (Thermo Scientific, Rockford, IL, USA), using the manufacturer's suggested protocol.

4.4 RESULTS AND DISCUSSION

Based on published reports of LPS stimulation resulting in TNF-α [149] and IL-10 secretion [150] in RAW264.7 murine macrophages, as well as the established suppression of TNF-α by IL-10 in RAW264.7 cells [149], we developed an integrated ODE model to represent the production of TNF-α and IL-10 in RAW264.7 cells upon LPS stimulation and their regulatory feedback loops. Eight parameters of the model are selected for estimation using local sensitivity analysis and hierarchical clustering (shown in Figure 15) [151,152]. The y-axis represents the parameter distance ranging from zero to one (the larger the distance, the smaller the similarity between the parameters). The red line presents the cutoff value, which groups the entire set of parameters into eight pairwise indistinguishable clusters. The normalized sensitivity magnitudes of the parameters are reflected in the histograms. The values of the selected parameters are estimated using the trust-region optimization technique and the advantage of this approach is that the selected parameters used for estimation result in a more robust dynamic model with an accurate prediction capability [152].

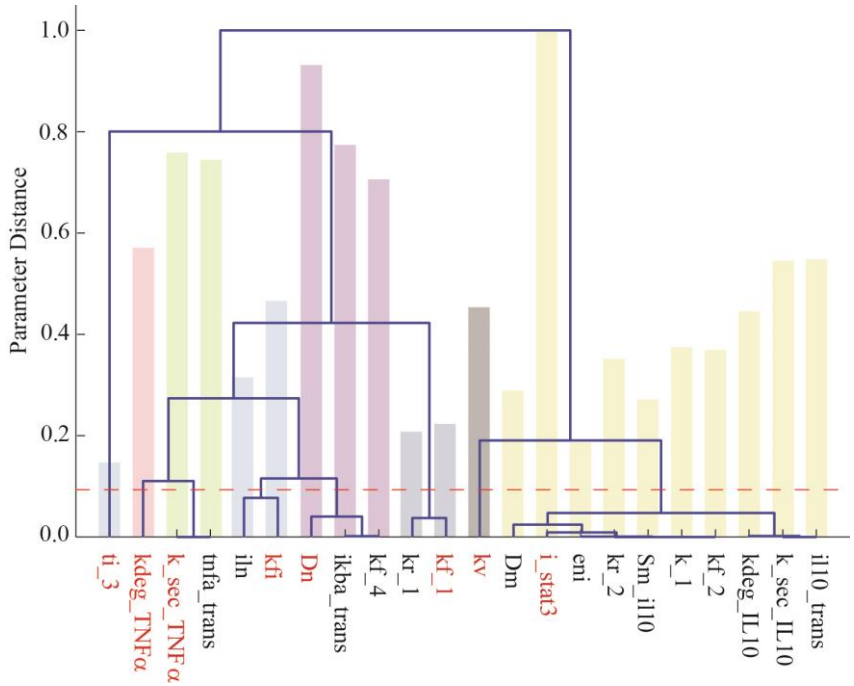

Figure 15. Representation of local sensitivity analysis results used for selecting pro- and anti-inflammatory ODE model parameters that are to be estimated. The y-axis represents the parameter distance ranging from zero to one (the larger the distance, the smaller the similarity between the parameters). The red line presents the cutoff value, which groups the entire set of parameters into eight pairwise indistinguishable clusters. The selected parameters, which have the largest sensitivity magnitude in each cluster, are highlighted in red. The normalized sensitivity magnitudes of the parameters are reflected in the histograms.

Model simulations after parameter estimation predict rapid phosphorylation of NF-κB upon exposure to LPS, as shown in Figure 16 (A). The maximum fold change in the ratio of phosphorylated NF-κB to total NF-κB in LPS-treated cells relative to control increased with increasing LPS concentration and varied from ~2.0 at the highest LPS concentration to being essentially unchanged at the lowest concentration as shown in Figure 16 (A).

Simulation of *de novo* synthesized TNF-α profile upon LPS stimulation shows that the TNF-α concentration reaches a maximum of ~1500 pg/mL at 4 hours and starts declining thereafter. Even though LPS is continuously present, TNF-α is undetectable at 24 hours for all LPS concentrations as shown in Figure 16 (B). The maximum TNF-α concentration at 4 hours increases with increasing concentrations of LPS. According to the model predictions, the *de novo* synthesized IL-10 concentration increases beyond 2 hours of LPS stimulation, as shown in Figure 16 (C), and the concentration of IL-10 produced increases with increasing LPS concentrations.

(A)

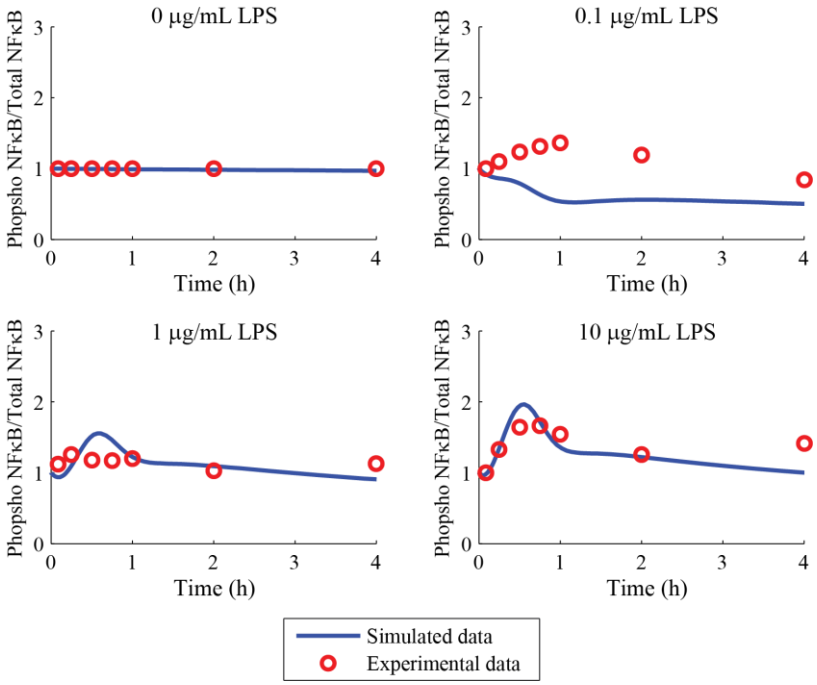

Figure 16. Comparison of model predictions and experimental data for LPS-stimulated RAW264.7 macrophages. (A) Profile of phosphorylated NF-κB/Total NF-κB in LPS-treated macrophages relative to the control; (B) Profile of *de novo* synthesized TNF-α (pg/mL) upon LPS stimulation; (C) Profile of *de novo* synthesized IL-10 (pg/mL) upon LPS stimulation.

(B)

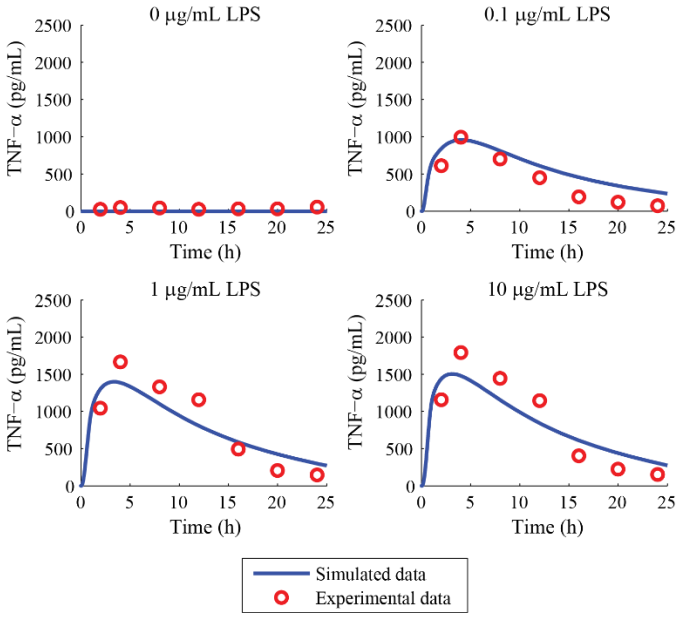

(C)

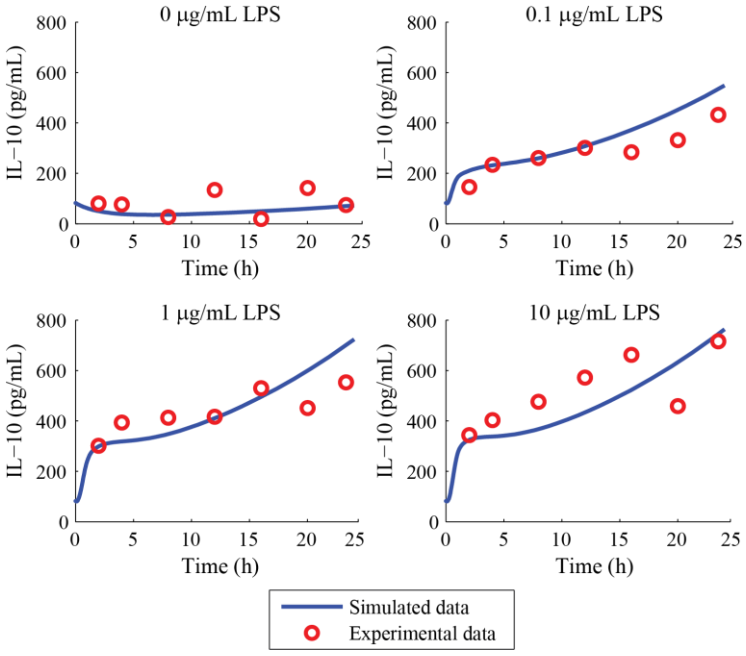

Figure 16. Continued.

Model simulations are validated by experimental data obtained from LPS-stimulated RAW264.7 cells. The comparison between simulated and experimental data for the fold change in NF-κB (phosphorylated NF-κB/Total NF-κB, relative to control), *de novo* TNF-α and IL-10 concentration profiles after parameter estimation are shown in Figures 16 (A), 16 (B) and 16 (C), respectively. In Figure 16 (A), the discrepancy between the model simulation and experimental data for 0.1 μg/mL LPS stimulation could arise from our assumption that the binding affinity between LPS and TLR4 is constant and concentrations of the LPS-TLR4 complex are linearly proportional to the concentrations of LPS tested. However, in reality, the ligand-receptor binding kinetics might follow a non-linear behavior, which is not accommodated in our computational model. The binding of LPS to TLR4 even at lower concentrations of LPS (e.g., 0.1 μg/mL) might result in higher concentrations of the LPS-TLR4 complex, resulting in more downstream phosphorylation of NF-*κ*B (as indicated by the higher phosphorylated NF-κB/total NF-κB ratio for the experimental data in Figure 16 (A) than the model is able to predict. However, the dynamic model where the parameters have been estimated exhibits a reasonably good fit for phosphorylated NF-κB/total NF-κB profiles (relative to control) at 0 μg/mL, 1 μg/mL and 10 μg/mL LPS stimulations. Furthermore, the model exhibits reasonable agreement between simulated and experimental data for both training and validation datasets for the TNF-α and IL-10 dynamic concentration profiles.

The model suggests that the initial increases in TNF-α and IL-10 are due to NF-*κ*B activation (*i.e.*, phosphorylation and dissociation of NF-κB from IκBα-NF-κB complex) in the cytoplasm and subsequent gene expression in the nucleus; and the

decrease in TNF-α concentration after 4 hour is due to the negative feedback of IL-10 on NF-κB activity (by inhibiting both IKK activation and nuclear translocation of phosphorylated NF-κB). Interestingly, the levels of IL-10 continue to increase, even when the levels of activated NF-κB are no longer increasing. It is possible that the initial burst of IL-10 produced through NF-κB activation can activate other transcription factors, which leads to an increase in IL-10 levels. An example of this could be the transcription factor STAT3, which has been shown to be activated by IL-10 [153]. Endogenous IL-10 in LPS stimulation of macrophages (RAW264.7) [154] forms the IL-10-IL10R complex that initiates phosphorylation of cytosolic STAT3, followed by its dimerization and translocation into the nucleus. The STAT3 dimer binds to the DNA response element and triggers transcription of IL-10 (Figure 17). Thus, increasing LPS concentration could lead to increasing concentrations of IL-10 due to the positive feedback of IL-10 on its own production.

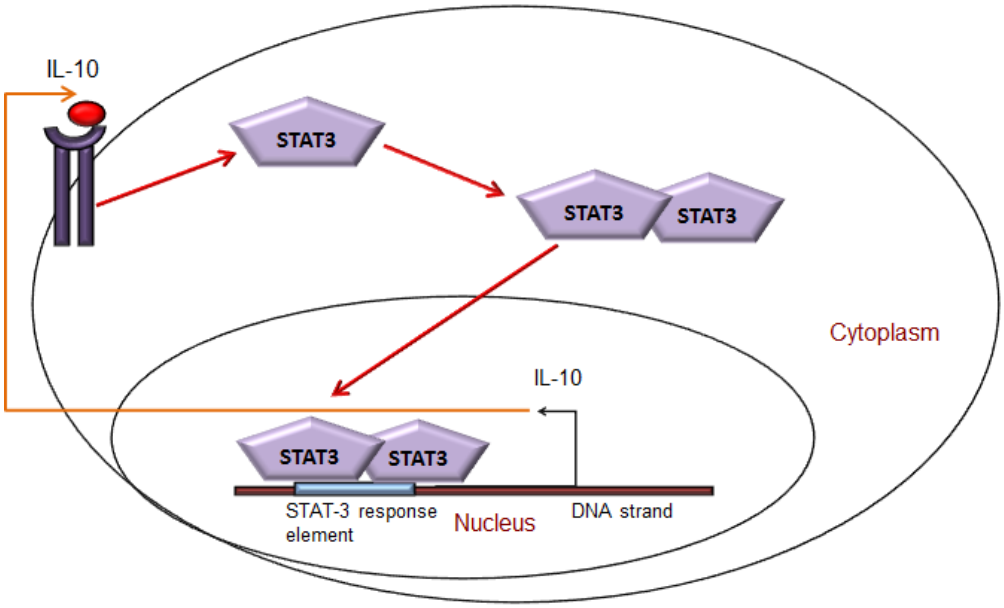

Figure 17. Schematic representation of STAT3 activation under LPS-induced *de novo* IL-10 production and feed-forward regulation in macrophages.

It can be seen that the model predictions and experimental data are in reasonable agreement, which demonstrates that biochemical reactions, which form the structure of the model, are physiologically relevant and can depict the interplay between pro-inflammatory and anti-inflammatory immune responses to maintain equilibrium (homeostasis). Furthermore, cross-talk between positive and negative feedback regulatory loops, incorporated in the model, is integral towards mathematically representing biochemical and gene regulatory networks, as mentioned by Tian *et al.* [155]. Our model also shows that the anti-inflammatory functions in the RAW264.7 macrophage cell line is initially triggered by pro-inflammatory stimulation. This model structure can be extended

to study other cell types with a modification in parameter values to fit model predictions to experimental datasets for specific cell types.

The integrated mathematical model of pro- and anti-inflammatory host immune response discussed in this chapter is a step towards assimilating our knowledge and developing a quantitative understanding of the signal transduction pathways involved in maintaining immune homeostasis, disruption of which can lead to inflammatory disorders. This mathematical model can be further used to study intra- and inter-kingdom signaling, *i.e.*, the effect of bacterial metabolites (e.g., indole) synthesized by micro flora present in the host gastro-intestinal tract on host immune response [29]. This model can be used as the basic structure to incorporate additional transcription factors, which will be needed to study the signaling of indole and their interactions with NF-κB, as described in Chapter V.

CHAPTER V

INTEGRATED INTRA- AND INTER-KINGDOM SIGNALING OF INFLAMMATORY RESPONSES

5.1 OVERVIEW

Inter-kingdom signaling in mammals arises from the complex interactions that take place between the mammalian hosts and indigenous bacteria (microbiota) residing in them. The microbiota is highly diverse in species and functions, ranging from indifferent commensal bacteria and beneficial mutualistic bacteria to disease causing pathobionts. It has been reported that the beneficial bacteria help in maintaining homeostasis in the host by modulating host immune responses against exogenous pathogenic and potentially harmful indigenous bacteria. However, the signal transduction induced by these beneficial bacteria in hosts and the molecular mechanisms involved in influencing host immune responses are not well understood. In this chapter we investigate a potential bacterial metabolite, indole-induced signaling in hosts that results in immunomodulation.

We studied indole-induced signal transduction pathway through activation of aryl hydrocarbon receptor (AHR) in down regulating nuclear factor- κ B (NF-κB) activation and inhibition of subsequent interleukin 8 (IL-8) production, by integrating mathematical modeling and experimental techniques. We observed that indole treatment at a concentration of 1 mM under moderately low pro-inflammatory stimuli (i.e., 0.1 and 1 ng/mL TNF-α) significantly down-regulates NF-κB activation and IL-8 synthesis whereas under 10 ng/mL TNF-α stimulation, inhibition of IL-8 lasts for only 4 hours post-

stimulation and down regulation of NF-κB activation is not statistically significant. 0.5 mM indole shows no significant NF-κB down regulation under any TNF-α concentrations but exhibits IL-8 inhibition for 12 hours post-TNF-α stimulation at 0.1 ng/mL and for 4 hours post-TNF-α stimulations at 1 and 10 ng/mL. 0.25 mM indole treatment on the other hand shows no significant down regulation of NF-κB under any concentration of TNF-α stimulus but exhibits IL-8 synthesis for 12 hours post-TNF-α stimulation at 0.1 ng/mL and for 4 and 2 hours post-TNF-α stimulations at 1 and 10 ng/mL respectively.

5.2 INTRODUCTION

Cross-talk between host and approximately 10^{14} indigenous bacterial cells belonging to ~1000 strains, inhabiting the gastro-intestinal (GI) tract in close proximity to host cells [10] is speculated to give rise to a complex network of inter-kingdom signaling between host and microbiota. Beneficial intestinal bacteria present in the mucous layer of the gastro-intestinal (GI) tract modulate mucosal immunity to prevent pathogenic exogenous and potentially harmful indigenous bacteria from colonizing the GI tract [13]. In this work we investigate intestinal bacteria-derived metabolite indole as a potential inter-kingdom signaling molecule.

Indole is a derivative of tryptophan (amino acid) which is produced by bacterial metabolism of tryptophan using enzyme tryptophanase A (encoded by *tnaA* in *Escherichia coli*). *Escherichia coli* also possesses *tnaB* that encodes for transporter protein TnaB which helps in internalizing dietary tryptophan which then gets hydrolyzed by tnaA to produce indole, pyruvate and ammonia [61,62]. *Escherichia coli*, one of the bacteria found in

mammalian GI tract produces ~600μM indole in suspension culture [58] which has also been detected in feces at comparable concentrations [59,60]. Indole had been known as bacteria-derived molecule over hundred years [63] however, only recently has it been recognized as an intercellular signaling molecule that regulates diverse physiological processes in both bacteria and eukaryotic cells. For example, indole has been reported to decrease motility and biofilm formation in EHEC [57], increase antibiotic resistance (by inducing xenobiotic efflux genes) [64] and decrease virulence in *candida albicans* [65]. Indole also increases intestinal epithelial cell tight junction resistance (likely increased protection against invading pathogens) and attenuate pro-inflammatory indicators by downregulating NF-κB in human intestinal epithelial cells *in vitro* [29]. Thus, indole appears to be an important intercellular signaling molecule that influences both bacterial as well as host cell responses. Several non-indole producing bacteria as well as mammalian cells in the GI tract possess enzymatic activity that can modify tryptophan and indole to produce other derivatives such as indole-3-propionic acid (identified as a powerful anti-oxidant), indoxyl sulphate [66] and 5-hydroxyindole (found in brain) [67].

The anti-inflammatory properties of indole as a NF-κB inhibitor and down-regulator of IL-8 reported by previous work in our laboratory [29] makes it a potential therapeutic candidate for inflammatory bowel disease. It is not clearly known yet if indole readily diffuses through the membrane of host cells or it requires exporter and importer proteins to facilitate its secretion and uptake, respectively [62]. Also, the molecular mechanisms involved in indole signaling in host cells are currently not well understood. Owing to its structural similarity with other well-known aromatic ligands of the cytosolic

ligand-activated aryl hydrocarbon receptor (AHR), such as 2,3,7,8-tetrachlorodibenzodioxin (TCDD), 6-formylindolo (3,2-b) carbazole (FICZ) [156], indigo dye and indirubin [157], we hypothesized in this work that indole might be a potential AHR ligand in intestinal epithelial cells that can mediate signaling through the AHR. Jin *et al.* recently demonstrated that indole is an agonist for AHR in Caco-2 intestinal epithelial cells based on approximately ten-fold induction in the mRNA levels of the canonical AHR-responsive gene cytochrome P450 (CYP1A1) [158]. In the current work we investigate a possible signal transduction pathway of indole signaling through activation of AHR that regulates host inflammatory signaling.

The AHR binds to a large number of exogenous aromatic hydrocarbons such as dioxins, polycyclic aromatic hydrocarbons (PAH), and polyphenolics and is known to regulate xenobiotic mediating enzymes such as cytochrome P450. AHR is sequestered in the cytoplasm as an inactive complex with a 90 kDa heat shock protein (HSP90), XAP2 and p23 in absence of a ligand [101]. Upon ligand binding the activated complex translocates into the nucleus and binds to aryl hydrocarbon receptor translocator protein (ARNT). AHR-ARNT complex formations induces dissociation of the chaperon proteins and AHR-ARNT complex binds to the dioxin response element (DRE) in the promoter region of responsive genes such as CYP1A1 (Figure 18).

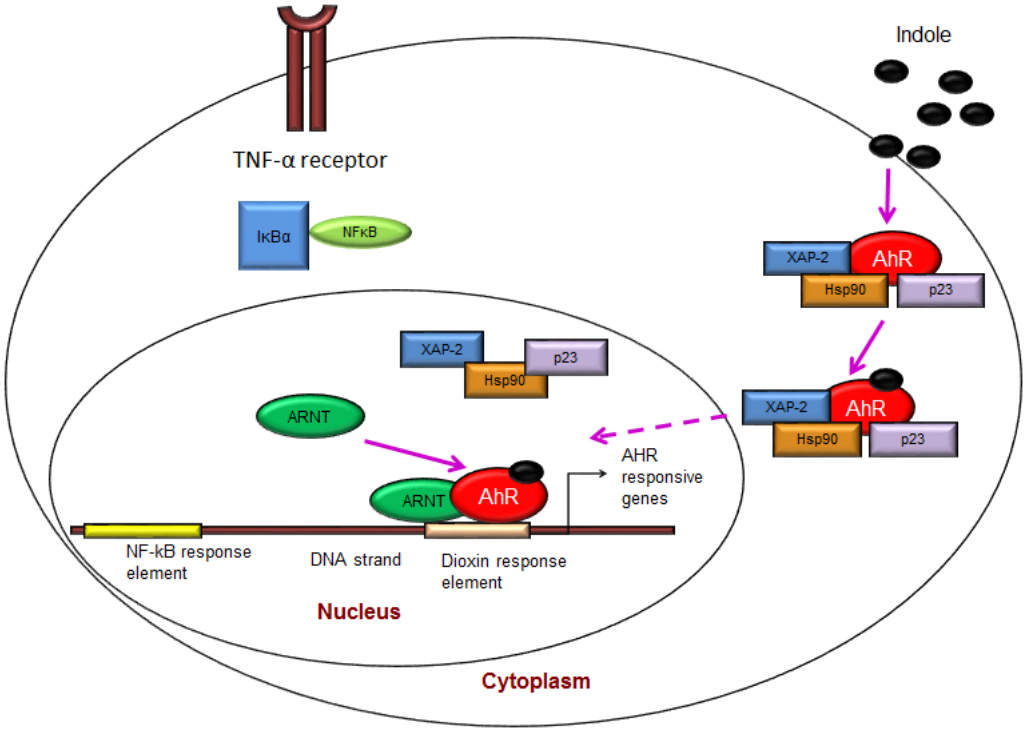

Figure 18. Schematic representation of indole signaling through activation of aryl hydrocarbon receptor (AHR).

The different chaperon proteins and ARNT tightly control AHR signaling. HSP90 helps mask the constitutive DNA binding affinity of AHR and maintains the receptor in a conformation that promotes high ligand binding affinity. XAP2 prevents ubiquitination of AHR prior to ligand binding and p23 prevents nuclear translocation of AHR complex and non-specific binding to ARNT in absence of bound ligand. Ligand binding causes conformational change in AHR complex (comprising AHR, three chaperon proteins and a ligand) that facilitates binding of importin β to the corresponding nuclear localization signal (NLS) which in turn promotes nuclear translocation of the complex.

AHR has been reported to be involved in regulatory T cell (T_{reg}) differentiation and down regulation of pro-inflammatory responses and use of natural AHR ligands (for example, plant flavonoids) have been reported as potential therapeutics for inflammatory disorder [102]. Although AHR activation has been shown to attenuate pro-inflammatory responses in hosts [159], specific molecular mechanisms by which it modulates inflammation is not fully understood. Tian *et al*. reported that ligand activated AHR can physically bind to activated pro-inflammatory nuclear factor –κ B (NF-κB) to form an inactive complex that is unable to translocate into the nucleus which results in mutual repression [160]. Based on this observation we extended our mathematical model of integrated pro- and anti-inflammatory immune responses centering around NF-κB activation (described in Chapter IV) to incorporate indole signaling through AHR and study its effect on regulating inflammation through AHR-NFκB interaction.

NF-κB is a prominent pro-inflammatory transcription factor found in most host cell types and is activated by pro-inflammatory stimuli such as LPS (bacterial component)

and TNF-α (mammalian cytokine). Upon activation, NF-κB can trigger synthesis of pro-inflammatory chemokine IL-8. In unstimulated cells, NF-κB is sequestered as an inactive complex by inhibitor –κ B α (IκBα). Upon stimulation, the complex is phosphorylated and dissociated into free NF-κB and free IκBα in the cytoplasm. Free NF-κB translocates into the nucleus and binds to its response elements in the promoter region of the responsive genes whereas IκBα is ubiquinated and eventually degraded (Figure 19).

We developed a mathematical model to describe the signal transduction pathways activated by simultaneous indole treatment and pro- inflammatory TNF-α stimulation thus leading to AHR and NF-κB activations respectively. Experimental data were used to train the model and validate model predictions.

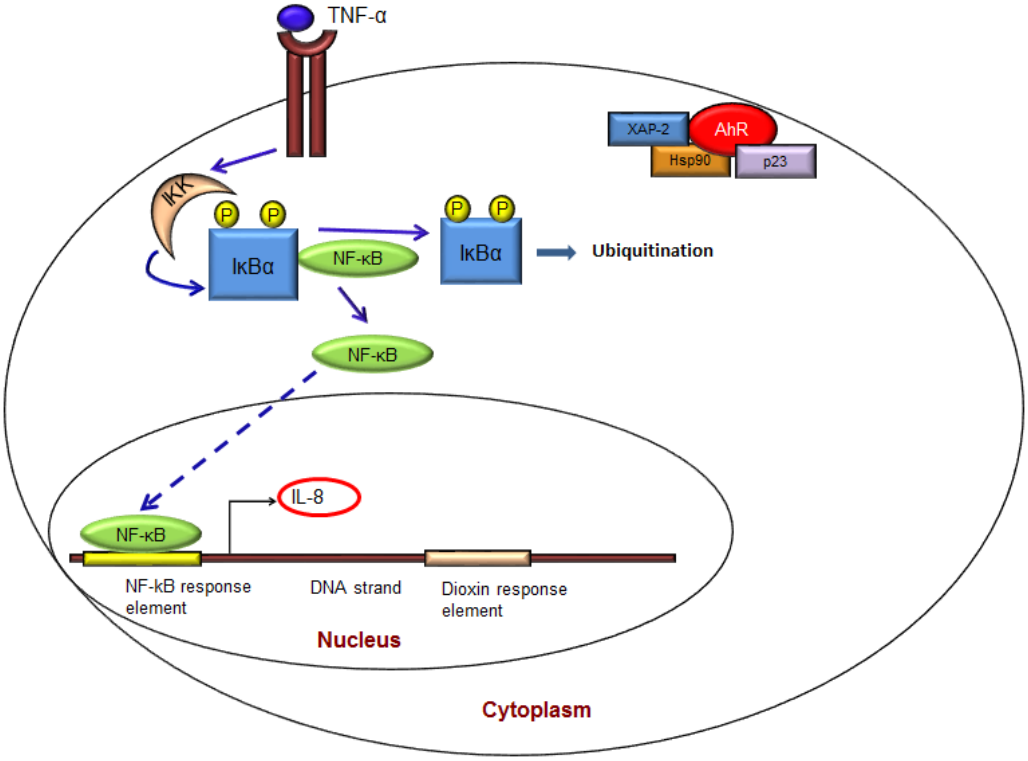

Figure 19. Schematic representation of TNF-α-induced signal transduction resulting in NF-κB activation and *de novo* IL-8 synthesis.

5.3 MATERIALS AND METHODS

5.3.1 Model formulation

In the current work we developed a dynamic computational model comprising non-linear ordinary differential equations (ODEs) to investigate molecular mechanisms involved in indole-induced attenuation of pro-inflammatory immune responses in intestinal epithelial cells based on its ability to down regulate NF-κB activation and subsequently inhibit IL-8 synthesis, observed by previous experimental work in our laboratory [29]. Until now most of the deterministic computational models relating to host immune responses have been focused towards predicting the effect of bacteria-derived pro-inflammatory signal such as lipopolysaccharide [161] by triggering pro-inflammatory responses in host. The current model is a step towards investigating a potential molecular mechanism that might be involved in eliciting host immune responses to indigenous bacterial metabolite (indole) with potential anti-inflammatory properties. It is an extension of our previously developed model representing cross-talk between pro- and anti-inflammatory immune responses in host macrophage cells (*de novo* synthesis of TNF-α and IL-10) through NF-κB activation under chronic inflammatory signal (LPS) as discussed in Chapter IV. In this chapter we describe the development of an integrated model that combines the effects of host-derived pro-inflammatory signal (TNF-α) on human intestinal epithelial cells (intra-kingdom) and cross-talk between human intestinal epithelial cells and microbiota-derived metabolite indole that influences host immune responses (inter-kingdom). Most of the computational models studying host-microbiota

interactions focus at metabolic pathways and contributions of microbiota to digestion of food in host which in turn help them survive. This is due to the availability of huge sets of metagenomic data and genome-scale metabolic models for some bacteria [118]. The current work focuses at studying signal transduction and investigation of a possible molecular mechanism involved in host immunomodulation by indigenous bacterial metabolite, indole.

The computational model comprises non-linear ordinary differential equations (ODE) that describe rate of change of the concentration of a particular component (protein/mRNA) involved in the signal transduction network. It is composed of 35 equations and 43 parameters. The model comprises important biochemical reactions in the signal transduction pathways induced by TNF-α (NF-κB activation) and indole (AHR activation) stimulation. The starting point of this model is the integrated model developed based on pro- and anti-inflammatory immune responses in murine macrophages (Chapter IV). The initial values of the parameters and initial protein concentrations are adapted from this model. Signal transduction pathway induced by TNF-α that leads to NF-κB activation is similar to the base model. No mathematical model has yet been developed for indole-induced AHR activation and AHR-NFκB interactions. Hence some of the model parameters involved in AHR activation and AHR-NF-κB interaction are initially assumed and later estimated using experimental data.

The ODE model can be structurally divided into two modules, namely, host-induced signal transduction under TNF-α stimulation and bacteria-induced signal transduction under indole stimulation.

Host-induced signal transduction through TNF-α stimulation:

1. In unstimulated cells, NF-κB is sequestered as an inactive complex bound to IκBα.
2. TNF-α binds to its cell surface receptor.
3. TNFα+receptor complex activates IKK.
4. IKK binds to inactive IκBα-NFκB, phosphorylates (activates) and dissociates the complex into free IκBα and NFκB.
5. Free phosphorylated NF-κB translocates into the nucleus of the cell whereas phosphorylated IκBα is ubiquinated and degraded in the cytoplasm.
6. Nuclear phosphorylated NF-κB binds to its response element in the promoter regions of IL-8, IκBα and A20 genes and initiates transcription.
7. IL-8, IκBα and A20 mRNA undergo translation in the cytoplasm.
8. *de novo* IL-8 is secreted out of the cell.
9. *de novo* cytoplasmic I*κ*Bα binds to free cytoplasmic NF-κB as well as translocates into the nucleus and sequesters free nuclear NF-κB. Nuclear IκBα- NF-κB complex translocates into the cytoplasm.
10. *de novo* A20 inactivates IKK.

Bacteria-induced signal transduction through indole stimulation:

1. In unstimulated cells, AHR is sequestered as an inactive complex bound to three chaperons, HSP90, XAP2 and p23.
2. Extracellular indole enters the cell and binds to AHR complex and activates it.
3. Indole bound AHR complex translocates into the nucleus.
4. Indole-AHR complex binds to ARNT.
5. Indole-AHR-ARNT complex binds to dioxin response elements.
6. No physical binding of AHR or NF-κB complexes takes place in absence of the respective ligands for AHR and NF-κB as shown in Figure 20 (A).
7. 'n' fraction of total activated AHR binds to 'm' fraction of activated NF-κB. The rest ('1-n' of activated AHR and '1-m' of activated NF-κB) is free to translocate into the nucleus and bind to their respective response elements as shown in Figure 20 (B).

(A)

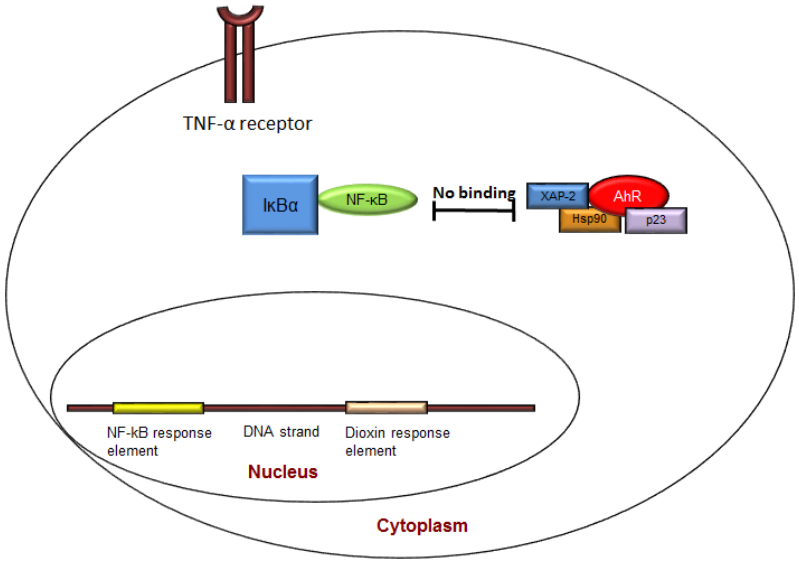

(B)

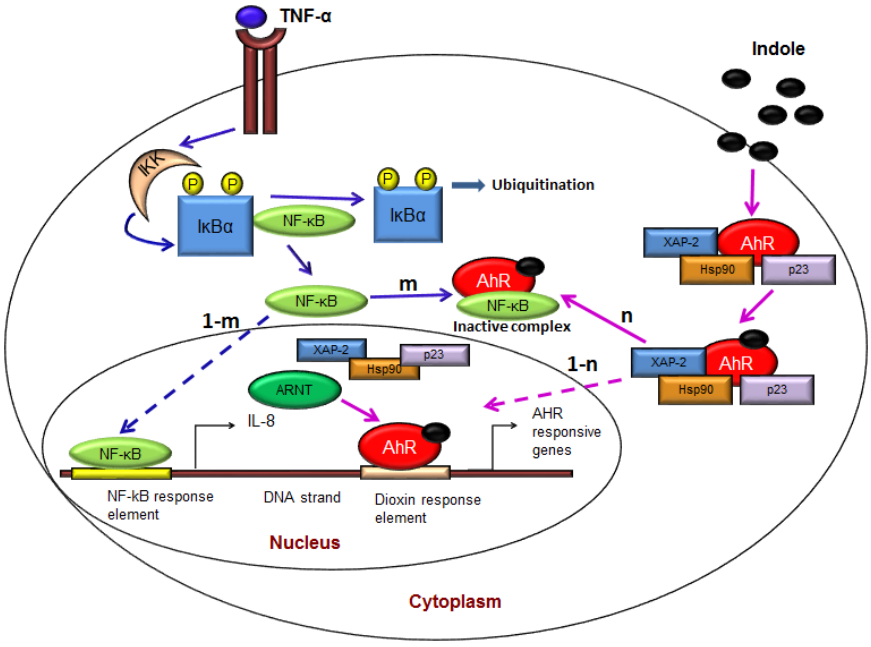

Figure 20. Simultaneous activation of NF-κB and AHR under TNF-α and indole-induced signal transduction pathways respectively. (A) In absence of stimulus (B) In presence of both TNF-α and indole stimuli.

A third transcription factor has been incorporated into the ODE model and its activation is described to be regulated by indole bound AHR. This transcription factor is modeled as a black box and is described to induce *de novo* synthesis of IL-10. Since connection between AHR and IL-10 in not clearly understood but IL-10 is known to be an important anti-inflammatory cytokine to maintain homeostasis in the GI tract, indole-induced AHR activation could be a signal for *de novo* synthesis of IL-10. We tried to investigate this mechanism through our experiments and model predictions.

ODEs describing host-induced signal transduction through TNF-α stimulation are multiplied with a variable TR where TR is 0 for 4 hours of indole pre-treatment and equal to 1 for TNF-α stimulation starting at time t_0 post-pretreatment. ODEs corresponding to indole-induced signal transduction do not have the term TR. ODEs used for formulating the current model and initial values of state variables (different components of the signal transduction pathways) are listed in Table 4 and Table 5 respectively**.**

Table 4. Differential equations representing biochemical reactions as used in the ODE model describing intra- and inter-kingdom signaling induced by bacterial metabolite indole.

1. $\frac{\mathrm{d[TNF-\alpha]}}{\mathrm{dt}} = \mathrm{TR}(-kf_1 \times [\mathrm{TNF} - \alpha_{\mathrm{sup}}][\mathrm{TNF} - \alpha\mathrm{R}] + kr1 \times [\mathrm{TNF}\alpha - \mathrm{TNF}\alpha\mathrm{R}])$
2. $\frac{\mathrm{d[TNF-\alpha R]}}{\mathrm{dt}} = \mathrm{TR}(-kf_1 \times [\mathrm{TNF} - \alpha_{\mathrm{sup}}][\mathrm{TNF} - \alpha\mathrm{R}] + kr1 \times [\mathrm{TNF}\alpha - \mathrm{TNF}\alpha\mathrm{R}])$
3. $\frac{\mathrm{d[TNF\alpha-TNF\alpha R]}}{\mathrm{dt}} = \mathrm{TR}(kf_1 \times [\mathrm{TNF} - \alpha_{\mathrm{sup}}][\mathrm{TNF} - \alpha\mathrm{R}] - kr_1 \times [\mathrm{TNF}\alpha - \mathrm{TNF}\alpha\mathrm{R}])$
4. $\frac{\mathrm{d[IKK_n]}}{\mathrm{dt}} = \mathrm{TR}(-kfi \times k_{in} \times [\mathrm{TNF}\alpha - \mathrm{TNF}\alpha\mathrm{R}] \times [\mathrm{IKK_n}] + ti \times [\mathrm{IKK_a} - \mathrm{I}\kappa\mathrm{B}\alpha\mathrm{NF}\kappa\mathrm{B_{cyto}}])$ where, $k_{in} = \max[(1 - \frac{[\mathrm{AIC\_R}]}{[\mathrm{AIC\_R_{max}}]}), 0]$ denoting inhibitory effect of anti-inflammatory cytokine (AIC)
5. $\frac{\mathrm{d[IKK_a]}}{\mathrm{dt}} = \mathrm{TR}(kfi \times k_{in} \times [\mathrm{TNF}\alpha - \mathrm{TNF}\alpha\mathrm{R}] \times [\mathrm{IKK_n}] - kk \times k_{in} \times [\mathrm{IKK_a}] \times [\mathrm{I}\kappa\mathrm{B}\alpha - \mathrm{NF}\kappa\mathrm{B_{cyto}}] - k_{a20} \times [\mathrm{IKK_a}] \times [\mathrm{A20_{cyto}}])$
6. $\frac{\mathrm{d[IKK_i]}}{\mathrm{dt}} = \mathrm{TR}(k_{a20} \times [\mathrm{IKK_a}] \times [\mathrm{A20_{cyto}}])$
7. $\frac{\mathrm{d[I\kappa B\alpha-NF\kappa B_{cyto}]}}{\mathrm{dt}} = \mathrm{TR}(kf_2 \times [\mathrm{NF}\kappa\mathrm{B_{cyto}}][\mathrm{I}\kappa\mathrm{B}\alpha_{\mathrm{cyto}}] + e\_nfkb\_ikba \times [\mathrm{I}\kappa\mathrm{B}\alpha - \mathrm{NF}\kappa\mathrm{B_{nuclear}}] \times kv - kk \times k_{in} \times [\mathrm{IKK_a}] \times [\mathrm{I}\kappa\mathrm{B}\alpha - \mathrm{NF}\kappa\mathrm{B_{cyto}}])$ Where *kv*=nuclear volume/cytoplasmic volume
8. $\frac{\mathrm{d[IKK_a-I\kappa B\alpha NF\kappa B_{cyto}]}}{\mathrm{dt}} = \mathrm{TR}(kk \times k_{in} \times [\mathrm{IKK_a}] \times [\mathrm{I}\kappa\mathrm{B}\alpha - \mathrm{NF}\kappa\mathrm{B_{cyto}}] - ti \times [\mathrm{IKK_a} - \mathrm{I}\kappa\mathrm{B}\alpha\mathrm{NF}\kappa\mathrm{B_{cyto}}])$
9. $\frac{\mathrm{d[NF\kappa B_{cyto}]}}{\mathrm{dt}} = \mathrm{TR}(-kf_2 \times [\mathrm{NF}\kappa\mathrm{B_{cyto}}][\mathrm{I}\kappa\mathrm{B}\alpha_{\mathrm{cyto}}] + ti \times [\mathrm{IKK_a} - \mathrm{I}\kappa\mathrm{B}\alpha\mathrm{NF}\kappa\mathrm{B_{cyto}}] - iln \times k_{in} \times [\mathrm{NF}\kappa\mathrm{B_{cyto}}])$
10. $\frac{\mathrm{d[NF\kappa B_{nuclear}]}}{\mathrm{dt}} = \mathrm{TR}((1 - \mathrm{m}) \times i\_nfkb \times k_{in} \times \frac{[\mathrm{NF}\kappa\mathrm{B_{cyto}}]}{\mathrm{kv}} - kf_2 \times [\mathrm{NF}\kappa\mathrm{B_{nuclear}}][\mathrm{I}\kappa\mathrm{B}\alpha_{\mathrm{nuclear}}])$
11. $\frac{\mathrm{d[I\kappa B\alpha_{phopsho}]}}{\mathrm{dt}} = \mathrm{TR}(ti \times [\mathrm{IKK_a} - \mathrm{I}\kappa\mathrm{B}\alpha\mathrm{NF}\kappa\mathrm{B_{cyto}}] - kdeg_{I\kappa B\alpha} \times [\mathrm{I}\kappa\mathrm{B}\alpha_{\mathrm{cyto}}])$
12. $\frac{\mathrm{d[A20_{mRNA}]}}{\mathrm{dt}} = \mathrm{TR}(Sm \times p \times \frac{[\mathrm{NF}\kappa\mathrm{B_{nuclear}}]}{\mathrm{C}+[\mathrm{NF}\kappa\mathrm{B_{nuclear}}]} - Dm \times [\mathrm{A20_{mRNA}}])$
13. $\frac{\mathrm{d[A20_{cyto}]}}{\mathrm{dt}} = \mathrm{TR}(a20_{trans} \times [\mathrm{A20_{mRNA}}] - kdeg_{A20} \times [\mathrm{A20_{cyto}}])$
14. $\frac{\mathrm{d[I\kappa B\alpha_{mRNA}]}}{\mathrm{dt}} = \mathrm{TR}(Sm \times p \times \frac{[\mathrm{NF}\kappa\mathrm{B_{nuclear}}]}{\mathrm{C}+[\mathrm{NF}\kappa\mathrm{B_{nuclear}}]} - Dm \times [\mathrm{I}\kappa\mathrm{B}\alpha_{\mathrm{mRNA}}])$
15. $\frac{\mathrm{d[I\kappa B\alpha_{cyto}]}}{\mathrm{dt}} = \mathrm{TR}(-kf_2 \times [\mathrm{NF}\kappa\mathrm{B_{cyto}}][\mathrm{I}\kappa\mathrm{B}\alpha_{\mathrm{cyto}}] + i\kappa b\alpha_{trans} \times [\mathrm{I}\kappa\mathrm{B}\alpha_{\mathrm{mRNA}}] - i\_ikba \times [\mathrm{I}\kappa\mathrm{B}\alpha_{\mathrm{cyto}}] + e\_ikba \times [\mathrm{I}\kappa\mathrm{B}\alpha_{\mathrm{nuclear}}] \times kv)$
16. $\frac{\mathrm{d[IL-8_{mRNA}]}}{\mathrm{dt}} = \mathrm{TR}(Sm \times p \times \frac{[\mathrm{NF}\kappa\mathrm{B_{nuclear}}]}{\mathrm{C}+[\mathrm{NF}\kappa\mathrm{B_{nuclear}}]} - Dm \times [\mathrm{IL} - 8_{\mathrm{mRNA}}])$
17. $\frac{\mathrm{d[IL-8_{cyto}]}}{\mathrm{dt}} = \mathrm{TR}(il8_{trans} \times [\mathrm{IL} - 8_{\mathrm{mRNA}}] - kdeg_{IL8} \times [\mathrm{IL} - 8_{\mathrm{cyto}}])$
18. $\frac{\mathrm{d[IL-8_{sup}]}}{\mathrm{dt}} = ksec_{IL8} \times [\mathrm{IL} - 8_{\mathrm{cyto}}] \times \frac{0.36}{200} - kdeg_{IL-8sup} \times [\mathrm{IL} - 8_{\mathrm{sup}}]$
19. $\frac{\mathrm{d[I\kappa B\alpha_{nuclear}]}}{\mathrm{dt}} = \mathrm{TR}(-kf_2 \times [\mathrm{NF}\kappa\mathrm{B_{nuclear}}][\mathrm{I}\kappa\mathrm{B}\alpha_{\mathrm{nuclear}}] + i\_ikba \times \frac{[\mathrm{I}\kappa\mathrm{B}\alpha_{\mathrm{cyto}}]}{\mathrm{kv}} - eki \times [\mathrm{I}\kappa\mathrm{B}\alpha_{\mathrm{nuclear}}])$
20. $\frac{\mathrm{d[I\kappa B\alpha-NF\kappa B_{nuclear}]}}{\mathrm{dt}} = \mathrm{TR}(kf_2 \times [\mathrm{NF}\kappa\mathrm{B_{nuclear}}][\mathrm{I}\kappa\mathrm{B}\alpha_{\mathrm{nuclear}}] - e\_nfkb\_ikba \times [\mathrm{I}\kappa\mathrm{B}\alpha - \mathrm{NF}\kappa\mathrm{B_{nuclear}}])$
21. $\frac{\mathrm{d[Indole]}}{\mathrm{dt}} - kf_3 \times \mathrm{ind_{transport}} \times [\mathrm{indole}][\mathrm{AHR_{complex}}] + kr_3 \times [\mathrm{indole} - \mathrm{AHR_{cyto}}]$
22. $\frac{\mathrm{d[AHR\ complex]}}{\mathrm{dt}} = -kf_3 \times \mathrm{ind_{transport}} \times [\mathrm{indole}][\mathrm{AHR_{complex}}] + kr_3 \times [\mathrm{indole} - \mathrm{AHR_{cyto}}]$
23. $\frac{\mathrm{d[indole-AHR_{cyto}]}}{\mathrm{dt}} = kf_3 \times \mathrm{ind_{transport}} \times [\mathrm{indole}][\mathrm{AHR_{complex}}] - kr_3 \times [\mathrm{indole} - \mathrm{AHR_{cyto}}]$

Table 4. Continued.

24.	$\frac{\mathrm{d[indole-AHR\ complex_{nuclear}]}}{\mathrm{dt}} = (1-n) \times i\_i_{indole_{ahr}} \times \frac{\mathrm{[indole-AHRcomplex_{cyto}]}}{\mathrm{kv}} - k_{ahr_{arnt}} \times [\mathrm{indole-AHR\ complex_{nuclear}}] \times [\mathrm{ARNT}]$
25.	$\frac{\mathrm{d[ARNT]}}{\mathrm{dt}} = k_{ahr_{arnt}} \times [\mathrm{indole-AHR\ complex_{nuclear}}] \times [\mathrm{ARNT}]$
26.	$\frac{\mathrm{d[indole-AHR-ARNT\ nuclear]}}{\mathrm{dt}} = k_{ahr_{arnt}} \times [\mathrm{indole-AHR\ complex_{nuclear}}] \times [\mathrm{ARNT}]$
27.	$\frac{\mathrm{d[indole-AHR-NF\kappa B\ complex_{cyto}]}}{\mathrm{dt}} = \mathrm{TR}(k_{ahr_{nfkb}} \times \mathrm{n} \times [\mathrm{indole-AHR_{cyto}}] \times \mathrm{m} \times [\mathrm{NF\kappa B_{cyto}}]$
28.	$\frac{\mathrm{d[TF\_AI_{cyto}]}}{\mathrm{dt}} = -kf_4 \times [\mathrm{TF\_IL10_{cyto}}] \times (1-\mathrm{n}) \times [\mathrm{indole-AHR\ complex_{nuclear}}]$
29.	$\frac{\mathrm{d[TF\_AI\_phospho_{cyto}]}}{\mathrm{dt}} = kf_4 \times [\mathrm{TF\_IL10_{cyto}}] \times (1-\mathrm{n}) \times [\mathrm{indole-AHR\ complex_{nuclear}}] - i\_tf\_ai \times [\mathrm{TF\_AI_{nuclear}}]$
30.	$\frac{\mathrm{d[TF\_AI\_phospho_{nuclear}]}}{\mathrm{dt}} = i\_tf\_ai \times [\mathrm{TF\_AI_{nuclear}}]$
31.	$\frac{\mathrm{d[IL-10_{mRNA}]}}{\mathrm{dt}} = \mathrm{TR} \times [\mathrm{a} \times Sm \times p \times \frac{[\mathrm{NF\kappa B_{nuclear}}]}{\mathrm{C}+[\mathrm{NF\kappa B_{nuclear}}]} + \mathrm{b} \times Sm\_il10 \times p \times \frac{[\mathrm{TF\_AI_{nuclear}}]}{\mathrm{C\_TF\_AI}+[\mathrm{TF\_AI_{nuclear}}]} - Dm \times [\mathrm{IL-10_{mRNA}}]$
32.	$\frac{\mathrm{d[IL-10_{cyto}]}}{\mathrm{dt}} = il10_{trans} \times [\mathrm{IL-10_{mRNA}}] - ksec_{IL10} \times [\mathrm{IL-10_{cyto}}] - Dn \times [\mathrm{IL-10_{cyto}}]$
33.	$\frac{\mathrm{d[IL-10_{sup}]}}{\mathrm{dt}} = -kf_4 \times [\mathrm{IL-10_{sup}}][\mathrm{IL-10R}] + kr_4 \times [\mathrm{IL10-IL10R}] + ksec_{IL10} \times [\mathrm{IL-10_{cyto}}] \times \frac{0.36}{200} - kdeg_{IL-10sup} \times [\mathrm{IL-10_{sup}}]$
34.	$\frac{\mathrm{d[IL-10R]}}{\mathrm{dt}} = -kf_4 \times [\mathrm{IL-10}][\mathrm{IL-10R}] + kr_4 \times [\mathrm{IL10-IL10R}]$
35.	$\frac{\mathrm{d[IL10-IL10R]}}{\mathrm{dt}} = kf4 \times [\mathrm{IL-10_{sup}}][\mathrm{IL-10R}] - kr_4 \times [\mathrm{IL10-IL10R}]$

Table 5. State variables and their initial values as used in intra- and inter-kingdom signaling ODE model.

Sr. No.	State variables	Initial values, μM
1.	TNF-α	Input concentrations
2.	TNF-αR	1.0×10^{-1}
3.	TNFα-TNFαR	0
4.	$\mathrm{IKK_{neutral}}$	2.0×10^{-1}
5.	$\mathrm{IKK_{active}}$	0
6.	$\mathrm{IKK_{inactive}}$	0
7.	$\mathrm{I\kappa B\alpha\text{-}NF\kappa B_{cyto}}$	2.5×10^{-1}
8.	IKK- $\mathrm{I\kappa B\alpha NF\kappa B}$	0
9.	$\mathrm{NF\kappa B_{cyto}}$	9.0×10^{-4}

Table 5 Continued.

Sr. No.	State variables	Initial values, µM
10.	$NF\kappa B_{nuclear}$	0
11.	$I\kappa B\alpha_{phopsho}$	0
12.	$A20_{mRNA}$	0
13.	$A20_{cyto}$	4.8×10^{-3}
14.	$I\kappa B\alpha_{mRNA}$	0
15.	$I\kappa B\alpha_{cyto}$	2.5×10^{-3}
16.	IL-8-α_{mRNA}	0
17.	IL-8-α_{cyto}	0
18.	IL-8-α_{sup}	0
19.	$I\kappa B\alpha_{nuclear}$	0
20.	$I\kappa B\alpha$-$NF\kappa B_{nuclear}$	0
21.	Indole	Input concentrations
22.	AHR $complex_{cyto}$	2.5×10^{-2}
23.	Indole-AHR $complex_{cyto}$	0
24.	Indole-AHR $complex_{nuclear}$	0
25.	ARNT	0
26.	Indole-AHR-$ARNT_{nuclear}$	0
27.	Indole-AHR-$NF\kappa B_{cyto}$	0
28.	TF_AI_{cyto}	2.5×10^{-1}
29.	TF_AI_$phospho_{cyto}$	3×10^{-4}
30.	TF_AI_$phospho_{nuclear}$	0
31.	$IL\text{-}10_{mRNA}$	0
32.	$IL\text{-}10_{cyto}$	0
33.	$IL\text{-}10_{supernatant}$	4.6×10^{-6}
34.	IL-10R	1.0×10^{-1}
35.	IL10-IL10R	0

5.3.2 Parameter selection and estimation

The parameter estimation problem for a dynamic system described by ordinary differential equations (ODEs) can be mathematically formulated as follows:

$$\min_{p} \sum_{i} \sum_{k} w_{ik} \left(y_{ik} - \hat{y}_{ik} \right)^2 \tag{5.1}$$

s.t.

$$\dot{x}(t) = f(x, u, p), \; x(0) = x_0 \tag{5.2}$$

$$y = g(x) \tag{5.3}$$

$$x^{lb} \le x \le x^{ub} \tag{5.4}$$

$$p^{lb} \le p \le p^{ub} \tag{5.5}$$

where y_{ik} and $\hat{y}_{ik}$ are the simulated and experimental data of the i-th component at sampling time t_k, respectively as shown in equation (5.1). In equation (5.2), x are the state variables of the dynamic system (as listed in Table 5), i.e., concentrations of individual components, with initial values x_0, u are the inputs to the system and p are the parameters to be estimated. The simulated output vector y in equation (5.3) is validated by experimental data of concentrations of intracellular phosphorylated NF-κB (relative to the unstimulated control) and extracellular IL-8 in cell culture supernatant. In addition, the state variables x and parameters p are restricted within certain ranges as shown in equations (5.4) and (5.5), determined by the underlying biology and prior knowledge based on mathematical models [31,32,112].

The experiments are conducted with different levels of inputs u (i.e., three different concentrations of TNF-α; 0.1, 1, and 10 ng/ml, and four different concentrations of indole; 0, 0.25, 0.5, and 1 mM). A total of 12 sets of measured outputs $\hat{y}_{ik}$ corresponding to different experimental conditions are obtained. These 12 measurements are randomly partitioned into training sets (to estimate model parameters) and validation sets (to validate model predictions).

Before performing parameter estimation, a local sensitivity analysis [162,163] is performed to identify the parameters that need to be estimated to fit the experimental data. In this method, sensitivity vectors for each parameter are calculated and clustered into a dendrogram. A cut off value for the clustering algorithm is chosen, in this case 0.05 resulting in the selection of eight parameters. The normalized sensitivity magnitudes of the parameters are reflected in the histograms in Figure 21. The y-axis represents correlation among parameters ranging from 0 to 1. The red line represents the cut-off value which results in clustering the entire set of parameters into eight pairwise indistinguishable groups (illustrated in different colors). The parameters with the largest sensitivity magnitude within each group are selected for estimation (highlighted in red).

Three other parameters (i.e., n, a, and b) were determined to be of significance *a priori* to investigate crosstalk between the AHR and NF-κB interactions. Therefore, a total of eleven parameters have been estimated using the experimental data.

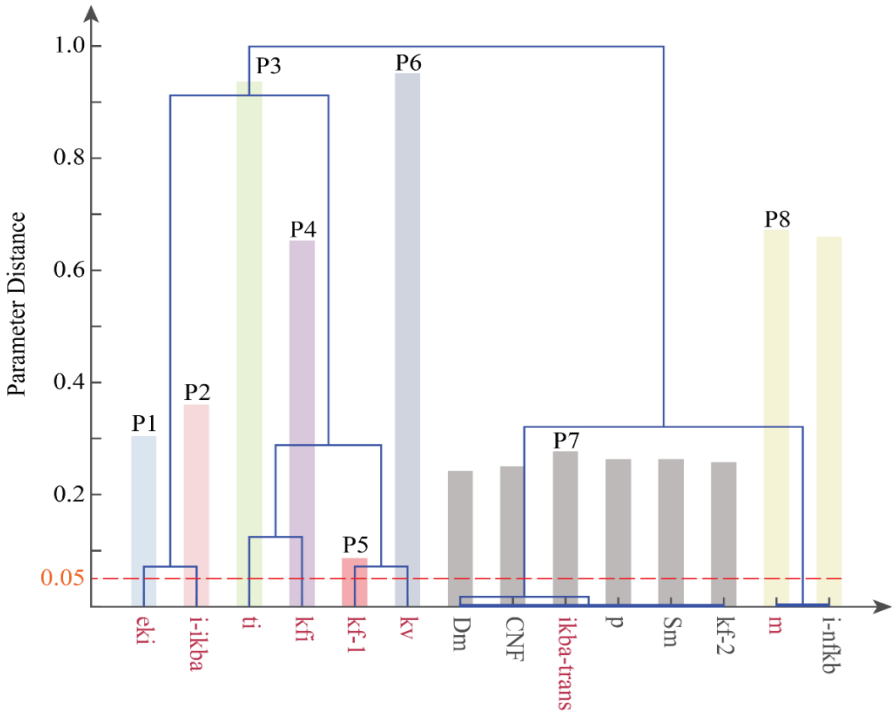

Figure 21. Representation of local sensitivity analysis results used for selecting parameters of intra- and inter-kingdom signaling ODE model that are to be estimated. The normalized sensitivity magnitudes of the parameters are reflected in the histograms. The *y*-axis represents correlation among parameters ranging from 0 to 1. The red line represents the cut-off value which results in clustering the entire set of parameters into eight pairwise indistinguishable groups (illustrated in different colors). The parameters with the largest sensitivity magnitude within each group are selected for estimation (highlighted in red).

A Trust-Region optimization technique is used to estimate the selected parameters. In this technique, an optimization algorithm is applied which requires repeated evaluation of the objective function and its gradients by numerical integration of the ODEs [145,164]. The eleven parameters selected in the previous step are estimated using the randomly selected training data sets. List of all parameters used in the intra- and inter-kingdom signaling ODE model are described in Table 6.

Table 6. List of parameters used in the intra- and inter-kingdom signaling ODE model. Estimated parameters after model optimization with experimental data are indicated in boldface.

Sr. No.	Parameter	Description	Value	Units	Comment
1.	***kv***	**Nuclear: Cytoplasmic (Volume)**	**4.094**	**NA**	**Estimated**
2.	$\boldsymbol{kf_1}$	**TNF-α binding to receptor**	**1.583**	$\boldsymbol{(\mu M^{-s})^{-1}}$	**Estimated**
3.	kr_1	Dissociation of TNF-α + receptor complex	1.25×10^{-3}	$(\mu M^{-s})^{-1}$	Rangamani *et al.* (2007) [112]
4.	***kfi***	**IKK activation**	**0.85**	$\boldsymbol{s^{-1}}$	**Estimated**
5.	*kk*	Association of IKK with IκBα-NFκB	1.0	$(\mu M^{-s})^{-1}$	Lipniacki *et al.* (2004) [31]
6.	***ti***	**Catalytic breakdown of IKK-IκBα-NFκB**	$\boldsymbol{6.7 \times 10^{-5}}$	$\boldsymbol{s^{-1}}$	**Estimated**
7.	*k_a*	Inactivation of IKK by A20	2.5×10^{-4}	$(\mu M^{-s})^{-1}$	Assumed
8.	kf_2	IκBa and NF-κB association	2.5×10^{-3}	$(\mu M^{-s})^{-1}$	Assumed
9.	***i_ikba***	**IκBα nuclear import**	$\boldsymbol{5.44 \times 10^{-3}}$	$\boldsymbol{s^{-1}}$	**Estimated**
10.	***e_ikba***	**IκBα nuclear export**	**4.094**	$\boldsymbol{s^{-1}}$	**Estimated**
11.	*e_nfkb_ikba*	IκBα-NFκB nuclear export	1.00×10^{-2}	s^{-1}	Lipniacki *et al.* (2004) [31]
12.	kf_4	IL-10 binding to receptor	2.50×10^{-4}	$(\mu M^{-s})^{-1}$	Assumed
13.	kr_4	Dissociation of IL-10 + receptor complex	6.11×10^{-4}	$(\mu M^{-s})^{-1}$	Assumed
14.	*i_nfkb*	NF-κB nuclear import	1.52×10^{-3}	s^{-1}	Estimated
15.	*e_nfkb_ikba*	NF-κB nuclear export	0.01	s^{-1}	Lipniacki *et al.* (2004) [31]
16.	*ind_transport*	Indole transport into cell cytoplasm	1.0×10^{-3}	s^{-1}	Assumed

Table 6. Continued.

Sr. No.	Parameter	Description	Value	Units	Comment
17.	*i_ind_ahr*	Indole-AHR nuclear transport	1.52×10^{-4}	s^{-1}	Assumed
18.	*i_TF_AI*	Phosphorylated TF_ anti-inflammatory nuclear import	1.52×10^{-3}	s^{-1}	Assumed
19.	*k_ahr_arnt*	Indole bound AHR-ARNT binding	2.5×10^{-3}	$(\mu M^{-s})^{-1}$	Assumed
20.	*k_ahr_nfkb*	Indole bound AHR-activated NF-κB binding	2.5×10^{-3}	$(\mu M^{-s})^{-1}$	Assumed
21.	$a20_{trans}$	A20 translation	5.00×10^{-1}	s^{-1}	Lipniacki *et al.* (2004) [31]
22.	$kdeg_{A20}$	Degradation of A20 protein	3.00×10^{-4}	s^{-1}	Lipniacki *et al.* (2004) [31]
23.	$\boldsymbol{i\kappa b\alpha_{trans}}$	**IκBα translation**	$\mathbf{6.6 \times 10^{-1}}$	$\mathbf{s^{-1}}$	**Estimated**
24.	$kdeg_{I\kappa B\alpha}$	Degradation of phosphorylated IκBα	1.28×10^{-4}	s^{-1}	Assumed half-life of 90 min
25.	$il8_{trans}$	IL-10 translation	5.00×10^{-1}	s^{-1}	Lipniacki *et al.* (2004) [31]
26.	$ksec_{IL8}$	Secretion of IL-8 from cytoplasm to supernatant	5.16×10^{-6}	s^{-1}	Assumed
27.	$kdeg_{IL8sup}$	Degradation of IL-8 in supernatant	7.46×10^{-7}	s^{-1}	Assumed
28.	$il10_{trans}$	IL-10 translation	5.00×10^{-1}	s^{-1}	Lipniacki *et al.* (2004) [31]
29.	$ksec_{IL10}$	Secretion of IL-10 from cytoplasm to supernatant	2.03×10^{-5}	s^{-1}	Assumed
30.	$kdeg_{IL10sup}$	Degradation of IL-10 in supernatant	7.40×10^{-5}	s^{-1}	Half-life of 2.6 h in supernatant. Fedorak *et al.* [148]

Table 6. Continued.

Sr. No.	Parameter	Description	Value	Units	Comment
31.	Dn	Degradation of intracellular cytokine	1.04×10^{-2}	s^{-1}	Huang *et al.* (2008) [32]
32.	kf_4	Indole-AHR complex induced activation TF_anti-inflammatory	2.5×10^{-4}	$(\mu M^{-s})^{-1}$	Assumed
33.	Sm	Transcription due to NF-κB	1.00×10^{-1}	s^{-1}	Huang *et al.* (2008) [32]
34.	Sm_il10	IL-10 translation due to TF_anti-inflammatory	1.5	s^{-1}	Maiti *et al*. [8]
35.	p	Transcription parameter	5.00×10^{-3}	µM	Huang *et al.* (2008) [32]
36.	Dm	Degradation of mRNA	1.04×10^{-2}	s^{-1}	Huang *et al.* (2008) [32]
37.	C	Maximum NF-κB concentration in nucleus	1.08×10^{-1}	µM	Huang *et al.* (2008) [32]
38.	C_{TF_AI}	Maximum TF_anti-inflammatory concentration in nucleus	5.00×10^{-2}	µM	Assumed
39.	$IL10\text{-}IL10R_{max}$	IL10-IL10R maximum concentration	2.56×10^{-6}	µM	Assumed
40.	***m***	**Fraction of activated NF-κB binding to AHR in the cytoplasm**	**0.948**	**NA**	**Estimated**
41.	***n***	**Fraction of activated AHR binding to NF-κB in the cytoplasm**	**0.733**	**NA**	**Estimated**
42.	***a***	**Impact of NF- κB on IL-10 transcription**	**0.879**	**NA**	**Estimated**
43.	***b***	**Impact of TF_anti-inflammatory on IL-10 transcription**	**0.314**	**NA**	**Estimated**

5.3.3 Cell culture and experimental-set up

All experiments were performed in human colon-cancer cell line HCT-8 (ATCC, Manassas, VA) derived from enterocytes at the junction of large and small bowel. HCT-8 cells were routinely cultured in Rosewell Park Memorial Institute (RPMI) 1640 medium with 10% equine serum, 1mM sodium pyruvate, 10mM HEPES, 100 U/ml penicillin and 100 µg/ml streptomycin at 37°C and 5% CO_2 according to standard ATCC protocols. HCT-8 cells were seeded in tissue culture treated well plates and allowed to attach overnight before indole treatment and TNF-α stimulation.

5.3.3.1 Indole treatment of colonic epithelial cells

HCT-8 cells were pre-treated with indole (Acros Organics, New Jersey, NJ) at titer concentrations of 0, 0.25, 0.5 and 1mM (initially dissolved in N,N-dimethylformamide and subsequently diluted in growth medium; final DMF concentration < 0.2%) in triplicates for 4 hours prior to TNF-α stimulation. Cells were continued to be exposed to corresponding concentrations of indole in presence TNF-α.

5.3.3.2 TNF-α stimulation of colonic epithelial cells

HCT-8 cells were stimulated with different concentrations (0.1 1 and 10 ng/mL) of recombinant human TNF-α (R&D Systems, Minneapolis, MN, USA) diluted in growth medium.

5.3.3.3 Transcription factor NF-κB quantification by ELISA

Indole treated and TNF-α stimulated (under conditions mentioned above) whole cells were used to measure phosphorylated NF-κB 5, 15, 30, 45, 60, 120 and 240 minutes post-TNF-α stimulation. Concentrations of phosphorylated NF-κB in HCT-8 epithelial cells were determined using a commercially-available enzyme-linked-immunosorbent assay (ELISA) kit (R&D Systems, Minneapolis, MN, USA) according to the manufacturer's suggested protocol.

5.3.3.4 IL-8 quantification by ELISA

Culture supernatants were collected 4, 8 and 12 hours post-TNF-α stimulation to measure *de novo* synthesized IL-8 concentrations by commercially available enzyme-linked immunosorbent assay (ELISA) kits (Thermo Scientific, Rockford, IL, USA), using the manufacturer's suggested protocol.

5.4 RESULTS AND DISCUSSION

The mathematical model presented in this section is based on observations of previous research work from our laboratory that showed indole-induced down-regulation NF-*κ*B activation and *de novo* IL-8 synthesis in HCT-8 cells [29]. However, the molecular mechanisms underlying indole's effects are not well understood. We investigated a possible mechanism of indole signaling through AHR activation and subsequent interaction with activated NF-κB, as suggested by Tian *et al*. [160]. We monitored NF-κB (p65) phosphorylation (activation) at different time points (5, 15, 30, 45, 60, 120 and 240 minutes post-TNF-α stimulation) and measured *de novo* IL-8 concentrations (2, 4, 8, 12 hours post-TNF-α stimulation) under different concentrations of TNF-α stimulations (0.1, 1, 10 ng/mL) and indole treatment (0, 0.25, 0.5 and 1mM) to establish dynamics of TNF-α and indole-induced intra- and inter-kingdom signaling.

The experimental data obtained for phosphorylated NF-κB (Rel A-p65) in TNF-α stimulated HCT-8 cells was normalized to unstimulated control at time t_0 to get a relative value. The unstimulated control has a value of 1 for phosphorylated NF-κB at time t when normalized to the phosphorylated NF-κB at time t_0 (TNF-α stimulation starts at time t_0). Thus, the data for normalized phosphorylated NF-κB for all the conditions have values higher than 1.

Figure 22 (A) shows levels of normalized phosphorylated NF-κB in HCT-8 cells after 4 hour pre-treatment with 0, 0.25, 0.5 and 1mM indole and 0.1 ng/mL TNF-α stimulation (in presence of indole). Phosphorylated NF-κB exhibits dose and time-dependent responses to indole concentrations. The phosphorylated levels of NF-κB are significantly reduced by 1mM indole treatment and the effect is observed from 5 minutes to 120 minutes post-TNF-α stimulation. In 0.5mM indole treated cells, significant reduction in phosphorylated NF-κB is observed after 30 minutes of TNF-α stimulation whereas 0.25mM indole treatment is able to reduce phosphorylated NF-κB levels only at 45 and 120 minutes post-TNF-α stimulation. Figure 22 (B) represents normalized phosphorylated NF-κB levels under indole treatment and 1 ng/mL TNF-α stimulation. Statistically significant reduction in phosphorylated NF-κB is observed for 0.5 and 1mM indole treatment at 120 minutes post-TNF-α stimulation only. As shown in Figure 22 (C), no concentration of indole treatment is able to significantly reduce activation of NF-κB under 10ng/mL TNF-α stimulation.

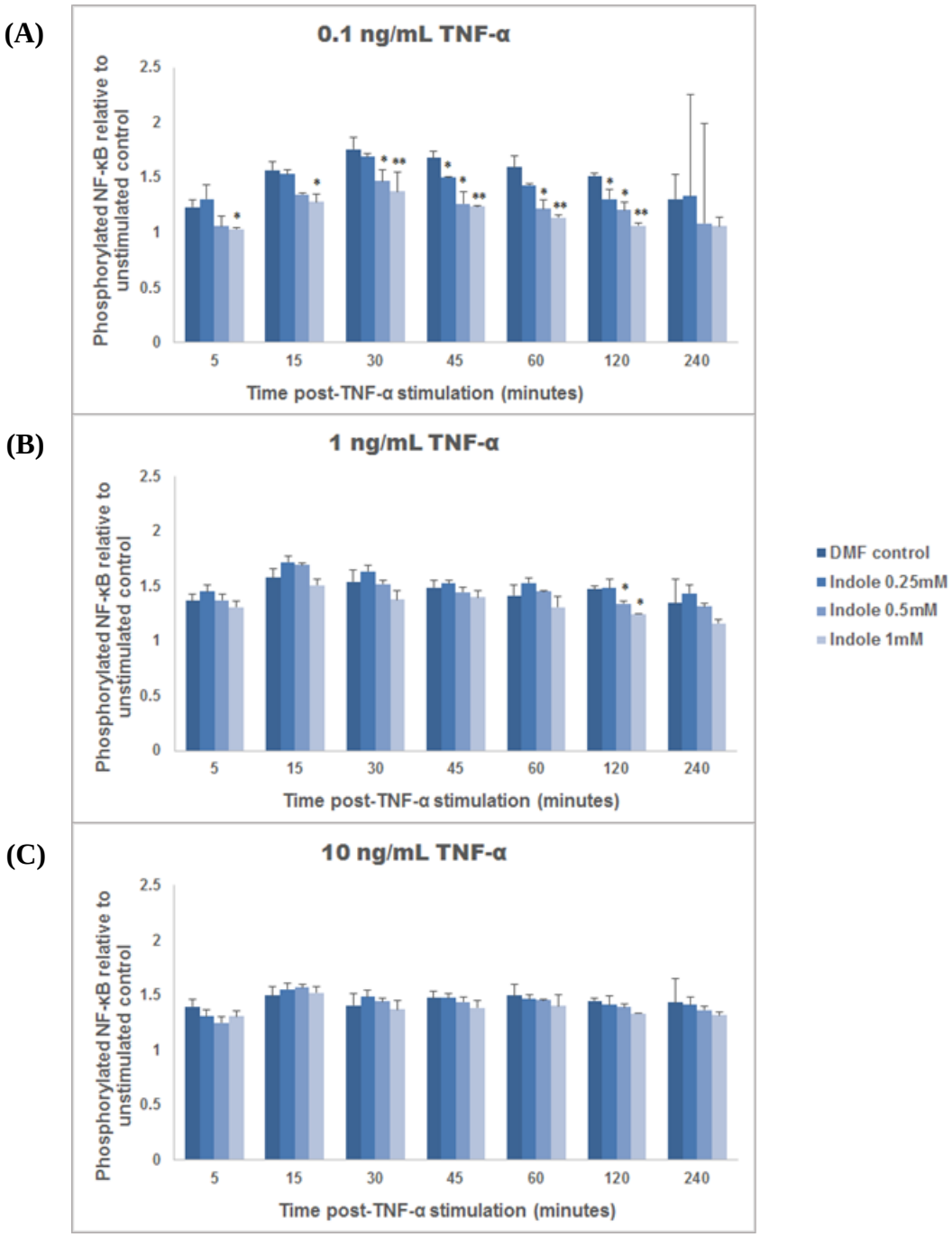

Figure 22. Experimental data of phosphorylated NF-κB (relative to unstimulated control at time t_0) in HCT-8 cells under different concentrations of indole treatment and TNF-α stimulation. (A) 0.1 ng/mL TNF-α stimulation; (B) 1 ng/mL TNF-α stimulation; (C) 10 ng/mL TNF- α stimulation. Statistical significance of phosphorylated NF-κB inhibition for $P < 0.05$ (*) and $P < 0.01$ (**) are indicated in the plots.

Figure 23 shows the concentrations of *de novo* synthesized IL-8 in HCT-8 cells in response to TNF-α stimulation and indole treatment. All concentrations of indole treatment used (0.25, 0.5 and 1 mM) were able to significantly down regulate IL-8 production in HCT-8 cells when stimulated with 0.1 ng/mL TNF-α for 2, 4, 8 and 12 hours as shown in Figure 23 (A). However, at a TNF-α concentration of 1 ng/mL, only 1 mM indole treatment was able to significantly reduce IL-8 production at all four time points (2, 4, 8, 12 hours post-TNF-α stimulation). Whereas, 0.5 mM indole treatment significantly down regulated IL-8 production for 4 hours and 0.25mM significantly reduced IL-8 synthesis only till 2 hours post-TNF-α stimulation at 1 ng/mL as shown in Figure 23 (B). In Figure 23 (C), under 10 ng/mL TNF-α stimulation all three concentrations of indole treatment significantly reduced IL-8 production until 2 hours post-stimulation. Beyond that, only 0.5 and 1mM indole concentrations were effective at downregulating IL-8 synthesis 4 hours post-TNF-α stimulation with no significant reduction observed after 4 hours.

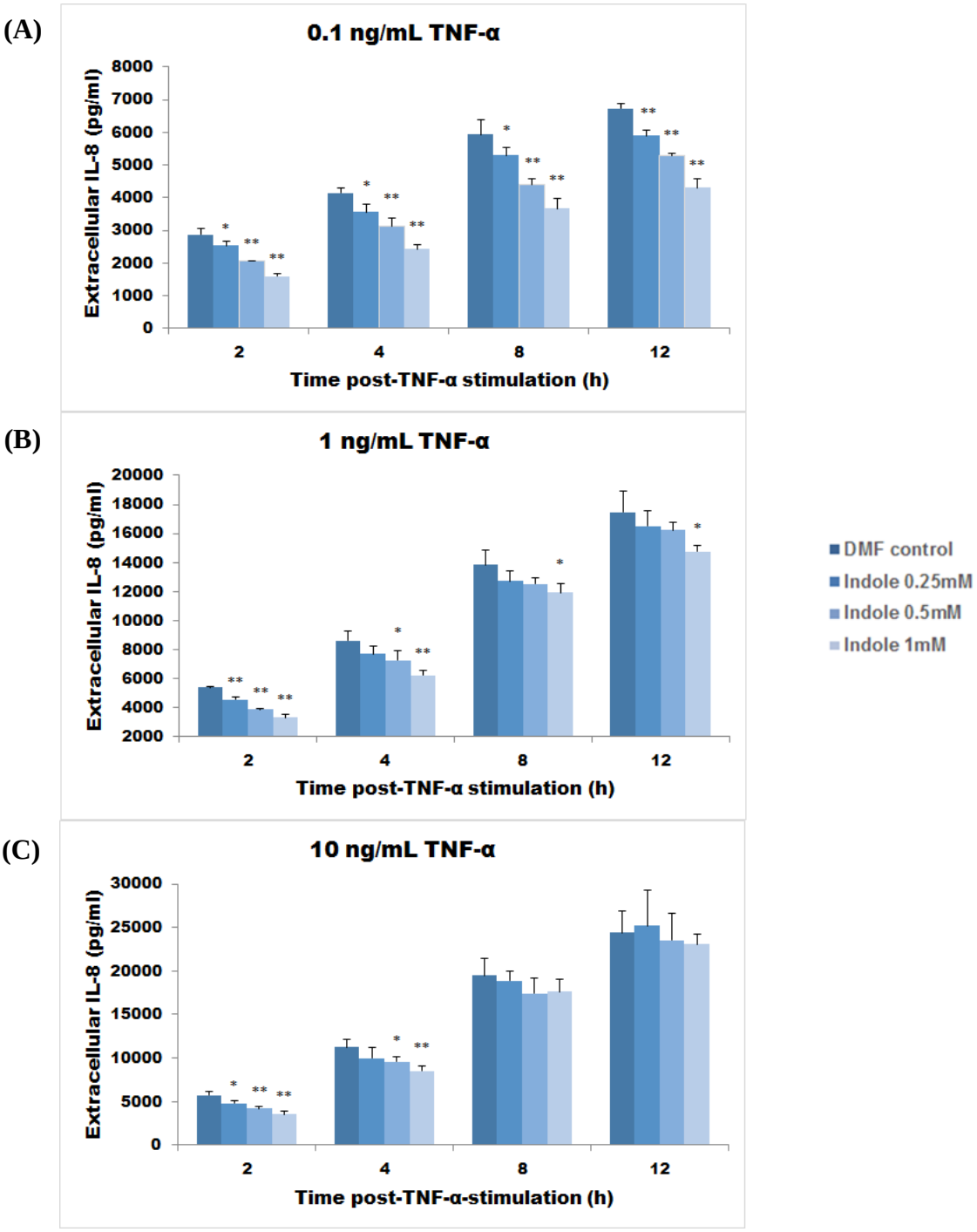

Figure 23. Experimental data of *de novo* synthesized IL-8 in HCT-8 cells under different concentrations of indole treatment and TNF-α stimulation. (A) 0.1 ng/mL TNF-α stimulation; (B) 1 ng/mL TNF-α stimulation; (C) 10 ng/mL TNF- α stimulation. Statistical significance of IL-8 inhibition for $P < 0.05$ (*) and $P < 0.01$ (**) are indicated in the plots.

A portion of the experimental data (randomly selected) was used to train the computational model and optimize model parameters under different exposure conditions. Model predictions for phosphorylated NF-κB and extracellular IL-8 were validated using the remaining data set. Figure 24 shows the comparison between model simulations and experimental data for intracellular phosphorylated NF-κB (normalized to unstimulated control at t_0). It can be seen that the simulation of both randomly selected training sets and validation sets agree with the experimental data with reasonable accuracy indicating that the parameter estimation is numerically robust.

(A)

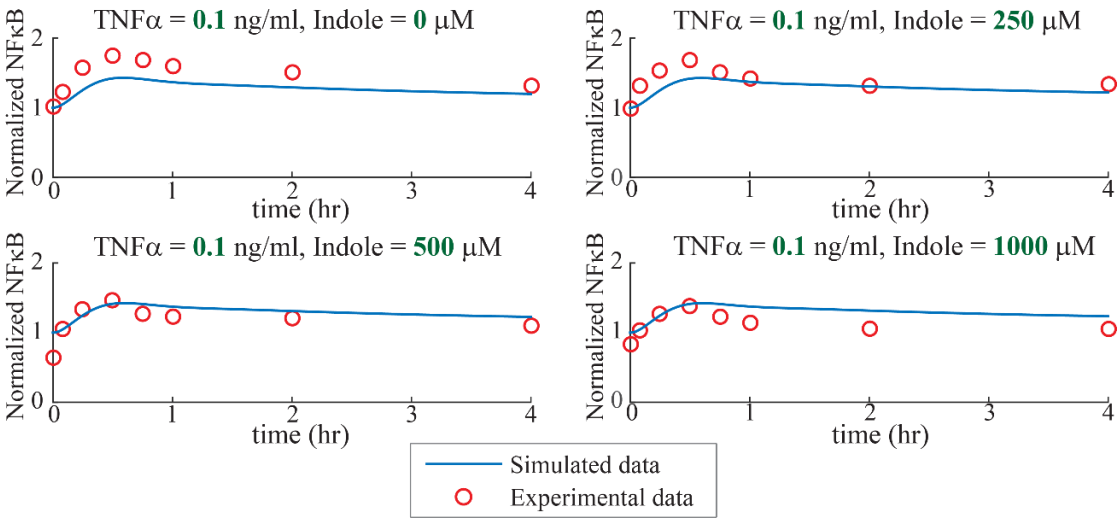

Figure 24. Comparison of model simulation with experimental data for phosphorylated NF-κB normalized to unstimulated control in HCT-8 cells under indole treatment and TNF-α stimulation. (A) 0.1 ng/mL TNF-α stimulation; (B) 1 ng/mL TNF-α stimulation; (C) 10 ng/mL TNF-α stimulation.

(B)

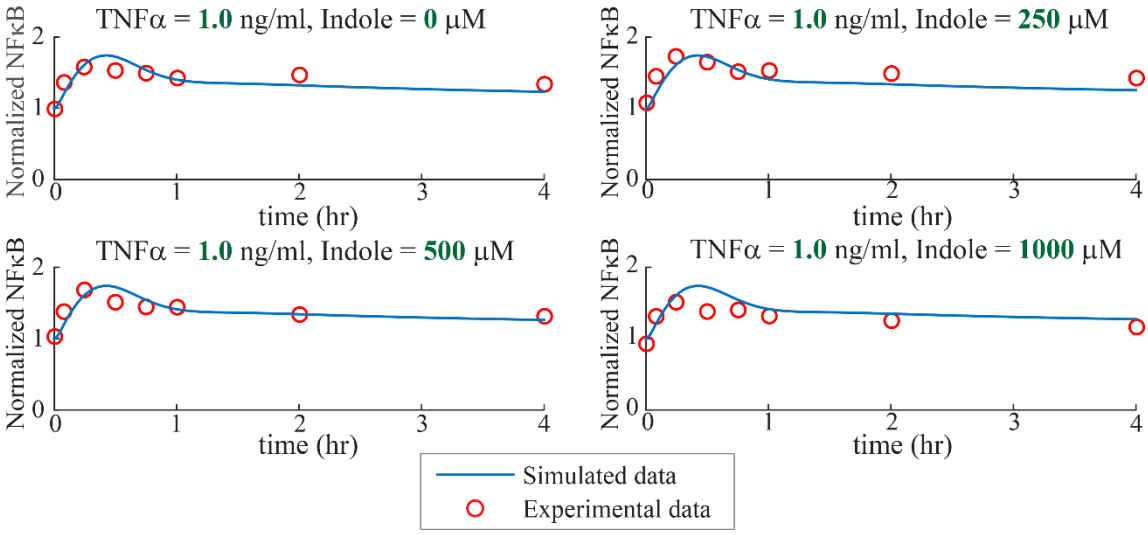

(C)

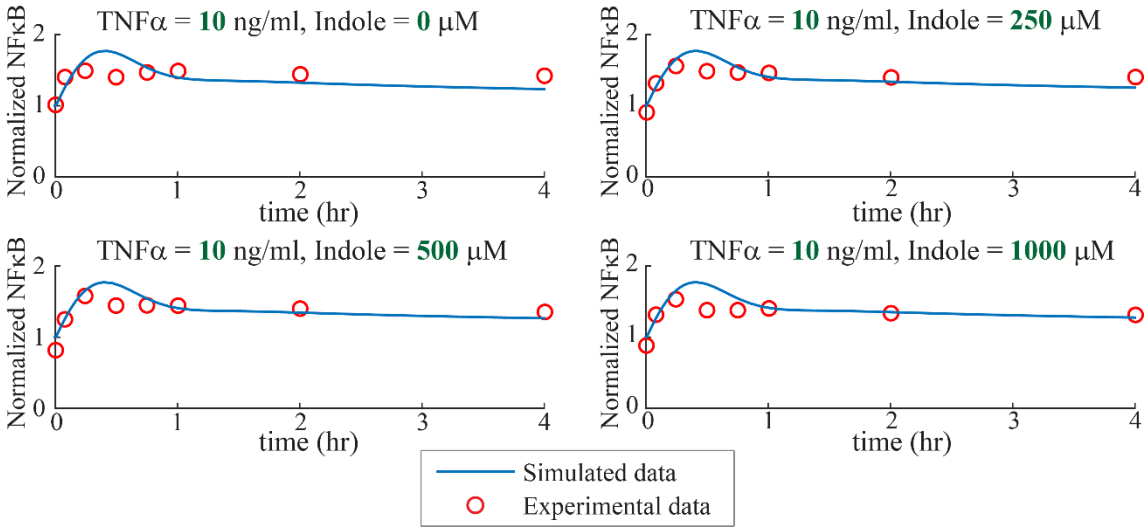

Figure 24. Continued.

Comparison of model predictions and experimental data for extracellular IL-8 under different inputs of TNF-α stimulation and indole treatment are shown in Figure 25. The model simulation of both training sets and validation sets show reasonably good agreement with experimental data. The model predictions for *de novo* IL-8 synthesis are able to capture the overall IL-8 concentration increase with an increasing TNF-α in a dose-dependent manner with a maximum of ~7000 pg/mL for 0.1ng/mL TNF-α stimulation, ~15,000 pg/mL for 1 ng/mL TNF-α stimulation and ~25,000 pg/mL for 10 ng/mL TNF-α stimulation.

(A)

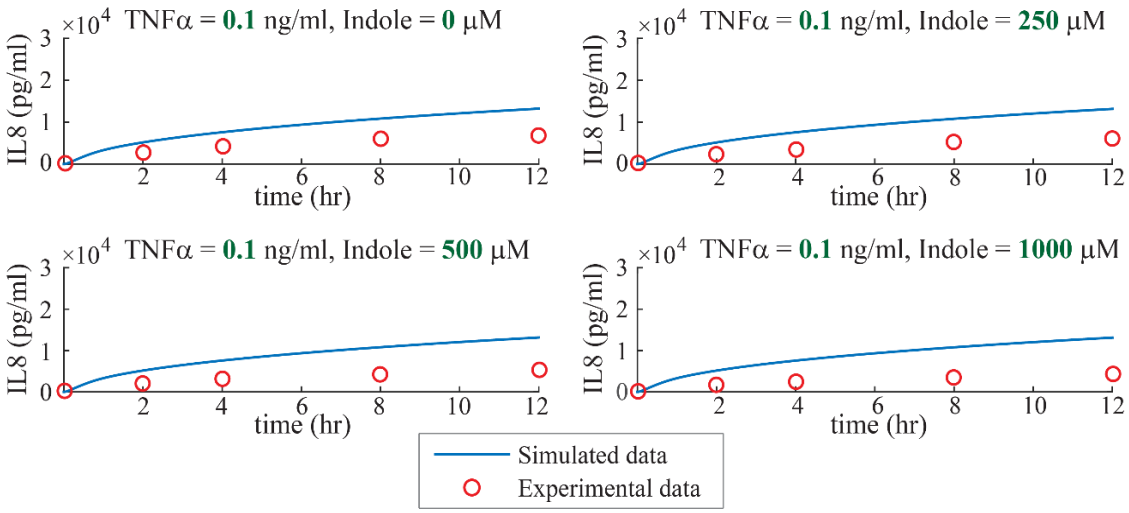

Figure 25. Comparison of model simulation with experimental data for *de novo* IL-8 synthesis in HCT-8 cells under indole treatment and TNF-α stimulation. (A) 0.1 ng/mL TNF-α stimulation; (B) 1 ng/mL TNF-α stimulation; (C) 10 ng/mL TNF-α stimulation.

(B)

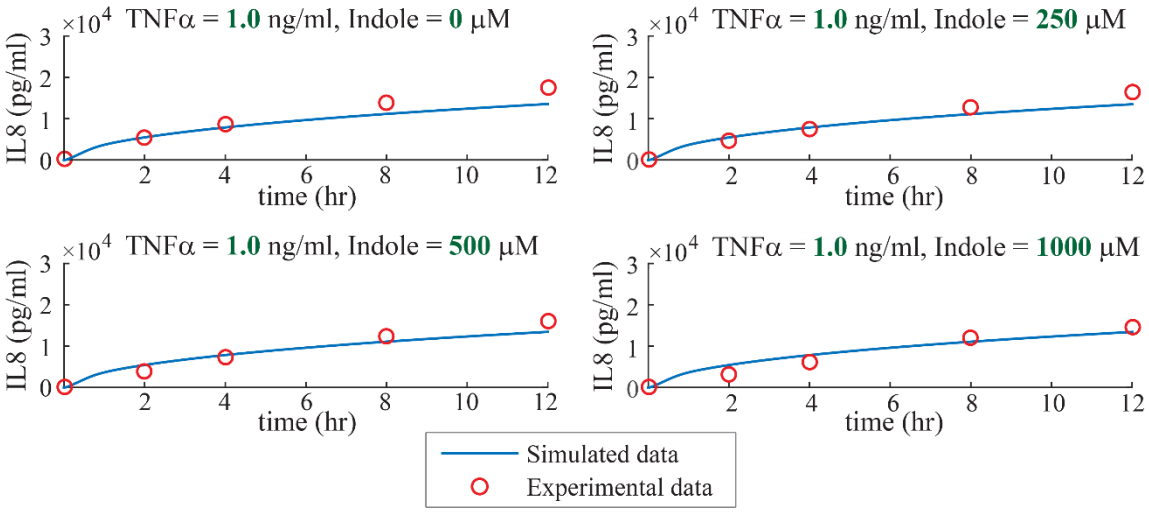

(C)

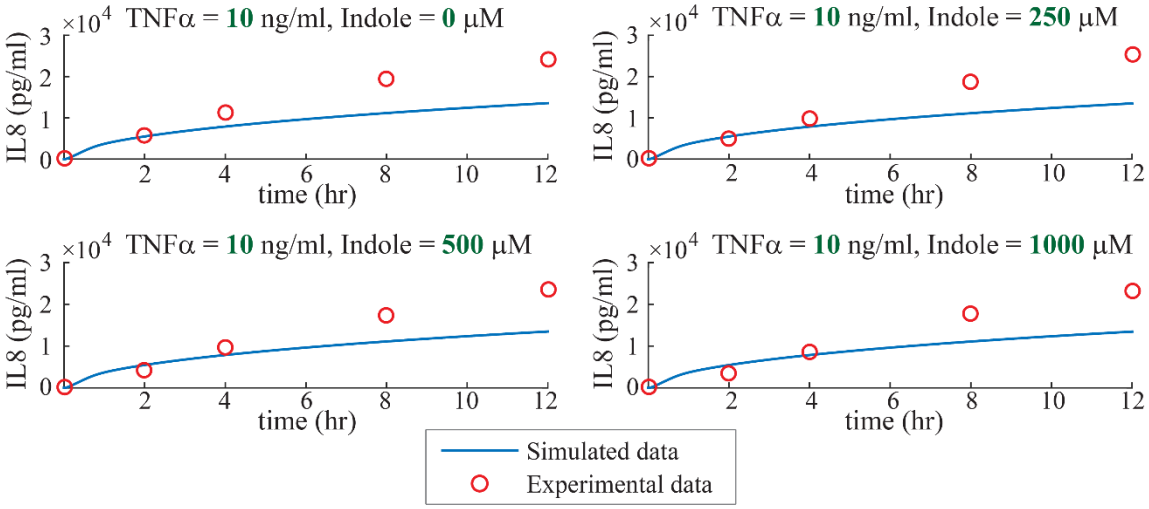

Figure 25. Continued.

In our model we have incorporated two mechanisms for the down-regulation of NF-κB through indole-activated AHR. First, the physical binding of activated transcription factors NF-κB and AHR observed experimentally by Tian *et al*. [160] which leads to cytoplasmic sequestration of NF-κB. Second, AHR-induced activation has been modeled to induce, either directly or indirectly through other transcription factors, the expression of an anti-inflammatory cytokine that down regulates NF-κB signaling. Based on our work [8] and prior studies [149], we hypothesized that the anti-inflammatory cytokine induced by AHR signaling is IL-10, given its ability to inhibit IKK activation as well as nuclear translocation of phosphorylated NF-κB [142,143].

Quantitative reverse transcription polymerase chain reaction (qRT-PCR) analysis of IL-10 expression in indole treated Caco-2 (human epithelial adenocarcinoma) cells showed a dose dependent increase in IL-10 mRNA in response to indole treatment. However, we were unable to detect an increase in IL-10 protein using ELISA or flow cytometry presumably due to the low expression of IL-10 by these cells. We speculate that the activation of IL-10 is mediated by the transcription factor Sp1 that is known to regulate IL-10 production [165] and is known to physically interact with the AHR protein [166]. It is also possible that the observed effect is mediated by an anti-inflammatory cytokine other than IL-10 such as TGF-β as AHR activation has been reported to induce differentiation of naïve T-cells to TGFβ producing regulatory T cells [167].

Our experimental data shows that 1mM indole is able to significantly down regulate TNF-α induced NF-κB activation from 5 minutes to 120 minutes and subsequent synthesis of IL-8 from 2 to 12 hours post-TNF-α stimulation at 0.1 ng/mL. Significant IL-8 inhibition is observed from 2 to 12 hours under 1 ng/mL TNF-α stimulation and only until 4 hours under 10 ng/mL TNF-α stimulation (though NF-κB down regulation is not statistically significant at under these two conditions). If the physical association between NF-κB and AHR were to be the mechanism through which inflammatory signaling is attenuated, our data are in support as more NF-κB would be expected to be activated at higher concentrations of TNF-α (i.e., more NF-κB is present than AHR can bind to). This is a distinct possibility as the abundance of NF-κB in cell cytoplasm is most likely many folds higher than AHR.

In addition, although 0.25 and 0.5 mM indole treatments do not show significant reduction in phosphorylated NF-κB levels, they inhibit IL-8 synthesis to varying degrees and time-points post-TNF-α stimulation. This suggests the involvement of a different transcription factor that might mediate pro-inflammatory responses and induce IL-8 production. One possible candidate could be CCAAT enhancer-binding protein β (CEBPβ; also known as NF-IL6) as it has been reported to activate transcription of IL-8 in synergy with NF-κB [89]. AHR has been shown to repress CEBPβ activation in addition to other transcription factors involved in acute phase response [168].

The model discussed in this chapter is a step towards assimilating our knowledge about host-microbiota interactions, investigating a potential signaling pathway induced by indigenous bacterial metabolite and develop a quantitative understanding of the inter-

kingdom signaling in mammalian hosts. This model can be further used to study the molecular mechanisms involved in immunomodulatory effects of other tryptophan derivatives found in the GI tract of hosts, such as tryptamine and 5-hydroxyindole [68]. The model developed in this work can be used to incorporate other transcription factors such as CEBPβ and Sp1 to represent the molecular mechanism involved in indole-induced anti-inflammatory immune responses of host cells and use experimental data to estimate the unknown parameters of the model.

CHAPTER VI

CONCLUSIONS AND FUTURE WORK

6.1 CONCLUSIONS

The increasing incidence of inflammatory disorders such as inflammatory bowel disease and multiple factors that significantly contribute to the initiation of the disorder such as genetics, diet and dysbiosis are not fully understood and hence motivated us in investigating the role of anti-inflammatory cytokines and intestinal microbiota that help maintain homeostasis. The interaction between intestinal microbiota residing in mammals and their immunomodulatory effects is rapidly emerging as an attractive area of research. The limiting factor in studying microbiota and metabolites secreted by them is the difficulty in culturing indigenous bacteria under laboratory conditions. Coupling mathematical modeling and experimental techniques could bridge the gap between the known and the unknown by understanding molecular mechanisms of host-microbiota interactions from predictions of experimentally validated models. Most of the computational models related to host-microbiota interactions are stochastic due to the unknown mechanisms involved in inter-kingdom signaling. In this dissertation we developed deterministic models based on biochemical reactions involved in intra-cellular signaling (as suggested by prior and current experimental data) to investigate possible mechanisms for maintaining immune homeostasis in the host.

In Chapter IV we developed an experimentally validated mathematical model that represented pro- and anti-inflammatory immune responses through *de novo* synthesis of

TNF-α (pro-inflammatory) and IL-10 (anti-inflammatory) under continuous LPS stimulation (mimicking chronic inflammation). We found that LPS stimulation of macrophages induces TNF-α synthesis which is then attenuated by subsequent synthesis of IL-10. This is likely one of the mechanisms utilized to regulate inflammation and maintain homeostasis in healthy individuals. Most of the inflammatory disorders are accompanied with high TNF-α and low IL-10 concentrations in the body. The use of *de-novo* synthesized anti-inflammatory cytokines could be a good therapeutic modality for alleviating chronic inflammation in patients suffering from auto-inflammatory disorders, provided the anti-inflammatory can be selectively induced.

In Chapter V we studied intra- and inter-kingdom signaling in hosts that arise from indigenous bacterial metabolite indole-induced host immune responses exhibited by down regulation of transcription factor NF-κB and chemokine IL-8 through signal transduction pathway involving activation of AHR host cells. With the extensive data sets generated, we could observe a time and dose dependent efficiency of indole as an anti-inflammatory molecule. Our data shows that 1mM indole is able to down regulate NF-κB activation and IL-8 synthesis for 2, 4, 8 and 12 hours post-TNF-α stimulation at low TNF-α dose such as 0.1 ng/mL. It can inhibit IL-8 production but not down regulate NF-κB at higher concentrations of TNF-α, indicating a possibility of another transcription factor (e.g. CEBPβ) that can induce IL-8 and is a possible target for indole bound AHR.

The contributions made by this dissertation can be summarized as follows:

1. The mathematical model was developed for pro- and anti-inflammatory responses in murine macrophage cell line. However, this is not restricted to macrophages and can be used for other inflammatory cell types as well. The parameters would need to be adjusted accordingly depending on the rates of the specific biochemical reactions represented in the model. Reaction rates are known to vary from one cell type to another. This model will be able to predict if the particular mammalian cell will be able to synthesize enough IL-10 upon inflammatory stimulus to counter-balance TNF-α produced by the cells and hence maintain homeostasis.
2. A mathematical model was developed for host-microbiota interaction through indole signaling in intestinal epithelial cells. This model is not limited to indole signaling and can be used to study the effects of any microbiota metabolite (e.g., other tryptophan-derived molecules, derivatives of indole or potential AHR ligands such as plant flavonoids) to investigate their effects on inflammatory signaling in intestinal epithelial cells or any other cell type. It can also be used as the basis for incorporating other transcription factors that are known to be activated by indole to study its effect on NF-κB activation and IL-8 synthesis.

6.2 RECOMMENDATIONS FOR FUTURE WORK

The primary focus of this dissertation is to develop deterministic models to study integrated pro- and anti-inflammatory immune responses in mammalian host under bacterial components LPS (pro-inflammatory signal) and indole (anti-inflammatory signal) as part of intra- and inter-kingdom signaling in host.

Some recommendations for future work are as follows:

1. Investigation of *de novo* synthesized anti-inflammatory cytokine in mammalian host cells under indole treatment. As indicated in Chapter V of this dissertation, the bacterial metabolite indole is able to attenuate pro-inflammatory markers such as activation of NF-κB and *de novo* synthesis of IL-8. Though physical binding of indole activated AHR and TNF-α activated NF-κB can explain the decrease in available free NF-κB and therefore reduction in IL-8 production, there might a second level of regulation that is involved. It could be activation of another transcription factor such as Sp1 that is known to regulate IL-10 production. We also observed that indole can increase IL-10 mRNA in a dose dependent manner. It would be worth investigating if indole upregulates other anti-inflammatory cytokines such as TGF-β in intestinal epithelial cells as TGF-β is known to be found in GI tract and its involvement in maintaining GI homeostasis is well established [169].

2. Indole has been reported to exhibit dual characteristics; at low concentrations (~50-100 μM) it is an AHR agonist and acts as an antagonist of TCDD-mediated induction of CYP1A1 at higher concentrations (~500 – 1000 μM) [158]. Agonist and antagonist behavior of several ligands have been attributed to their preference for specific binding sites under different conditions, thereby leading to distinct conformational changes in the receptor that results in the induction of different signals. The specific criteria for indole's dual characteristic is not well understood. It would be interesting to investigate what leads to the duality in indole's function as a potential AHR ligand. In the GI tract indole is present in conjunction with other potential endogenous ligands for AHR. Hence, studying indole's preference for specific binding sites on AHR in presence of other competitors can inform us on mechanisms of interaction with other molecules *in vivo*.
3. Indole and other indole-derived molecules have been shown to induce anti-inflammatory immune responses in hosts. Co-culturing bacterial cells and mammalian cells in micro-fluidic devices using bacterial consortia from cecal contents would be an interesting step towards studying the effect of multiple *de novo* bacteria-derived metabolites on host cells. This might reveal some new signaling pathways that are integral in mediating bacteria-derived signals.

REFERENCES

1. Firestein, G.S. Evolving concepts of rheumatoid arthritis. *Nature* **2003**, *423*, 356-361.
2. Barnes, P.J. Immunology of asthma and chronic obstructive pulmonary disease. *Nat Rev Immunol* **2008**, *8*, 183-192.
3. Gottlieb, A.B. Psoriasis: emerging therapeutic strategies. *Nat Rev Drug Discov* **2005**, *4*, 19-34.
4. Goldenberg, M.M. Multiple sclerosis review. *Pharmacol Ther* **2012**, *37*, 175-184.
5. Kaser, A.; Zeissig, S.; Blumberg, R.S. Inflammatory bowel disease. *Annu Rev Immunol* **2010**, *28*, 573-621.
6. Neurath, M.F. Cytokines in inflammatory bowel disease. *Nat Rev Immunol* **2014**, *14*, 329-342.
7. Poltorak, A.; He, X.; Smirnova, I.; Liu, M.-Y.; Huffel, C.V.; Du, X.; Birdwell, D.; Alejos, E.; Silva, M.; Galanos, C., *et al.* Defective LPS signaling in C3H/HeJ and C57BL/10ScCr mice: mutations in Tlr4 gene. *Science* **1998**, *282*, 2085-2088.
8. Maiti, S.; Dai, W.; Alaniz, R.; Hahn, J.; Jayaraman, A. Mathematical modeling of pro- and anti-inflammatory signaling in macrophages. *Processes* **2014**, *3*, 1-18.
9. Gerritsen, J.; Smidt, H.; Rijkers, G.T.; de Vos, W.M. Intestinal microbiota in human health and disease: the impact of probiotics. *Genes Nutr* **2011**, *6*, 209-240.
10. Berg, R.D. The indegenous gastrointestinal microflora. *Trends Microbiol* **1996**, *4*, 430-435.

11. Ley, R.E.; Peterson, D.A.; Gordon, J.I. Ecological and evolutionary forces shaping microbial diversity in the human intestine. *Cell* **2006**, *124*, 837-848.

12. Sears, C.L. A dynamic partnership: celebrating our gut microflora. *Anaerobe* **2005**, *11*, 247-251.

13. Kamada, N.; Seo, S.-U.; Chen, G.Y.; Nunez, G. Role of the gut microbiota in immunity and inflammatory disease. *Nat Rev Immunol* **2013**, *13*, 321-335.

14. Mazmanian, S.K.; Round, J.L.; Kasper, D.L. A microbial symbiosis factor prevents intestinal inflammatory disease. *Nature* **2008**, *453*, 620-625.

15. Cerf-Bensussan, N.; Gaboriau-Routhiau, V. The immune system and the gut microbiota: friends or foes? *Nat Rev Immunol* **2010**, *10*, 735-744.

16. Doré, J.; Simrén, M.; Buttle, L.; Guarner, F. Hot topics in gut microbiota. *United European Gastroenterol J* **2013**, *1*, 311-318.

17. Limbergen, J.V.; Russell, R.K.; Drummond, H.E.; Aldhous, M.C.; Round, N.K.; Nimmo, E.R.; Smith, L.; Gillett, P.M.; McGrogan, P.; Weaver, L.T., *et al.* Definition of phenotypic characteristics of childhood-onset inflammatory bowel disease. *Gastroenterol* **2008**, *135*, 1114-1122.

18. Heuschkel, R.; Salvestrini, C.; Beattie, M.R.; Hildebrand, H.; Walters, T.; Griffiths, A. Guidelines for the management of growth failure in childhood inflammatory bowel disease. *Inflamm Bowel Dis* **2008**, *14*, 839-849.

19. Manichanh, C.; Borruel, N.; Casellas, F.; Guarner, F. The gut microbiota in IBD. *Nat Rev Gastroenterol Hepatol* **2012**, *9*, 599-608.

20. Katz, J.A. Treatment of inflammatory bowel disease with corticosteroids. *Gastroenterol Clin North Am* **2004**, *33*, 171-189.

21. Ardizzone, S.; Cassinotti, A.; Manes, G.; Porro, G.B. Immunomodulators for all patients with inflammatory bowel disease? *Therap Adv Gastroenterol* **2010**, *3*, 31-42.

22. Ford, A.C.; Achkar, J.-P.; Khan, K.J.; Kane, S.V.; Talley, N.J.; Marshall, J.K.; Moayyedi, P. Efficacy of 5-aminosalicylates in ulcerative colitis: systematic review and meta-analysis. *Am J Gastroenterol* **2011**, *106*, 601-616.

23. Ford, A.C.; Kane, S.V.; Khan, K.J.; Achkar, J.-P.; Talley, N.J.; Marshall, J.K.; Moayyedi, P. Efficacy of 5-aminosalicylates in Crohn's disease: systematic review and meta-analysis. *Am J Gastroenterol* **2011**, *106*, 617-629.

24. Khanna, R.; Sattin, B.D.; Afif, W.; Benchimol, E.I.; Bernard, E.J.; Bitton, A.; Bressler, B.; Fedorak, R.N.; Ghosh, S.; Greenberg, G.R., *et al.* Review article: a clinician's guide for therapeutic drug monitoring of infliximab in inflammatory bowel disease. *Aliment Pharmacol Ther* **2013**, *38*, 447-459.

25. Danese, S. IBD: Golimumab in ulcerative colitis: a 'menage a trois' of drugs. *Nat Rev Gastroenterol Hepatol* **2013**, *10*, 511-512.

26. McLean, L.P.; Shea-Donohue, T.; Cross, R.K. Vedolizumab for the treatment of ulcerative colitis and Crohn’s disease. *Immunotherapy* **2012**, *4*, 883-898.

27. Kumar, A.; Auron, M.; Aneja, A.; Mohr, F.; Jain, A.; Shen, B. Inflammatory bowel disease: perioperative pharmacological considerations. *Mayo Clin Proc* **2011**, *86*, 748-757.

28. Larson, D.W.; Pemberton, J.H. Current concepts and controversies in surgery for IBD. *Gastroenterol* **2004**, *126*, 1611-1620.

29. Bansal, T.; Alaniz, R.C.; Wood, T.K.; Jayaraman, A. The bacterial signal indole increases epithelial-cell tight-junction resistance and attenuates indicators of inflammation. *Proc Natl Acad Sci U S A* **2010**, *107*, 228-233.

30. Shimada, Y.; Kinoshita, M.; Harada, K.; Mizutani, M.; Masahata, K.; Kayama, H.; Takeda, K. Commensal bacteria-dependent indole production enhances epithelial barrier function in the colon. *Plos One* **2013**, *8*, doi: 10.1371/journal.pone.0080604.

31. Lipniacki, T.; Paszek, P.; Brasier, A.R.; Luxon, B.; Kimmel, M. Mathematical model of NF-κB regulatory module. *J Theor Biol* **2004**, *228*, 195-215.

32. Huang, Z.; Senocak, F.; Jayaraman, A.; Hahn, J. Integrated modeling and experimental approach for determining transcription factor profiles from fluorescent reporter data. *BMC Syst Biol* **2008**, *2*, 64-74.

33. Moya, C.; Huang, Z.; Cheng, P.; Jayaraman, A.; Hahn, J. Investigation of IL-6 and IL-10 signalling via mathematical modelling. *IET Syst Biol* **2011**, *5*, 15-26.

34. Matinon, F.; Jurg, T. Inflammatory caspases: linking an intracellular innate immune system to autoinflammatory diseases. *Cell* **2004**, *117*, 561-574.

35. Medzhitov, R.; Janeway, C., Jr. Innate immune recognition: mechanisms and pathways. *Immunol Rev* **2000**, *173*, 89-97.

36. Crispe, I.N. The liver as a lymphoid organ. *Annu Rev Immunol* **2009**, *27*, 147-163.

37. Swirski, F.K.; Nahrendorf, M.; Etzrodt, M.; Wildgruber, M.; Cortez-Retamozo, V.; Panizzi, P.; Figueiredo, J.-L.; Kohler, R.H.; Chudnovskiy, A.; Waterman, P., *et al.* Identification of splenic reservoir monocytes and their deployment to inflammatory sites. *Science* **2009**, *325*, 612-616.

38. Jung, C.; Hugot, J.-P.; Barreau, F. Peyer's patches: the immune sensors of the intestine. *Int J Inflam* **2010**, *2010*, 823710-823736.

39. Andersen-Nissen, E.; Smith, K.D.; Bonneau, R.; Strong, R.K.; Aderem, A. A conserved surface on Toll-like receptor 5 recognizes bacterial flagellin. *J Exp Med* **2007**, *204*, 393-403.

40. Adams, D.O.; Hamilton, T.A. The cell biology of macrophage activation. *Annu Rev Immunol* **1984**, *2*, 283-318.

41. Kolaczkowska, E.; Kubes, P. Neutrophil recruitment and function in health and inflammation. *Nat Rev Immunol* **2013**, *13*, 159-175.

42. University of Washington. Phagocytosis. http://courses.washington.edu/conj/bloodcells/phagocytosis.htm (27/12/14).

43. Steinman, R.M.; Hemmi, H. Dendritic cells: translating innate to adaptive immunity. *From innate immunity to immunological memory*, Springer Berlin Heidelberg **2006**; *311*, 17-58.

44. Sun, Z.; Andersson, R. NF-κB activation and inhibition: A review. *Shock* **2002**, *18*, 99-106.

45. Opal, S.M.; DePalo, V.A. Anti-inflammatory cytokines. *Chest* **2000**, *117*, 1162-1172.

46. Rahman, I.; MacNee, W. Role of transcription factors in inflammatory lung diseases. *Thorax* **1998**, *53*, 601-612.

47. Fujio, K.; Okamura, T.; Yamamoto, K. The family of IL-10-secreting CD4+ T Cells. *Adv Immunol* **2010**, *105*, 99-130.

48. Martinez, F.O.; Gordon, S. The M1 and M2 paradigm of macrophage activation: time for reassessment. *F1000 Prime Rep* **2014**, *6*, doi: 10.12703/P6-13.

49. Martinez, F.O.; Sica, A.; Mantovani, A.; Locati, M. Macrophage activation and polarization. *Front Biosci* **2008**, *13*, 453-461.

50. Gill, S.R.; Pop, M.; DeBoy, R.T.; Eckburg, P.B.; Turnbaugh, P.J.; Samuel, B.S.; Gordon, J.I.; Relman, D.A.; Fraser-Liggett, C.M.; Nelson, K.E. Metagenomic analysis of the human distal gut microbiome. *Science* **2006**, *312*, 1355-1359.

51. Tlaskalová-Hogenováa, H.; Štěpánkováa, R.; Hudcovica, T.; Tučkováa, L.; Cukrowskab, B.; Lodinová-Žádníkovác, R.; Kozákováa, H.; Rossmanna, P.; Bártovád, J.; Sokola, D., *et al.* Commensal bacteria (normal microflora), mucosal immunity and chronic inflammatory and autoimmune diseases. *Immunol Lett* **2004**, *93*, 97-108.

52. Cummings, J.H.; Macfarlane, G.T. Role of intestinal bacteria in nutrient metabolism. *Clin Nutr* **1997**, *16*, 3-11.

53. Arpaia, N.; Campbell, C.; Fan, X.; Dikiy, S.; van der Veeken, J.; deRoos, P.; Liu, H.; Cross, J.R.; Pfeffer, K.; Coffer, P.J., *et al.* Metabolites produced by commensal bacteria promote peripheral regulatory T-cell generation. *Nature* **2013**, *504*, 451-455.

54. O'Hara, A.M.; Shanahan, F. The gut flora as a forgotten organ. *EMBO Reports* **2006**, *7*, 688-693.

55. Kucharzik, T.; LÜGering, N.; Rautenberg, K.; LÜGering, A.; Schmidt, M.A.; Stoll, R.; Domschke, W. Role of M Cells in intestinal barrier function. *Ann NY Acad Sci* **2000**, *915*, 171-183.

56. Yang, J.Y.; Karr, J.R.; Watrous, J.D.; Dorrestein, P.C. Integrating `-omics' and natural product discovery platforms to investigate metabolic exchange in microbiomes. *Curr Opin Chem Biol* **2011**, *15*, 79-87.

57. Bansal, T.; Englert, D.; Lee, J.; Hegde, M.; Wood, T.K.; Jayaraman, A. Differential effects of epinephrine, norepinephrine, and indole on *Escherichia coli* O157:H7 chemotaxis, colonization, and gene expression. *Infect Immun* **2007**, *75*, 4597-4607.

58. Domka, J.; Lee, J.; Wood, T.K. YliH (BssR) and YceP (BssS) regulate *Escherichia coli* K-12 biofilm formation by influencing cell signaling. *Appl Environ Microbiol* **2006**, *72*, 2449-2459.

59. Karlin, D.A.; Mastromarino, A.J.; Jones, R.D.; Stroehlein, J.R.; Lorentz, O. Fecal skatole and indole and breath methane and hydrogen in patients with large bowel polyps or cancer. *J Cancer Res Clin Oncol* **1985**, *109*, 135-141.

60. Zuccato, E.; Venturi, M.; Di Leo, G.; Colombo, L.; Bertolo, C.; Doldi, S.; Mussini, E. Role of bile acids and metabolic activity of colonic bacteria in increased risk of colon cancer after cholecystectomy. *Dig Dis Sci* **1993**, *38*, 514-519.

61. Li, G.; Young, K.D. Indole production by the tryptophanase TnaA in *Escherichia coli* is determined by the amount of exogenous tryptophan. *Microbiology* **2013**, *159*, 402-410.

62. Lee, J.-H.; Lee, J. Indole as an intercellular signal in microbial communities. *Microbiol Rev* **2010**, *34*, 426-444.

63. Smith, T. A modification of the method for determining the production of indol by bacteria *J Exp Med* **1897**, *2*, 543-547.

64. Hirakawa, H.; Inazumi, Y.; Masaki, T.; Hirata, T.; Yamaguchi, A. Indole induces the expression of multidrug exporter genes in *Escherichia coli*. *Mol Microbiol* **2005**, *55*, 1113–1126.

65. Oh, S.; Go, G.W.; Mylonakis, E.; Kim, Y. The bacterial signalling molecule indole attenuates the virulence of the fungal pathogen Candida albicans. *J App Microbiol* **2012**, *113*, 622-628.

66. Wikoff, W.R.; Anfora, A.T.; Liu, J.; Schultz, P.G.; Lesley, S.A.; Peters, E.C.; Siuzdak, G. Metabolomics analysis reveals large effects of gut microflora on mammalian blood metabolites. *Proc Natl Acad Sci U S A* **2009**, doi: 10.1073/pnas.0812874106.

67. Crumeyrolle-Arias, M.; Tournaire, M.-C.; Rabot, S.; Malpaux, B.; Thiéry, J.-C. 5-hydroxyoxindole, an indole metabolite, is present at high concentrations in brain. *J Neuro Res* **2008**, *86*, 202-207.

68. Sridharan, G.V.; Choi, K.; Klemashevich, C.; Wu, C.; Prabakaran, D.; Pan, L.B.; Steinmeyer, S.; Mueller, C.; Yousofshahi, M.; Alaniz, R.C., *et al.* Prediction and

quantification of bioactive microbiota metabolites in the mouse gut. *Nat Commun* **2014**, *5*, doi: 10.1038/ncomms6492.

69. Ashcroft, S.J.; Crossley, J.R.; Crossley, P.C. The effect of N-acylglucosamines on the biosynthesis and secretion of insulin in the rat. *Biochem J* **1976**, *154*, 701-707.

70. Tonndorf, J. Davis-1961 revisited. Signal transmission in the cochlear hair cell-nerve junction. *Arch Otolaryngol* **1975**, *101*, 528-535.

71. Foxwell, M.B.; Barrett, K.; Feldmann, M. Cytokine receptors: structure and signal transduction. *Clin Exp Immunol* **1992**, *90*, 161-169.

72. Raghuwanshi, S.K.; Su, Y.; Singh, V.; Haynes, K.; Richmond, A.; Richardson, R.M. The chemokine receptors CXCR1 and CXCR2 couple to distinct G Protein-coupled receptor kinases to mediate and regulate leukocyte functions. *J Immunol* **2012**, *189*, 2824-2832.

73. Sensory receptors. http://www.seehint.com/word.asp?no=13043 (27/12/14).

74. Aggarwal, B.B. Signalling pathways of the TNF superfamily: a double-edged sword. *Nat Rev Immunol* **2003**, *3*, 745-756.

75. Popa, C.; Netea, M.G.; van Riel, P.L.C.M.; van der Meer, J.W.M.; Stalenhoef, A.F.H. The role of TNF-α in chronic inflammatory conditions, intermediary metabolism, and cardiovascular risk. *J Lipid Res* **2007**, *48*, 751-762.

76. B, C.W. The treatement of malignant tumors by repeated inoculations of erysipelas. With a report of ten original cases. *Am J Med Sci* **1893**, *105*, 487-511.

77. Carswell, E.A.; Old, L.J.; Kassel, R.L.; Green, S.; Fiore, N.; Williamson, B. An endotoxin-induced serum factor that causes necrosis of tumors. *Proc Natl Acad Sci U S A* **1975**, *72*, 3666-3670.

78. Beutler, B.A.; Milsark, I.W.; Cerami, A. Cachectin/tumor necrosis factor: production, distribution, and metabolic fate in vivo. *J Immunol* **1985**, *135*, 3972-3977.

79. Sandborn, W.J.; Hanauer, S.B. Antitumor necrosis factor therapy for inflammatory bowel disease: a review of agents, pharmacology, clinical results, and safety. *Inflam Bowel Dis* **1999**, *5*, 119-133.

80. van Heel, D.A.; Udalova, I.A.; De Silva, A.P.; McGovern, D.P.; Kinouchi, Y.; Hull, J.; Lench, N.J.; Cardon, L.R.; Carey, A.H.; Jewell, D.P., *et al.* Inflammatory bowel disease is associated with a TNF polymorphism that affects an interaction between the OCT1 and NF-κB transcription factors. *Hum Mol Gen* **2002**, *11*, 1281-1289.

81. Aggarwal, B.B.; Kohr, W.J.; Hass, P.E.; Moffat, B.; Spencer, S.A.; Henzel, W.J.; Bringman, T.S.; Nedwin, G.E.; Goeddel, D.V.; Harkins, R.N. Human tumor necrosis factor. Production, purification, and characterization. *J Biol Chem* **1985**, *260*, 2345-2354.

82. Smith, R.A.; Baglioni, C. The active form of tumor necrosis factor is a trimer. *J Biol Chem* **1987**, *262*, 6951-6954.

83. Naudé, P.J.; den Boer, J.A.; Luiten, P.G.; Eisel, U.L. Tumor necrosis factor receptor cross-talk. *FEBS J* **2011**, *278*, 888-898.

84. Maury, C.P.J. Tumour Necrosis Factor—an overview. *Acta Med Scand* **1986**, *220*, 387-394.

85. Idriss, H.T.; Naismith, J.H. TNF-α and the TNF receptor superfamily: Structure-function relationship(s). *Microsc Res Tech* **2000**, *50*, 184-195.

86. Fiorentino, D.F.; Zlotnik, A.; Mosmann, T.R.; Howard, M.; O'Garra, A. IL-10 inhibits cytokine production by activated macrophages. *J Immunol* **1991**, *147*, 3815-3822.

87. Brat, D.J.; Bellail, A.C.; Van Meir, E.G. The role of interleukin-8 and its receptors in gliomagenesis and tumoral angiogenesis. *Neuro-Oncol* **2005**, *7*, 122-133.

88. Rossi, D.; Zlotnik, A. The Biology of Chemokines and their Receptors. *Annu Rev Immunol* **2000**, *18*, 217-242.

89. Matsusaka, T.; Fujikawa, K.; Nishio, Y.; Mukaida, N.; Matsushima, K.; Kishimoto, T.; Akira, S. Trancription factors NF-IL6 and NF-kB synergistically activate transcription of the inflammatory cytokines, interleukin 6 and interleukin 8. *Proc Natl Acad Sci U S A* **1993**, *90*, 10193-10197.

90. Horcher, M.; Rot, A.; Aschauer, H.; Besemer, J. IL-8 derivatives with a reduced potential to form homodimers are fully active *in vitro* and *in vivo*. *Cytokine* **1998**, *10*, 1-12.

91. Rajarathnam, K.; Sykes, B.D.; Kay, C.M.; Dewald, B.; Geiser, T.; Baggiolini, M.; Clark-Lewis, I. Neutrophil activation by monmeric interleukin-8. *Science* **1994**, *264*, 90-92.

92. Singh, J.; Simoes, B.; Howell, S.; Farnie, G.; Clarke, R. Recent advances reveal IL-8 signaling as a potential key to targeting breast cancer stem cells. *Breast Cancer Res* **2013**, *15*, 210-218.

93. Ouyang, W.; Rutz, S.; Crellin, N.K.; Valdez, P.A.; Hymowitz, S.G. Regulation and functions of the IL-10 family of cytokines in inflammation and disease. *Annu Rev Immunol* **2011**, *29*, 71-109.

94. Fiorentino, D.F.; Bond, M.W.; Mosmann, T.R. Two types of mouse T helper cell. IV. Th2 clones secrete a factor that inhibits cytokine production by Th1 clones. *J Exp Med* **1989**, *170*, 2081-2095.

95. Kühn, R.; Löhler, J.; Rennick, D.; Rajewsky, K.; Müller, W. Interleukin-10-deficient mice develop chronic enterocolitis. *Cell* **1993**, *75*, 263-274.

96. Human Genome Sequencing, C.I. Finishing the euchromatic sequence of the human genome. *Nature* **2004**, *431*, 931-945.

97. Sen, R.; Baltimore, D. Multiple nuclear factors interact with the immunoglobulin enhancer sequences. *Cell* **1986**, *46*, 705-716.

98. Sen, R.; Baltimore, D. Inducibility of κ immunoglobulin enhancer-binding protein NF-κB by a posttranslational mechanism. *Cell* **1986**, *47*, 921-928.

99. Baeuerle, P.A.; Baltimore, D. IκB: A specific inhibitor of the NF-κB transcription factor. *Science* **1988**, *242*, 540-545.

100. Barnes, P.J.; Karin, M. Nuclear factor-κB — a pivotal transcription factor in chronic inflammatory diseases. *New Engl J Med* **1997**, *336*, 1066-1071.

101. Stockinger, B.; Meglio, P.D.; Gialitakis, M.; Duarte, J.H. The aryl hydrocarbon receptor: multitasking in the immune system. *Annu Rev Immunol* **2014**, *32*, 403-432.

102. Busbee, P.B.; Rouse, M.; Nagarkatti, M.; Nagarkatti, P.S. Use of natural AhR ligands as potential therapeutic modalities against inflammatory disorders. *Nutr Rev* **2013**, *71*, 353-369.

103. Kewley, R.J.; Whitelaw, M.L.; Chapman-Smith, A. The mammalian basic helix–loop–helix/PAS family of transcriptional regulators. *Int J of Biochem Cell Biol* **2004**, *36*, 189-204.

104. Westerhoff, H.V.; Palsson, B.O. The evolution of molecular biology into systems biology. *Nat Biotech* **2004**, *22*, 1249-1252.

105. Bandyopadhyay, S.; Soto-Nieves, N.; Macián, F. Transcriptional regulation of T cell tolerance. *Semin Immunol* **2007**, *19*, 180-187.

106. Eungdamrong, N.J.; Iyengar, R. Modeling cell signaling networks. *Biol Cell* **2004**, *96*, 355-362.

107. Hoffmann, A.; Natoli, G.; Ghosh, G. Transcriptional regulation via the NF-[kappa]B signaling module. *Oncogene* **2006**, *25*, 6706-6716.

108. Hoffmann, A.; Levchenko, A.; Scott, M.L.; Baltimore, D. The IκB-NF-κB signaling module: temporal control and selective gene activation. *Science* **2002**, *298*, 1241-1245.

109. Vodovotz, Y. Deciphering the complexity of acute inflammation using mathematical models. *Immunol Res* **2006**, *36*, 237-245.

110. Ideker, T.; Lauffenburger, D. Building with a scaffold: emerging strategies for high- to low-level cellular modeling. *Trends Biotechnol* **2003**, *21*, 255-262.

111. Arnosti, D.N.; Ay, A. Boolean modeling of gene regulatory networks: Driesch redux. *Proc Natl Acad Sci U S A* **2012**, *109*, 18239-18240.

112. Rangamani, P.; Sirovich, L. Survival and apoptotic pathways initiated by TNF-α: Modeling and predictions. *Biotechnol Bioeng* **2007**, *97*, 1216-1229.

113. Brown, A.J. Enzyme action. *J Chem Soc* **1902**, *81*, 373-388.

114. Moya, C.; Huang, Z.; Cheng, P.; Jayaraman, A.; Hahn, J. Investigation of IL-6 and IL-10 signalling via mathematical modelling. *IET Syst Biol* **2011**, *5*, 15-26.

115. Karlsson, F.H.; Nookaew, I.; Petranovic, D.; Nielsen, J. Prospects for systems biology and modeling of the gut microbiome. *Trends Biotechnol* **2011**, *29*, 251-258.

116. Shoaie, S.; Karlsson, F.; Mardinoglu, A.; Nookaew, I.; Bordel, S.; Nielsen, J. Understanding the interactions between bacteria in the human gut through metabolic modeling. *Sci Rep* **2013**, *3*, doi: 10.1038/srep02532.

117. Marino, S.; Baxter, N.T.; Huffnagle, G.B.; Petrosino, J.F.; Schloss, P.D. Mathematical modeling of primary succession of murine intestinal microbiota. *Proc Natl Acad Sci U S A* **2014**, *111*, 439-444.

118. Christley, S.; Cockrell, C.; An, G. Computational studies of the intestinal host-microbiota interactome. *Computation* **2014**, *3*, 2-28.

119. Beerenwinkel, N.; Sing, T.; Lengauer, T.; Rahnenführer, J.; Roomp, K.; Savenkov, I.; Fischer, R.; Hoffmann, D.; Selbig, J.; Korn, K., *et al.* Computational methods

for the design of effective therapies against drug resistant HIV strains. *Bioinformatics* **2005**, *21*, 3943-3950.

120. Mandal, S.; Sarkar, R.R.; Sinha, S. Mathematical models of malaria - a review. *Malaria J* **2011**, *10*, 202-220.

121. Marino, S.; Linderman, J.; Kirschner, D.E. A multi-faceted approach to modeling the immune response in Tuberculosis. *Interdiscip Rev Syst Biol* **2011**, *3*, 479-489.

122. Smith, A.M.; Ribeiro, R.M. Modeling the viral dynamics of influenza A virus infection. *Crit Rev Immunol* **2010**, *30*, 291-298.

123. Nathan, C. Points of control in inflammation. *Nature* **2002**, *420*, 846-852.

124. Hansson, G.K.; Libby, P.; Schönbeck, U.; Yan, Z.-Q. Innate and adaptive immunity in the pathogenesis of atherosclerosis. *Circ Res* **2002**, *91*, 281-291.

125. Mantovani, A.; Cassatella, M.A.; Costantini, C.; Jaillon, S. Neutrophils in the activation and regulation of innate and adaptive immunity. *Nat Rev Immunol* **2011**, *11*, 519-531.

126. Lodes, M.J.; Cong, Y.; Elson, C.O.; Mohamath, R.; Landers, C.J.; Targan, S.R.; Fort, M.; Hershberg, R.M. Bacterial flagellin is a dominant antigen in Crohn disease. *J Clin Invest* **2004**, *113*, 1296-1306.

127. Montuschi, P. Pharmacotheraphy of patients with mild persistent asthma: strategies and unresolved issues. *Front Pharmacol* **2011**, *2*, doi: 10.3389/fphar.2011.00035.

128. Trivedi, P.J.; Adams, D.H. Mucosal immunity in liver autoimmunity: A comprehensive review. *J Autoimmun* **2013**, *46*, 97-111.

129. Ghosh, G.; Wang, V.Y.-F.; Huang, D.-B.; Fusco, A. NF-κB regulation: lessons from structures. *Immunol Rev* **2012**, *246*, 36-58.

130. Baeuerle, P.A.; Baltimore, D. A 65-kappaD subunit of active NF-kappaB is required for inhibition of NF-kappaB by I kappaB. *Genes Dev* **1989**, *3*, 1689-1698.

131. Hayden, M.S.; Ghosh, S. Shared principles in NF-κB signaling. *Cell* **2008**, *132*, 344-362.

132. Bogdan, C.; Vodovotz, Y.; Nathan, C. Macrophage deactivation by interleukin 10. *Journal Exp Med* **1991**, *174*, 1549-1555.

133. Collart, M.A.; Baeuerle, P.; Vassalli, P. Regulation of tumor necrosis factor alpha transcription in macrophages: involvement of four kappa B-like motifs and of constitutive and inducible forms of NF-kappa B. *Mol Cell Biol* **1990**, *10*, 1498-1506.

134. Saraiva, M.; Christensen, J.R.; Tsytsykova, A.V.; Goldfeld, A.E.; Ley, S.C.; Kioussis, D.; O′Garra, A. Identification of a macrophage-specific chromatin signature in the IL-10 locus. *J Immunol* **2005**, *175*, 1041-1046.

135. Scott, M.L.; Fujita, T.; Liou, H.C.; Nolan, G.P.; Baltimore, D. The p65 subunit of NF-kappa B regulates I kappa B by two distinct mechanisms. *Genes Dev* **1993**, *7*, 1266-1276.

136. Zhang, S.Q.; Kovalenko, A.; Cantarella, G.; Wallach, D. Recruitment of the IKK signalosome to the p55 TNF receptor: RIP and A20 bind to NEMO (IKKγ) upon receptor stimulation. *Immunity* **2000**, *12*, 301-311.

137. Benkhart, E.M.; Siedlar, M.; Wedel, A.; Werner, T.; Ziegler-Heitbrock, H.W.L. Role of Stat3 in lipopolysaccharide-induced IL-10 gene expression. *J Immunol* **2000**, *165*, 1612-1617.

138. Lang, R.; Patel, D.; Morris, J.J.; Rutschman, R.L.; Murray, P.J. Shaping gene expression in activated and resting primary macrophages by IL-10. *J Immunol* **2002**, *169*, 2253-2263.

139. Niemand, C.; Nimmesgern, A.; Haan, S.; Fischer, P.; Schaper, F.; Rossaint, R.; Heinrich, P.C.; Müller-Newen, G. Activation of STAT3 by IL-6 and IL-10 in primary human macrophages is differentially modulated by suppressor of cytokine signaling 3. *J Immunol* **2003**, *170*, 3263-3272.

140. Lee, K.-C.; Chang, H.-H.; Chung, Y.-H.; Lee, T.-Y. Andrographolide acts as an anti-inflammatory agent in LPS-stimulated RAW264.7 macrophages by inhibiting STAT3-mediated suppression of the NF-κB pathway. *J Ethnopharmacol* **2011**, *135*, 678-684.

141. Bhattacharyya, S.; Sen, P.; Wallet, M.; Long, B.; Baldwin, A.S.; Tisch, R. Immunoregulation of dendritic cells by IL-10 is mediated through suppression of the PI3K/Akt pathway and of IκB kinase activity. *Blood* **2004**, *104*, 1100-1109.

142. Driessler, F.; Venstrom, K.; Sabat, R.; Asadullah, K.; Schottelius, A.J. Molecular mechanisms of interleukin-10-mediated inhibition of NF-κB activity: a role for p50. *Clin Exp Immunol* **2004**, *135*, 64-73.

143. Schottelius, A.J.G.; Mayo, M.W.; Sartor, R.B.; Baldwin, A.S. Interleukin-10 signaling blocks inhibitor of κB kinase activity and nuclear factor κB DNA binding. *J Biol Chem* **1999**, *274*, 31868-31874.

144. Singh, A.; Jayaraman, A.; Hahn, J. Modeling regulatory mechanisms in IL-6 signal transduction in hepatocytes. *Biotechnol Bioeng* **2006**, *95*, 850-862.

145. Tjoa, I.B.; Biegler, L.T. Simultaneous solution and optimization strategies for parameter estimation of differential-algebraic equation systems. *Ind Eng Chem Res* **1991**, *30*, 376-385.

146. Kravaris, C.; Hahn, J.; Chu, Y. Advances and selected recent developments in state and parameter estimation. *Comp Chem Eng* **2013**, *51*, 111-123.

147. Gray, P.W.; Barrett, K.; Chantry, D.; Turner, M.; Feldmann, M. Cloning of human tumor necrosis factor (TNF) receptor cDNA and expression of recombinant soluble TNF-binding protein. *Proc Natl Acad Sci U S A* **1990**, *87*, 7380-7384.

148. Fedorak, R.N.; Gangl, A.; Elson, C.O.; Rutgeerts, P.; Schreiber, S.; Wild, G.; Hanauer, S.B.; Kilian, A.; Cohard, M.; LeBeaut, A., *et al.* Recombinant human interleukin 10 in the treatment of patients with mild to moderately active Crohn's disease. *Gastroenterology* **2000**, *119*, 1473-1482.

149. Riley, J.K.; Takeda, K.; Akira, S.; Schreiber, R.D. Interleukin-10 receptor signaling through the JAK-STAT pathway: requirement for two distinct receptor-derived signals for anti- inflammtory action. *J Biol Chem* **1999**, *274*, 16513-16521.

150. Rahim, S.S.; Khan, N.; Boddupalli, C.S.; Hasnain, S.E.; Mukhopadhyay, S. Interleukin-10 (IL-10) mediated suppression of IL-12 production in RAW 264.7 cells also involves c-rel transcription factor. *Immunology* **2005**, *114*, 313-321.

151. Chu, Y.; Hahn, J. Parameter set selection via clustering of parameters into pairwise indistinguishable groups of parameters. *Ind Eng Chem Res* **2008**, *48*, 6000-6009.

152. Dai, W.; Bansal, L.; Hahn, J.; Word, D. Parameter set selection for dynamic systems under uncertainty via dynamic optimization and hierarchical clustering. *AIChE J.* **2014**, *60*, 181-192.

153. Murray, P.J. The primary mechanism of the IL-10-regulated anti-inflammatory response is to selectively inhibit transcription. *Proc Natl Acad Sci USA* **2005**, *102*, 8686-8691.

154. Carl, V.S.; Gautam, J.K.; Comeau, L.D.; Smith, M.F. Role of endogenous IL-10 in LPS-induced STAT3 activation and IL-1 receptor antagonist gene expression. *J. Leukoc. Biol.* **2004**, *76*, 735-742.

155. Tian, X.J.; Zhang, X.P.; Liu, F.; Wang, W. Interlinking positive and negative feedback loops creates a tunable motif in gene regulatory networks. *Phys Rev E* **2009**, *80*, doi:10.1103/PhysRevE.1180.011926.

156. Wincent, E.; Amini, N.; Luecke, S.; Glatt, H.; Bergman, J.; Crescenzi, C.; Rannug, A.; Rannug, U. The suggested physiologic aryl hydrocarbon receptor activator and cytochrome P4501 substrate 6-formylindolo[3,2-b]carbazole is present in humans. *J Biol Chem* **2009**, *284*, 2690-2696.

157. Adachi, J.; Mori, Y.; Matsui, S.; Takigami, H.; Fujino, J.; Kitagawa, H.; Miller, C.A.; Kato, T.; Saeki, K.; Matsuda, T. Indirubin and indigo are potent aryl hydrocarbon receptor ligands present in human urine. *J Biol Chem* **2001**, *276*, 31475-31478.

158. Jin, U.-H.; Lee, S.-O.; Sridharan, G.; Lee, K.; Davidson, L.A.; Jayaraman, A.; Chapkin, R.S.; Alaniz, R.; Safe, S. Microbiome-derived tryptophan metabolites and their aryl hydrocarbon receptor-dependent agonist and antagonist activities. *Mol Pharmacol* **2014**, *85*, 777-788.

159. Monteleone, I.; Rizzo, A.; Sarra, M.; Sica, G.; Sileri, P.; Biancone, L.; MacDonald, T.T.; Pallone, F.; Monteleone, G. Aryl hydrocarbon receptor-induced signals up-regulate IL-22 production and inhibit inflammation in the gastrointestinal Tract. *Gastroenterology* **2011**, *141*, 237-248.

160. Tian, Y.; Ke, S.; Denison, M.S.; Rabson, A.B.; Gallo, M.A. Ah receptor and NF-κB interactions, a potential mechanism for dioxin toxicity. *J Biol Chem* **1999**, *274*, 510-515.

161. Rivière, B.; Epshteyn, Y.; Swigon, D.; Vodovotz, Y. A simple mathematical model of signaling resulting from the binding of lipopolysaccharide with Toll-like ceceptor 4 demonstrates inherent preconditioning behavior. *Math Biosci* **2009**, *217*, 19-26.

162. Dai, W.; Bansal, L.; Hahn, J. Parameter set selection for signal transduction pathway models including uncertainties. *19th IFAC World Congress* **2013**, *19*, 815-820.

163. Dai, W.; Bansal, L.; Hahn, J.; Word, D. Parameter set selection for dynamic systems under uncertainty via dynamic optimization and hierarchical clustering. *AIChE J* **2014**, *60*, 181-192.

164. Dai, W.; Word, D.P.; Hahn, J. Modeling and dynamic optimization of fuel-grade ethanol fermentation using fed-batch process. *Control Eng Prac* **2014**, *22*, 231-241.

165. Tone, M.; Powell, M.J.; Tone, Y.; Thompson, S.A.J.; Waldmann, H. IL-10 gene expression is controlled by the transcription factors Sp1 and Sp3. *J Immunol* **2000**, *165*, 286-291.

166. Kobayashi, A.; Sogawa, K.; Fujii-Kuriyama, Y. Cooperative interaction between AhR·Arnt and Sp1 for the drug-inducible expression of CYP1A1 Gene. *J Biol Chem* **1996**, *271*, 12310-12316.

167. Mezrich, J.D.; Fechner, J.H.; Zhang, X.; Johnson, B.P.; Burlingham, W.J.; Bradfield, C.A. An interaction between kynurenine and the aryl hydrocarbon receptor can generate regulatory T cells. *J Immunol* **2010**, *185*, 3190-3198.

168. Patel, R.D.; Murray, I.A.; Flaveny, C.A.; Kusnadi, A.; Perdew, G.H. Ah receptor represses acute-phase response gene expression without binding to its cognate response element. *Lab Invest* **2009**, *89*, 695-707.

169. Konkel, J.E.; Chen, W. Balancing acts: the role of TGF-β in the mucosal immune system. *Trends Mole Med* **2011**, *17*, 668-676.